UNIVERSITY FOR DEVELOPMENT STUDIES

HYDRO-GEOPHYSICAL ASSESSMENT OF GROUNDWATER POTENTIAL FOR IRRIGATED-AGRICULTURE IN THE SAWLA TUNA KALBA DISTRICT OF SAVANNAH REGION, GHANA

PROSPER, KPIEBAYA

2022

UNIVERSITY FOR DEVELOPMENT STUDIES

HYDRO-GEOPHYSICAL ASSESSMENT OF GROUNDWATER POTENTIAL FOR IRRIGATED-AGRICULTURE IN THE SAWLA TUNA KALBA DISTRICT OF SAVANNAH REGION, GHANA

BY

PROSPER, KPIEBAYA (B.Sc. Earth Science)

ID NUMBER; UDS/MSWC/0001/19

[DISSERTATION/THESIS SUBMITTED TO THE DEPARTMENT OF AGRICULTURAL MECHANIZATION AND IRRIGATION TECHNOLOGY, FACULTY OF AGRICULTURE, FOOD AND CONSUMER SCIENCES, UNIVERSITY FOR DEVELOPMENT STUDIES IN PARTIAL FULFILLMENT OF THE REQUIREMENTS FOR THE AWARD OF MASTER OF PHILOSOPHY DEGREE IN SOIL AND WATER CONSERVATION AND MANAGEMENT]

FEBRUARY, 2022

DECLARATION

Student

I hereby declare that this dissertation/thesis is the result of my original work and that no part of it has been presented for another degree in this University or elsewhere:

Candidate:

Signature:……..…… Date:……

Name: ……...……..

Supervisors

I hereby declare that the preparation and presentation of the dissertation/thesis was supervised following the guidelines on supervision of dissertation/thesis laid down by the University for Development Studies.

Principal Supervisor's

Signature:……..…… Date:……

Name: ……...……..

Co-Supervisor

Signature:……..…… Date:……

Name: ……...……..

ABSTRACT

Despite Africa having huge groundwater potential, we are still behind in terms of groundwater irrigated agriculture. The main objective of this study is to appraise the groundwater potential in the Sawla Tuna Kalba District for irrigated agriculture. The Schoeller equation was used to estimate the groundwater storage and extractable storage within the basin. Hargreaves equation and remote sensing data from November to February (planting to maturity) in the year 2020 for tomato and maize were used to determine the total crop water requirements (CWR) using the extractable growth storage. Moreover, the Geographic Information System (GIS) was used to develop a groundwater potential map of the study area and however, used to create a groundwater quality suitability map for irrigation. Results from the hydro-geophysical survey show that the study area is predominantly underlined by the Precambrian and Paleozoic units. The groundwater storage and extractable storage were found to be approximately 2.4×10^6 Km^3 and 9.8×10^6 Km^3 respectively. The total Irrigation Water Requirements (IR) for a hectare of tomato and maize were 5,097 m^3/ha/growing season and 5960 m^3/ha/growing season respectively. The total land area available for agricultural use was computed to be around 1282.7 Km^2 (128,270 hectares), but the total area that can be irrigated with tomato and maize using groundwater was found to be 143.6 Km^2 (14,360 ha) and 196.2 Km^2 (19,620 ha) respectively. The groundwater suitability map showed that areas of excellent quality for irrigation had an area of 507.88 Km^2, areas of very good quality were found to be 3277.99 Km^2, good areas was about 790.21 Km^2, less restricted areas was around 24.21 Km2 and areas of that are extremely restricted had area of 1.11 Km^2. Moving forward, an indepth geophysical survey should be conducted to determine the nature of aquifer which can be the basis of any hydrogeological study.

ACKNOWLEDGEMENT

First of all, I will like to thank the almighty for how far he has brought us and most especially for the gift of life.

My first thanks go to my Supervisor Prof. Ganiyu and Dr. Baatuuwie for nurturing this work to see the light of day but both later became more than just supervisors to me, may the almighty God bring your wishes to light and also grant you eternal wisdom so that we can learn from you first hand.

Dr. Joseph, my HoD can not be left out, it is him that encouraged me and thought me the skill of patience and knowing that everything would fall in place at the right time like this moment. I am most indebted to him now and in years to come.

I will like to thank my lecturers who squeezed time to ensure that I finish my course work on time, especially lecturers from the department and outside the department. Also, special thanks go to my senior brother Amadu Inusah and Gordon Tanga of AESL for giving me the opportunity to being a consultant at the firm, and it is through my consultancy I develop an interest in further studies and importantly discovering this research topic.

My utmost appreciation goes to my family for their incredible support from the beginning of this work to now, may God bless them. To my colleagues at WACWISA, they know what I feel because no amount of thank you can make up for the room they gave me to work.

DEDICATION

This work is been dedicated to my grandfather and grandmother who are in blessed memory.

TABLE OF CONTENTS

LIST OF TABLES

LIST OF FIGURES

LIST OF PLATE

LIST OF APPENDICES

CHAPTER ONE

GENERAL INTRODUCTION

1.0 Introduction and Background

Groundwater is all water that exists in layers of soil or rock beneath the subsurface, which can also serve as a future water resource, especially in agriculture (Lin *et al.,* 2018). The term surface refers to water in the soil surface area (rainwater, lake water, and so on), then moves into the soil layer in recharge areas and then flows to the discharge area (Sikandar & Christen, 2012). Water in the subsurface will join to form a layer called the soil-water zone. In most cases, plants and other organisms utilize the surface water and, to some extent, the groundwater as well.

Water is essential for agriculture, but its availability for irrigation has been jeopardized by several factors, the most serious of which is climate change (Havril *et al.*, 2018). According to the National Environment Policy (2004), anthropogenic climate change has a negative impact on precipitation patterns, ecosystems, agricultural potential, forests, coastal and marine resources. The Intergovernmental Panel on Climate Change (IPCC) explained climate as "the average weather in terms of the mean and its variability over a certain time-span and a certain area" and the significant variation of the mean state of climate lasting for decades is referred to as climate change. Precipitation and evapotranspiration affect groundwater through the challenges of climatic change. Mall *et al.* (2006) in a review, itemised the gases that pose a threat to climatic issues which tend to offset the rainfall structure influencing the groundwater recharge.

Mall *et al.* (2006) in a study rebutted the idea of climate change is the sole factor of groundwater fluctuations. The reasons were the demand for groundwater has increased due to urbanization and industrialization, changes in the cropping patterns and land-use patterns, over-abstraction of groundwater, and changes in irrigation and drainage. Olesen *et al.* (2007) argued that replacing natural vegetation with crops can increase and improve the natural recharge of groundwater. The compelling fact was, if the climatic change affects the vegetation in the forest or savanna, then this too can enhance the natural groundwater recharge. However, the direction of net impact will depend on the changes in the natural ecosystem. Simulation models developed by Australian scientists have shown that temporal variations and rainfall influence vegetation growth rates and leaf area of plants that affect groundwater recharge (Kundzewicz *et al.*, 2008; Birkenholtz, 2017*;* Havril *et al.*, 2018). Comparatively, (Dong *et al.*, 2013) confirmed that the occurrence of groundwater is influenced by climate, morphology, geology, and natural vegetation. Biodiversity helps in the process of water absorption into the soil (Wahyudi & Moersidik, 2016).

The storage capacity of groundwater is of great essence in the context of sustainable agriculture and irrigation. A study conducted by Martin & van de Giesen. (2005) within the White Volta indicated that the main variables in the estimation of groundwater storage are the rate of recharge and available storage. The study's main finding was that groundwater utilisation was less than 1% of the recharge rate and that the border between Ghana and Burkina Faso was about 3.7% of the recharge rate.

The availability of groundwater for irrigation is fundamentally necessary, however, the quality of the water used cannot be overlooked. Groundwater's suitability for irrigation is dependent on the presence of dissolved constituents in it. The presence of salts beyond certain acceptable limits uptake of water through modification of osmotic processes, or chemically by metabolic reactions such as those caused by toxic constituents (Saeedi *et al.*, 2010; Ewida *et al.*, 2020). In this regard, it is very important to carry out the required quality test in a recognized laboratory before exploiting and adopting it for groundwater irrigation. In the past, many irrigational schemes have failed due to the presumption that groundwater is desirable for domestic and industrial use. For instance, a typical example is the failed scheme at Gung in the Kumbungu District of the Northern Region as a result of high salinity in groundwater.

The economic benefits derived from irrigation in some developed parts of the world are irrefutable. Asia is the largest cultivator of groundwater-irrigated agriculture, accounting for 15.6% of the irrigated land area of the world (Siebert *et al.*, 2010). Research has shown that the Asia economy is boosted through irrigation with groundwater as its main source of supply (Wada *et al.*, 2012). Comparably, Africa and the Sub-Saharan areas have encountered challenges in the utilization of groundwater for irrigation schemes. These challenges include; little knowledge of the groundwater resource potential limited or fragmented data on groundwater, inadequate ongoing monitoring of groundwater, limited capacity to plan, develop or manage the groundwater resource, low groundwater potential or issues on groundwater quality, high cost of exploration, and lack of operational experience (Kumar *et al.*, 2018).

Another unmentioned content is the geological and hydrogeological disparity that defines the occurrence and existence of groundwater. There is a wide acceptance that geology is the major controller of groundwater availability (Pavelic *et al.,* 2012; Rahmati *et al.,* 2015; Tolche, 2020). There are four major hydrogeological provinces in Africa: a) the crystalline basement complex, which supports approximately half of the settlements in Sub-Saharan Africa with variable borehole yields; b) consolidated sedimentary formation, which supports approximately a quarter of the population with moderate-low yields; and c) unconsolidated alluvial sediments, which supports approximately 15% of the population with moderate-low yields (MacDonald *et al.,* 2009; Abdul-ganiyu *et al.,* 2020). The research area falls under the Crystalline Basement complex which is believed to have high groundwater potential that can be exploited for irrigated agriculture if proper feasibility studies are carried with the appropriate techniques such as hydro-geophysical methods.

Hydro-geophysical techniques exploit contrasts in physical properties (example, dielectric permittivity, apparent electrical conductivity or resistivity, and magnetic susceptibility) to indirectly measure, profile, and monitor differences in physico-chemical soil properties; delineate suitable soil, lithological, and stratigraphic boundaries, and characterize soil patterns and features (Piccoli *et al.,* 2020). Another component of Apparent Electrical Resistivity (ERa) of soils in the context of hydro-geophysics is becoming more popular in the framework of precision agriculture (Gebbers & Lück, 2005). Apparent Electrical Resistivity (ERa) is of holistic importance because it correlates to soil physical properties which are prime factors in soil fertility assessment (Abidin *et al.,* 2017).

Romero-Ruiz *et al.* (2018) and Dampney *et al.* (2004) studied that hydro-geophysical techniques can be used to estimate salinity, soil texture, water content, organic matter content, and compaction. There are numerous geophysical exploration methods, but three of these methods that are commonly used in soil and agriculture surveys are Electromagnetic Induction (EMI), Electrical Resistivity (ER), and Ground-Penetrating Radar (GPR) (Allred & Redman, 2009). Electrical Resistivity and Electromagnetic Induction methods were initially used to assess soil salinity but their use has greatly expanded in agriculture with the development of precision agriculture in the 1990s (Allred & Redman, 2009). Since the late 1970s, GPR has been used extensively as a quality control tool to improve soil data interpretations (Allred & Redman, 2009).

Hydro-geophysical technique is a non-disturb method of an observed object which results in electrical resistivity value at each soil depth (Bahri & Saibi, 2010; Swileam *et al.*, 2019). The resistivity value is inversely proportional to the groundwater content (Abidin *et al.*, 2017). The adoption of the Schlumberger configuration was to profile the geological formation stratigraphically to achieve a realistic objective, while the dipole-dipole configuration has proven to be a prolific groundwater-finder array within the Palaeozoic sedimentary formation (Yidana *et al.*, 2012; Abd El-Gawad *et al.*, 2018).

1.1 Problem Statement and Justification

Fundamentally, irrigation should have unimpeded access to a water supply. Groundwater is abundant in this part of the world (Sub-Saharan Africa), according to past and current studies, and it is also gaining widespread recognition as an invaluable untapped resource for irrigated agriculture (Giordano, 2006; Masiyandima and Giordano, 2007). Research has

proven that the Asian continent has boosted its economy through groundwater irrigation despite Africa having high groundwater reserves. Africa currently has the least irrigated land area while groundwater availability is unquestionable (Giordano, 2006; Allaire, 2009) Climate change and irregularities in rainfall structure stand to pose a huge threat to agriculture and food security in decades to come if resilient solutions are not implemented. Based on literature and field research, the most effective solution to the looming problem is groundwater exploration for irrigation (Anornu *et al.*, 2009). The matter in question is why the potential of groundwater irrigation is not fully exploited in this part of the world? This can be attributed to little knowledge on groundwater resources and their potential, limited or fragmented data, no ongoing groundwater monitoring to assess various aquifers, limited capacity to plan, poor quality of groundwater in some parts of the study area, high operating costs, and a lack of personal experience. Hence, this research sought to study the geological profile using appropriate techniques and methods to locate areas viable for groundwater irrigation for agricultural productivity.

The study of groundwater potential using hydro-geophysical methods can be the cutting-edge solution to the problem of why Ghana and specifically the Sawla-Tuna Kalba areas have not fully explored groundwater irrigation despite the enormous groundwater availability. Hydro-geophysical surveys are economically affordable as it ranges from USD 120 to USD 450 for a 1 Km^2 area depending on the study (Groundwater delineation, Geological Characterization, and Agricultural Survey). Also, the operational service and accessibility to geophysical equipment are of moderate access, implying that the field of professionalism is held to a high standard. Considerably, a hydro-geophysical survey has

a high versatility rate, suggesting that it can be used from one geographic area to the other with the right calibration (Yidana et al., 2013; Kpiebaya & Abanyie, 2017).

The imminence of this survey is to inform future policymakers to consider groundwater irrigation as an alternative solution that can shield Ghana and Africa from food insecurity with climate change at its peak. Furthermore, the results of this research will serve as a stepping stone toward establishing a groundwater potential knowledge base on which the government, donors, stakeholders, and well-doing farmers can rely for future irrigation decisions. This will go a long way to achieve a number of the Sustainable Development Goals (SDGs 1, 2, 3, 8, 10, 13, 14, and 15) that Ghana and the world at large are aiming at. This will also contribute enormously to the Ghana government's development agenda of the Planting for Food and Jobs.

1.3 Research Questions

1. What are the resistivity and apparent resistivity of the geological formation in the study area?
2. What is the groundwater yields under these geological formations for irrigation in the area
3. What is the quality of the groundwater for irrigation in the area?
4. Where are the zones of occurrence of the groundwater resource for possible future irrigation projects

1.4 Objective of the Study

1.4.1 Aim of the Study

This research aimed to study and delineate the groundwater potential using hydro-geophysical techniques for irrigated agriculture in the Sawla-Tuna-Kalba District of Ghana.

1.4.2 Specific objectives of the Study

1. To evaluate the resistivity and apparent resistivity of the geological formation.
2. To determine the groundwater yield potential and quality for irrigation in the study area.
3. Delineate the occurrence of groundwater resources for possible future irrigation projects.

1.5 Organization of study:

The study is organized into five (5) chapters. Chapter one introduced the study by providing the background of the study, followed by the problem statement and justification, the research questions, and the objectives of the study. Chapter two reviewed the relevant literature on the use of groundwater for irrigation and also, the use of various techniques and methods for groundwater assessment. Chapter three highlighted the study area as well as the research methods and materials used. This chapter first described the study area both with respect to its physical and anthropogenic features. The second section explained the research methodology and data analysis of the study. Chapter four presented the results of the study and discussions. Chapter five provided a summary of the results, conclusions, and recommendations.

CHAPTER TWO

REVIEW OF RELATED LITERATURE

2.0 Overview

This chapter is a review of research and other related literature relevant to the study questions. It discussed some of the theoretical perspectives on the use of groundwater for irrigation. The following research headings were used to guide the review of the literature:

1. Review of theoretical perspectives of the study
2. Hydro-geophysics
3. Groundwater potential in the study area
4. Groundwater quality for irrigation
5. Groundwater Irrigated Agriculture in Ghana

2.1 Groundwater

Groundwater is documented as the most valuable resource on the planet, found within the subsurface, which includes sediments, cracks, fractures, crevices, faults, and many other features (www.nationalgeographic.org). These subsurface features are also known as a hydrogeological environment or a province (www.nationalgeographic.org). Groundwater is defined as water that exists beneath the water table and typically fills all void spaces (hydrogeological environment) in the saturated zone of the rocks (Kresic, 2007). However, these context-specific spaces must be well interconnected with one another to ensure a high-yielding environment. Groundwater, according to the International Groundwater Resources Assessment Centre (IGRAC, 2013), is a "*hidden resource*". Thus IGRAC (2013) defined groundwater as a naturally occurring resource that is replenished by rainwater, snowmelt, or water that leaks into the ground from rivers and lakes. Kresic (2007) and IGRAC both have a fundamental concept for describing groundwater in terms

of its location on Earth and natural phenomena. The United Nations Educational, Scientific, and Cultural Organization (UNESCO-IHP, 2019) explained groundwater on the IGRAC concept, but more importantly, outlined groundwater as an abundant source of fresh water on earth, despite remaining hidden in many ways. The UNESCO-IHP (2019) definition of groundwater is still contradictory because a resource that is both "plentiful" and "*hidden*" does not add up. It is undeniably plentiful on earth, but the processes involved in locating this resource are strategic and have recently become laborious. As a result, groundwater is considered "*hidden*" while also abundant.

2.2 Groundwater Classification

Classification of groundwater is varied and is based on several parameters over the past decades but the globally recognized classification standard is vividly discussed in sections (2.2.1, 2.2.2, 2.2.3, and 2.2.4) (https://en.wikipedia.org/wiki/Groundwater). The global classes are based on the position and location of groundwater and it consists of the confined aquifer, unconfined aquifer, and perched aquifer. However, few authors have attempted to classify this resource based on other factors affecting groundwater which include; quantity and quality (George *et al.,* 2009). George *et al.* (2009) in a study in Canada (Alberta) classified the groundwater resource based on Total Dissolved Solids (TDS) but noticed that the TDS varied in Texas, Utah, and Wyoming. It was found that the groundwater was grouped into six (6) classes (I, II, III, IV, V, and VI) with class VI considered to be unsuitable for any use and class IV showing high TDS values around 10000 mg/L suggesting the groundwater type to be brackish. In the same study in the United States, groundwater was classified based on quality, uses, and vulnerability. The classes were found to be in class I, class II, and class III. Class I, was a groundwater that is highly

vulnerable and ecologically vital, class II was groundwater that is a potential source of drinking, and class III was groundwater with insufficient yield and with intermediate quality. George *et al.* (2009), noticed that groundwater in South Africa was grouped based on the geological units (aquifer system) and was classified into five (5) classes. These were sole-source aquifer, major aquifer, minor aquifer, non-aquifer system, and special aquifer system. The sole source aquifer was described as one that supplies about 50% for domestic use, major and minor aquifers were based on productivity and abstraction while a special aquifer system was described as an aquifer that has been designated by a government official.

2.2.1 Aquifer

An aquifer, according to the web dictionary (https://en.wikipedia.org), is any geological formation or underground layer of water-bearing rock that yields groundwater in sufficient quantities for human consumption. In geological terms, an aquifer is a saturated rock through which water can easily move (permeability). In layman's terms, an aquifer is a formation that can store large amounts of water. An aquifer is distinguished by two main characteristics that determine whether it is high or low yielding. Porosity and permeability are two common characteristics used to describe an aquifer in which groundwater is held or stored (Huang *et al.,* 2020). The ability to store and the ability of water to flow through it distinguishes porosity and permeability. While porosity is concerned with the ability of groundwater to be stored, permeability is concerned with the ability of groundwater to flow within the spaces. However, porosity and permeability go hand in hand; for example, an aquifer made of clay may be low-yielding because clay has a lot of pores but they are tiny, resulting in low permeability. Because of the tiny pores, it is more difficult for water to

move through it, and thus less water is held within the pores, making any aquifer of clay formation low yielding. Because of the cemented phase, an aquifer with hard rock as the bedrock (granite, sandstone, shale, limestone, siltstones, and many others) has no pores and can only yield groundwater if it has cracks and fractures. Hard rock with fractures can hold a lot of water, and if the fractures are well connected, the formation becomes very permeable. Aquifers are classified into three types: confined, unconfined, and perched aquifers (Arumugam & Elangovan, 2009).

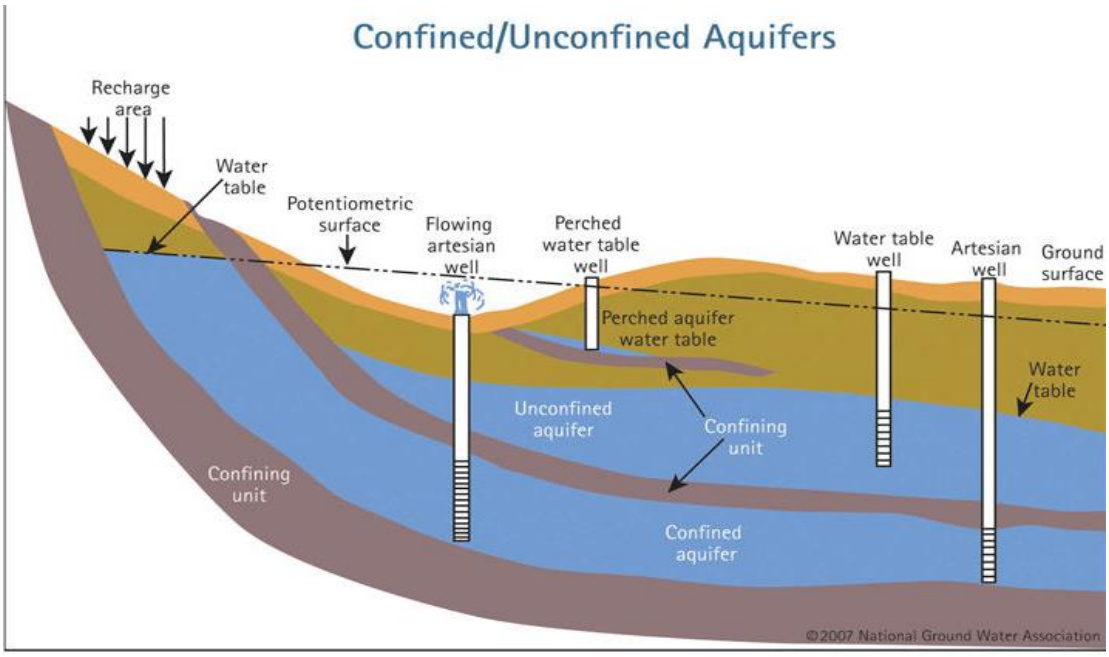

Figure 2.1: Showing a Confined, Unconfined, and Perched Aquifer (John, 2014)

2.2.2 Confined Aquifer

This type of aquifer stores water in a permeable rock that is surrounded by two impermeable rock layers known as confining beds (Fenta *et al.,* 2020). The confining bed may be composed of clay, shale, granite, or other bodies that tend to protect groundwater from contamination caused by surface activities such as leakage and seepage (Hassan *et al*., 2019; Fenta *et al.,* 2020). Due to the extreme nature of these confining beds, the existing

water is subjected to pressures that may be greater than atmospheric pressure. Confined aquifers are also known as "Artesian Aquifers." Drilled wells sourced from artesian aquifers typically have unstable water levels due to a greater change in pressure than the amount of water stored.

2.2.3 Unconfined Aquifer

Unconfined aquifers are geological bodies that store water and are found very close to the land surface. They have no confining or impermeable bed covering them. The water table is the uppermost layer of groundwater within an unconfined aquifer. As a result of infiltration by land pollutants, this type of aquifer is more prone to contamination and pollution than confined aquifers. Groundwater level fluctuation is determined by the amount of water stored and the atmospheric pressure acting on the water storage (Hassan *et al.,* 2019; Fenta *et al.,* 2020).

2.2.4 Perched Aquifer

This is closely related to a confined aquifer which has confining layers, but these layers are below groundwater but above the main water table. This type of aquifer is formed when groundwater rises above unsaturated rock formations due to a discontinuous impermeable layer (Arumugam & Elangovan, 2009). This type of groundwater is extremely rare, and in some parts of the world, it is only available during certain seasons of the year.

2.3 Importance of groundwater

2.3.1 Domestic and Industrial use

The use of groundwater has been described to be an exceptional source of water supply and the top five countries that extract groundwater mainly for domestic and industrial use

include; China, the United States, India, Pakistan, and Iran (https://en.wikipedia.org/wiki/Groundwater). IGRAC, (2013) and UNESCO-WWAP, (2009) estimated that about 1000 Km^3 of the world's aggregated groundwater is abstracted yearly for domestic and industrial uses. In Africa, the greatest man-made river was created from the Nubian Sandstone aquifer and supplies most of the groundwater for domestic and industrial uses (Banoeng-Yakubo, 2017). In the study, groundwater in Sub-Saharan countries is the main source of water for agriculture, drinking, and domestic uses. In Ghana, Yeleliere *et al.* (2018), Gracia-de-Rentería *et al.* (2020), and Chegbeleh *et al.* (2020) in separate studies discussed the various uses of groundwater but found the major uses of groundwater fell in either domestic and industrial. The individual uses of groundwater according to the latter studies included; drinking, washing, cooking, bathing, watering of animals, irrigating gardens, and many more.

2.3.2 Groundwater usage for Irrigation

Irrigation is the most important use of groundwater because of the benefits it provides. Its economic potential for a country and an individual is immeasurable. Groundwater is often the most obvious alternative in some parts of the world where surface water is unable to meet the water supply demand for irrigation. Agriculture uses approximately 70% of the groundwater drawn for human consumption globally, and approximately 53% of the groundwater in the United States (Rosenberg *et al.*, 2000; KhoKhar, 2017). The world's total irrigable land is about 301 million ha of which 38% are equipped for irrigation with groundwater (Siebert *et al.*, 2010; Lebdi, 2016). The total groundwater that is been consumed around the world for agricultural purposes is around 545 Km^3yr^{-1} (Siebert *et al.*, 2010; Lebdi, 2016). Moreover, countries with the largest extent in terms of land area for

irrigation are India (39 million ha), China (19 million ha), and the USA (17 million ha) (Siebert *et al.*, 2010). Groundwater irrigation is currently on the rise both in percentage and in absolute terms. Siebert *et al.* (2010) and Grogan *et al.* (2017) conducted a study that uncovered the uncertainties associated with the availability of statistical data to track patterns and developments of groundwater use for irrigation.

In 2013, the Africa Climate Policy Center (ACPC) identified one of three major factors driving Africa's intense interest in groundwater development. The United Nations Millennium Development Goals (MDGs 7. C) was one of the pressing factors that needed to be addressed in order to provide safe and sustainable drinking water to the African people (Lomazzi *et al.*, 2014). Groundwater was the primary source of water, particularly in rural areas, and the commercialization of this resource brought it to the forefront of attention (ARCC, 2014). In addition, providing access to groundwater for agriculture (livestock water and small-scale or commercial irrigation) is a critical step in reducing poverty and raising living standards. The ACPC. (2013) recommendation on irrigation was to manage the storage capacity both within the regolith and the aquifer to sustain irrigation schemes against harsh conditions and hydrological shocks.

On the 16th of May, 2016, the 2nd Asia Pacific Water Summit in Chiang Mai presented the reasons why irrigation should be practiced more and the opportunities for small-holder farmers around the world. A few examples of its significance presented are as follows:

1. Increase crop intensification and diversification
2. On-demand irrigation (high water productivity)
3. Secure agricultural productivity during droughts and long dry spells
4. Boost food security and improve livelihood

5. Creates employment opportunities and some associated indirect benefits
6. As pro-poor; it makes irrigation democratic, spatially, and supports private enterprise.

Kwoyiga & Stefan (2018) in a study found out that groundwater for irrigation in Ghana is gaining currency. This was conducted around the northeast part of the country where the potential of groundwater is extremely high. In the study, groundwater irrigation was aimed at the natives to assess local knowledge in the understanding and utilization of this resource for irrigation. According to their findings, local knowledge in groundwater irrigation enables irrigators to locate groundwater points for the construction of wells and dugouts. It also prompts local people on the period to construct wells for irrigation and how to use groundwater to cope with the insufficiency of surface water resources during the dry seasons. *(*Abdul-ganiyu *et al.,* 2020; Prosper *et al.,* 2020; Loh *et al.,* 2020) investigated suitable alternatives for irrigation in the absence of surface water during the dry season in similar studies in Ghana's Northern and Upper West Regions. According to the findings of the study, climate change and temporal variations are endangering food security in this part of the world, and thus other approaches must be implemented to protect agricultural productivity.

2.4 Assessment of groundwater

Groundwater resource can only be assessed through exploration and exploitation methods which involves drilling of boreholes, well digging, and so on (NGWA, 2014). In this study, groundwater assessment is based on geophysical methods. Several methods exist but the recognized ones include; areal methods, surface methods, subsurface methods, and traditional methods (https://openei.org/wiki/Geophysical_Methods). Kpiebaya & Abanyie. (2017) and Ylaya *et al.* (2020) noticed that areal method, surface methods,

subsurface methods can be considered as modern geophysics and traditional methods can be considered traditional geophysics. Traditional geophysics evolved around the 17th century to locate groundwater points using indigenous techniques, these techniques included; water-witching, water divining, dowing, and many more (Shishaye, 2017). These methods in recent years have been considered to have numerous uncertainties in some parts of the world and Ghana, Kpiebaya & Abanyie. (2017) in a study in the upper west region of Ghana noticed that these methods still have an appreciable success rate but may vary from one geologic setting to the other. This current study deployed subsurface methods (electromagnetic and electrical) in assessing the potential of groundwater for irrigated agriculture in the study area and this is discussed in sections 2.5.1 to 2.6.3.

2.5 Geophysical Techniques – Concepts and Principles

Geophysics, which dates back to ancient times, was recognized around the 17th century (Shishaye, 2017). It is the science that deals with the use of physics in geological studies to investigate specific physical properties of the earth (Robinson *et al.,* 2015). Reynolds (1997) defined geophysics as the application of physical principles to the study of the earth. The two main branches of geophysics are pure geophysics and applied geophysics (Ylaya *et al.,* 2020). Pure geophysics involves the study of the solid part of the earth, whereas applied geophysics deals with the study of the earth's interior by taking measurements near the earth's surface and drawing informed conclusions (Ylaya *et al.,* 2020). In terms of economics and development, the essence of geophysics is not far-fetched. Predominantly, geophysics is a prominent process used in the investigation and exploration of some natural resources such as gold, petroleum, diamond, bauxite, and others (David *et al.,* 2001). Its application in groundwater assessment is still evolving and not widely known. Geophysical

methods are commonly classified based on the source of earth, and thus they can be active or passive methods (Li *et al.*, 2020).

Active methods, involve artificial processes, while passive methods, too, involve natural processes (Reynolds, 1997). Geophysical techniques also differ depending on the operation principle (Robinson *et al.*, 2015), the purpose of the investigation (At & Fields, 2020), the nature of the geology, and even the cost of the investigation (Adamo *et al.*, 2020). These techniques mostly include electrical resistivity methods, electromagnetic methods, magnetic methods, seismic methods, and gravitational methods (Best, 2015; Manivannan & Elango, 2019). Each of these methods is only appropriate based on the purpose of the investigation. For example, the magnetic method is often preferred in the search for rock deposits with specific magnetic properties. Because of the depth of deposition associated with coal, seismic methods are preferred in the search for petroleum (David *et al.*, 2001; At & Fields, 2020). Similarly, seismic and electrical resistivity methods are preferable to one another for groundwater delineation because they can distinguish saturated rock from dry rock due to higher seismic velocity or electrical conductivity (Kearey and Brooks, 2002; Arjwech *et al.*, 2021).

2.5.1 The Electromagnetic Method (EM)

Electromagnetic (EM) surveys are used in groundwater exploration. They are also used in mineral exploration and metalliferous mineral deposits (Guo, 2020; Peng & Han, 2020), geotechnical studies (Abidin *et al.*, 2011; Mohammed *et al.*, 2020), anthropological studies (Sea & Ernenwein, 2020), and investigation to locate buried artifacts such as pipes, barrels, walls, and others (Espindola-Canata *et al.*, 2020; Liu *et al.*, 2020). It can also be used to investigate geothermal resources, map contaminated land, geological and environmental

mapping, map contaminant plumes, detect natural and artificial cavities, and locate geological faults (Youssouf *et al.,* 2021; Espindola-Canata *et al.,* 2020).

The EM uses a device called the Geonics EM34 which is used for the EM profiling. Its constituent parts are the transmitter and receiver coils, the transmitter and receiver console, and the separation coils (Figure 2.2) (Parnow *et al.*, 2021; Kpiebaya *et al.*, 2021). The EM of profiling is effective in the presence of water-bearing rocks or thin overburden. It measures the properties of magnetic fields that are induced into the ground. These fields consist of an alternating electric intensity and a magnetizing force.

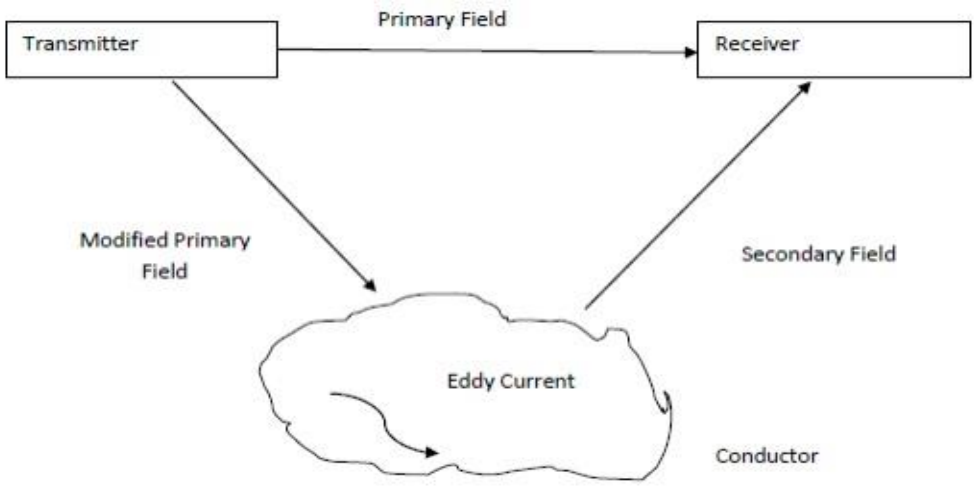

Figure 2.2: Schematic diagram of EM field (Kearey and Brooks, 2002)

This method, on the other hand, can be used as a reconnaissance tool due to its quick data generation and ease of interpretation. A primary or inducing field is created by passing an alternating current into the ground through a coil, which is made up of a wire loop known as a transmitter coil (Chegbeleh *et al.,* 2009). Eddy current is produced when the primary field generates spreads out in space both above and below (John, 2014). The eddy current creates a secondary electromagnetic field that can interfere with the primary field. The

receiver coil detects the resultant of the primary and secondary fields, and thus all bodies with conductive effects are detected (Oghenekohwo, 2008). In summary, an induced current is introduced into the ground by the transmitter coil and measured by the receiver coil, which is located a short distance from the transmitter as in plate 1. The apparent conductivity is measured on the receiver and is expressed in millimhos/meter (m mhos/m).

The preference of the Electromagnetic method over other geophysical techniques are stated below;

1. It is quicker to carry out EM surveys in larger areas.
2. Because EM methods are based on induction, they do not require direct contact with the ground and thus do not require the use of electrodes.
3. The EM method is versatile, which means it can be used in the air, at sea, or on land.

Despite having these merits, the EM34 device has few shortcomings and they include;

1. The depth of investigation is fixed depending on the separation coil used.
2. Because of the magnetic fields that may be created during the survey, it cannot be used near high-tension electrical lines. The high-tension lines would interfere with these magnetic fields, causing reading errors.
3. More sophisticated quantitative interpretation of electromagnetic anomalies.

Plate 1: The application of EM34 in the current study

2.5.2 The Electromagnetic Theory

The EM34 conductivity measurement is dependent on electromagnetic fields and the alternating induce current on the surface caused by the primary fields. The science that generates these values is based on scientific formulae and principles. The electromagnetic phenomenon was first derived from Maxwell's wave equations (Ward and Hohmann, 1987) and has recently been used in several studies (John, 2014; Roy, 2020; Africa *et al.*, 2020).

2.5.3 Depth of Penetration in Electromagnetism

Depth of penetration, also known as skin depth, is defined as the depth at which the amplitude of an electromagnetic wave is reduced to 1/e or 37% of its original value A_o (Lange & Seidel, 2007). Mathematically is been described as the amplitude of electromagnetic radiation as a function of depth (z) relative to its original amplitude A_o seen in equation 2.1:

$$A_z = A_o e^{-1} \qquad (2.1)$$

Mathematically, the skin depth is expressed as in equation 2.2;

$$\delta = \sqrt{\frac{2}{\omega\sigma\mu}} = 503\sqrt{(f\sigma)} \qquad (2.2)$$

Where, $\omega = 2\pi f$, f = frequency in Hz, σ = conductivity in S/m and μ = magnetic permeability (usually ≈ 1).

A realistic estimate of the depth to which a conductor would give rise to a detectable EM anomaly is $\approx \frac{\delta}{5}$ (Reynolds, 1997). As the frequency of the electromagnetic field and the conductivity of the ground both decrease, so does the depth of penetration. As a result, the electromagnetic method is constrained by the frequency (f) dependence of the depth of penetration. The power of electromagnetic radiation or wave to penetrate to a certain distance is worth investigating in an EM survey (Reynolds, 1997). In theory, an electromagnetic wave can travel indefinitely through an isotropic medium, in practice, it travels through geological media to detect the presence of groundwater. In comparison to other theoretical phenomena, an electromagnetic wave has a difficult time penetrating the earth's subsurface. Because the frequencies used in EM surveys are frequently less than 5 kHz, the effects of attenuation are negligible, but signal losses occur due to diffusion.

2.6 The Electrical Resistivity (ER) Method

In comparison to the electromagnetic magnetic method, this is the oldest and most popular modern geophysical method. In Africa and some parts of the world, the ER method is commonly used for borehole siting and other related water sitting activities (Mohamaden *et al.,* 2016; K *et al.,* 2020; Taha *et al.,* 2021). This method works based on the electrical

resistivity of a specific rock, implying that every rock or geological material has a certain amount of conductivity that can be estimated and interpreted. Two main activities can be performed during an electrical resistivity survey; Profiling and Depth sounding (Taha *et al.*, 2021).

The survey is carried out at each interval along the groundwater zone, and measurements are taken at each point of an interval with the configuration arrays, these are discussed in section 2.6.2. This method is commonly used in groundwater exploration. In sounding, the survey is carried out at a predetermined point, and measurements are taken at each depth. Sounding is more common in lateral soil or lithological investigation, but the two processes can be used concurrently (Romero-Ruiz *et al.*, 2018). During ER surveys, profiling is used first to detect points of suitable groundwater occurrence, and sounding can be used to authenticate the suspected point (Romero-Ruiz *et al.*, 2018; Kpiebaya *et al.*, 2021). This is because it involves complex data collection and interpretation to locate an appropriate point of groundwater occurrence, its application in the field requires the use of a specialist with extensive experience. It is the more reason why the use of ER is more precise in rural water supply applications (MacDonald & Davies, 2000).

Furthermore, Vertical Electrical Sounding (VES) is known to be the most widely used method in Africa (Mcdowell *et al.*, 2002). This method is used to investigate the vertical change in resistivity of geology while gradually increasing the electrode spacing between points of the interval while keeping the center of the entire array constant. The current permeates to greater depths as the electrode spacing is increased (Mcdowell *et al.*, 2002; Abidin *et al.*, 2011; Riwayat *et al.*, 2018). The resistivity measured is multiplied by the

geometric factor (K) to get the apparent resistivity (Kpiebaya *et al.*, 2021). The apparent resistivity is then plotted against the distance intervals (stations) to get a graph or image of the change of apparent resistivity with depth.

Both the electrical resistivity and electromagnetic techniques continuously measure the bulk resistivity of the subsurface. The only difference is how the electric current is transferred into the ground. In the electromagnetic method, a current is induced by magnetic fields, whereas in the electrical resistivity method, the current is sent directly through the electrodes (John, 2014). MacDonald & Davies (2000) discovered that one of the benefits of electrical resistivity is that the data collected can be quantitatively interpreted using the Microsoft Excel package to obtain precise estimates of depth thickness and resistivity of the subsurface layers. In groundwater exploration, the electrical resistivity of the subsurface can be used to estimate the saturating fluid in the formation, which is linked to the concentration of Total Dissolved Solids in the fluid (Dampney *et al.*, 2004; Romero-Ruiz *et al.*, 2018). This gives the ER method a significant advantage over the EM method. When compared to the EM method, this advantage is described as being non-destructive (Bahri & Saibi, 2010; Swileam *et al.*, 2019).

Nevertheless, the use of electrical resistivity presents several challenges, the most significant of which is its labour intensive and time-consuming (Abidin et al., 2017). The minimum electrodes in each survey are four, implying that the survey requires up to five people (Abdul-ganiyu *et al.*, 2020). In addition, each suspected groundwater point would have to go through sounding (VES) to confirm the degree of groundwater occurrence which involves a considerable amount of time (Abdul-ganiyu *et al.*, 2020; Kpiebaya *et al.*, 2021).

Another limitation of the ER survey is its lack of adaptability (John, 2014). It is not suitable for close spaces such as industrial areas, quarters, or crowded housing (Kpiebaya & Abanyie, 2017). This is because, in open spaces, more data can be collected and thus interpreted to a greater degree of precision, whereas in closed areas, less data is collected and interpreted to a lesser degree of precision, resulting in failures in groundwater exploration (Benoit *et al.*, 2019). Most importantly, an electrical resistivity survey cannot be performed on wetlands. This is because, with ER direct electricity is transmitted in the ground, and if performed on wetlands, anyone in the vicinity will likely be electrocuted (Kpiebaya and Abanyie, 2017).

2.6.1 Basic Principles of the Electrical Resistivity Method

The electrical resistivity employs the use of ABEM Terrameter which measures electrical resistivity by passing an electrical current into the ground via electrodes (C1 and C2) and measuring the resulting potential via two or more electrodes (P1, P2, …or more). Figure 2.3 shows how resistivity is measured in detail (Walton, 2010). Ohms law is commonly used to calculate resistance, which is then multiplied by a geometric factor (usually referred to as a K factor) to calculate resistivity. (MacDonald & Case, 2005).

According to ohms law, a Current (I) passing through an electrical circuit is directly proportional to the Potential difference (V) across the circuit.

The summarized equation is given as (equation 2.3 and 2.4) with full derivation in (John, 2014);

$$V = \frac{\rho l}{K} \qquad (2.3)$$

Resistivity is then estimated from equation (2.4)

$$\rho = \frac{KV}{I}\ R_{app}K \qquad (2.4)$$

Where $\rho = resistivity\ (ohm),\ R_{app} = Apparent\ Resistivity\ (ohm.m) and\ K = Geometric\ Factor(m)$

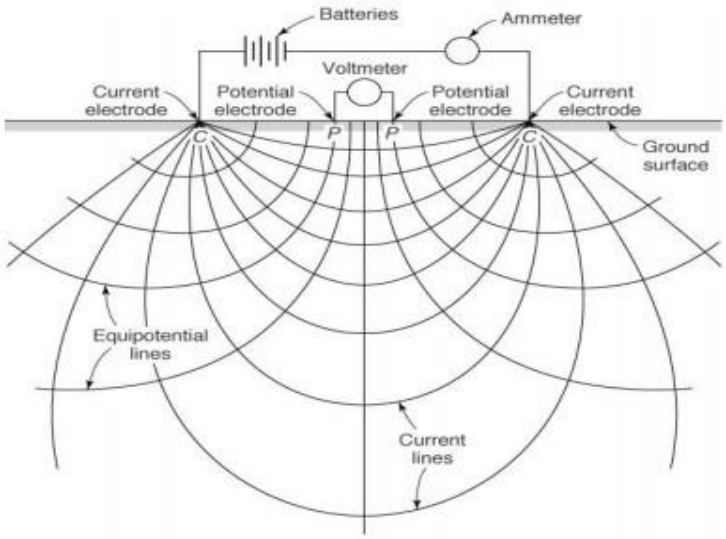

Figure 2.3: Schematic diagram of how Resistivity is measured (Walton, 2010)

2.6.2 Electrode Configuration

Electrode configuration has to do with the arrangements of the ABEM terrameter in the field survey to determine the presence and depth of groundwater. The depth of investigation is determined by the electrode spacing during a survey (Prosper *et al.*, 2020). The wider the electrode spacing, the greater the depth of investigation. Depending on the rock resistivity, the depth of investigation is typically 20% - 40% of the current electrode spacing (Abidin *et al.*, 2011).

The choice of electrode configuration in groundwater exploration depends on a variety of factors. The geological structures to be delineated, subsurface heterogeneities, the sensitivity of the resistivity meter, background noise level, and electromagnetic coupling are all factors that influence the selection of an electrode array (Aizebeokhai, 2010). Several array methods exist, including Schlumberger, Wenner, Dipole-Dipole, and others. Until 1960, the Wenner and Schlumberger configuration was the most common electrode array configuration (Abidin et al., 2017). Some arrays that have recently been discovered include dipole-dipole, pole-dipole, square, and gradient arrays (Aizebeokhai, 2010). Though most of the arrays are still in use, the Schlumberger method is the most preferred array in Sub-Saharan Africa for groundwater exploration because of its depth of penetration (Abidin *et al.*, 2011; Abidin et al., 2017). Each electrode configuration is better suited to a specific geological investigation.

The Schlumberger and Wenner (alpha) arrays are sensitive to vertical variation in subsurface resistivity beneath the array in a profile but less sensitive to horizontal variation in resistivity, which is their main shortcoming. Because of its high signal strength, the Wenner array outperforms other arrays in noisy fields, but it falls short of 3D structures (Dahlin & Loke, 2014; John, 2014).

Conversely, the dipole-dipole array is the most sensitive of all the arrays (both vertical and horizontal variation of resistivity) (Aizebeokhai, 2010). This type of array makes it the most preferred in mapping vertical structures like dykes and cavities. It is also the most desired in 3D structures among the other arrays (Dahlin & Loke, 2014; Riwayat *et al.*,

2018). A limitation associated with this array in the probing depth is its ability to be used to investigate shallow depth only (Dahlin & Loke, 2014).

Another electrode array configuration used in groundwater exploration is the pole-pole array configuration. This configuration uses one of the current and potential electrodes closer to the terrameter, while the other current and potential electrodes in a profile are placed at a greater distance (Aizebeokhai, 2010). In a survey, this type of electrode is known for its ability to withstand a telluric noisy environment. As a result, this electrode is known to have low resolution. It is also known for its greater horizontal distance coverage and greater depth of investigation (Aizebeokhai, 2010; Dahlin & Loke, 2014; Zainal Abidin et al., 2017; Kpiebaya & Abanyie, 2017). In areas with smaller places, the pole-pole array configuration may be preferred. Figures 2.4 to 2.8 represent the different electrode configurations.

Figure 2.4: Wenner Array

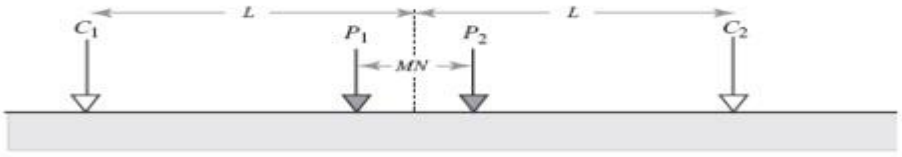

Figure 2.5: Schlumberger Array

Figure 2.6: Dipole-Dipole Array

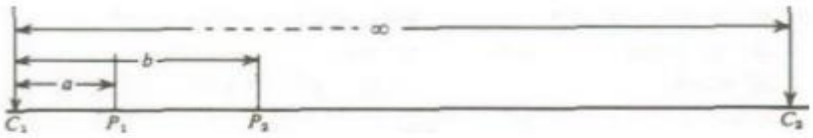

Figure 2.7: Pole-Dipole Array

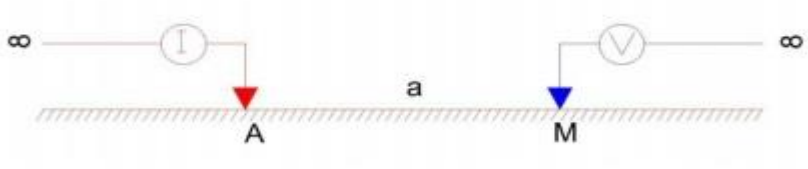

Figure 2.8: Pole-Pole Array

2.6.3 Application of the Electrical Resistivity Method

Electrical resistivity has been widely used in hydrogeological exploration (Chegbeleh et al., 2009; Riwayat *et al.*, 2018; Taha *et al.*, 2021), geotechnical (Abidin *et al.*, 2011; Gunn *et al.*, 2015), and mining investigation over the years (Peng & Han, 2020; Youssouf *et al.*, 2021). The use of this geophysical method improved the precision of hydrogeological and mining operations (Siena *et al.*, 2020). Electrical resistivity has recently been used in environmental surveys (Loke, 2001; Walsh, 2017). It is used in agricultural surveys for sounding (VES) to study lateral variation in soils to determine crop suitability (Gebbers & Lück, 2005; Ismailia & Rode, 2017). Furthermore, it was used in groundwater irrigated agriculture to map out zones of groundwater occurrence as well as study the soil for irrigation (Mohamaden *et al.*, 2016). ER methods are commonly used to locate potential

quarry mining sites (Abudulawal *et al.,* 2017; Mesbah *et al.,* 2017), detect buried metals (Liu *et al.,* 2020; Espindola-Canata *et al.,* 2020), map geological features (Kowalczyk *et al.,* 2017; Krietsch *et al.,* 2018; Sanuade *et al.,* 2018), and many other things (Peng & Han, 2020).

2.7 Groundwater Quality for Irrigation

Groundwater pollution has become the most challenging issue facing the world in recent times as a result of industrialization and urbanization (Umar *et al.,* 2009; Hassan Rashid *et al.,* 2018; Faroque & South, 2021). A number of factors contribute to the quality of groundwater existence (Bahri & Saibi, 2010; Liaqat *et al.,* 2021b): subsurface geochemical processes, precipitation, recharge water, and inland surface water (Chegbeleh *et al.,* 2020). The quality of groundwater has attracted global attention due to high-quality water demand for domestic and irrigation purposes (Siebert *et al.,* 2010). Groundwater quality parameters are classified into three types: physicochemical parameters, bacterial parameters, and trace metals (Yidana *et al.,* 2012; Bodrud-Doza *et al.,* 2020).

The physiochemical parameters, as the name implies, are the branches of chemistry that deal with the interrelationship between the composition and properties of matter (Belkhiri et al., 2010; Dehnavi, 2018). pH, Turbidity, Temperature, Total Dissolved Solids (TDS), Alkalinity, Turbidity, Temperature, Electrical Conductivity (EC), Total Hardness, Magnesium, Manganese, Nitrate, Zinc, Lead, Copper, Chromium, Calcium, Sulfate, and others are some of the chemical parameters that consist of some anions, cations, and trace metals (Dehnavi, 2018; Loh *et al.,* 2020; Ram *et al.,* 2021). Groundwater's physicochemical quality and temperature are relatively stable, and it can be consumed without even bacteriological treatment in some cases (Hoover *et al.,* 2017). Bacteriological

analysis, on the other hand, is a scientific method used to determine the number of bacteria present in a sample and whether it is safe for consumption or use. These bacteria are not only edible, but they also cause diseases that are extremely dangerous to human health (Yeleliere *et al.*, 2018). The Escherichia coli (E.coli) parameter is a subgroup of the group of the total coliforms that are commonly found in excreta (feces) (Yeleliere *et al.*, 2018). Total and Faecal Coliforms is another parameter found in feces but with no discernible differences.

Water's chemical composition changes as it moves through the aquifer due to dissolution, precipitation, ion exchange, concentration, and other chemical reactions (Bahri & Saibi, 2010). The chemical activity of the water, the aquifer, and the flow pattern contribute to the characteristic of groundwater. Groundwater is reported to have a low total dissolved solids content in recharge areas and a high total dissolved solids content in discharge areas (Kumar *et al.*, 2014). Only a few of the many solutes found in groundwater are present at concentrations greater than 1 mg/l under natural conditions (Abanyie *et al.*, 2020). Major ion constituents are those with concentrations greater than 10 mg/l while minor constituents are those with concentrations ranging from 0.01 mg/l to 10 mg/l, and trace elements are those with concentrations less than 0.01 mg/l (Abanyie e*t al.*, 2020).

A lot of studies have been conducted on the hydrochemistry of groundwater in recent years to determine its suitability for domestic and irrigational purposes (HARTINA, 2017; Kumar *et al.*, 2018; Etikala *et al.*, 2019; Chegbeleh *et al.*, 2020; Abanyie *et al.*, 2020; Oseke *et al.*, 2021). Early studies on the characterization of groundwater facies and chemical evolutionary history made use of graphical representations of groundwater's major ionic

composition (Kwoyiga & Stefan, 2018). Several studies including (Yidana *et al.,* 2012; Sahu & Sikdar, 2008; Umar *et al.,* 2009; Sadat-Noori *et al.,* 2014; Of *et al.,* 2008) have used Sodium Adsorption Ratio (SAR) and Water Quality Index (WQI) to determine the suitability of water for irrigation, domestic and drinking purposes.

Belkhiri *et al.* (2010) conducted a study on groundwater quality and its suitability for drinking and agricultural use in the Ain Azel plain, Algeria, and discovered that the dominant hydrochemical facies in the study area are Ca-Mg-HCO_3 and Ca-Mg-Cl-SO_4. In a study to assess the quality of groundwater for domestic and irrigation purposes in and around Gubrunde, Borno State, in north-eastern Nigeria. Arabi *et al.* (2012), confirmed that all the tests were under-saturated in calcite and aragonite, while most of the major anion and cations fall within World Health Organization and Nigeria Industrial Standard for Drinking water values. In general, the groundwater quality in the area was found to be adequate for agricultural and domestic use.

CHAPTER THREE

METHODOLOGY

3.0 Overview

This study sought to look at groundwater potential in the Sawla Tuna Kalba District in the Savannah Region of Ghana. It demanded an open and in-depth approach in delineating zones of high groundwater yield. This chapter deals with the description of the study area, research design, data source, research instrument for data collection, and data analysis.

3.1 Study Area

Sawla Tuna Kalba District (Figure 3.1) is one of the twenty (20) administrative districts of the Savannah Region of Ghana. It shares boundaries with Upper West Region to the North, Ivory Coast to the West, North and West Gonja to the East, and Bole Bamboo to the South. The total land area of Sawla Tuna Kalba is about 4601 Km^2 (http://sawlatunakalbadistrict.gov.gh/profile.html). The study area falls between latitudes 8^o 40′ and 9^o 40′ North and longitudes 1^o 50′ and 2^o 45′ west.

3.2 Topography and Drainage

The district is generally undulating in terms of relief. The altitude ranges between 400 to 800 ft. above sea level with the southern part being slightly flat and sloping gently towards the North. The Black Volta and its tributaries are the province's primary drainage system. This system impact is most noticeable in the district's northern reaches, which stretch from Gindabor to Jermakuraa. Because these locations are susceptible to flooding during the rainy season, they are ideal for rice farming (Loh *et al.*, 2020). The study area receives an average annual rainfall of 1050 mm, which is considered adequate for one agricultural

season. Temperatures are typically hot, averaging around 34 degrees Celsius (Loh *et al.*, 2020). The maximum temperature might reach 42°C, while the lowest could drop to 16°C. Cooler temperatures prevail from December to late February, when the North-East Trade Winds (harmattan) have a significant impact on the study area (Loh *et al.*, 2020). The extreme temperature, combined with the low humidity caused by the dry harmattan winds, encourage high rates of evaporation and transpiration, resulting in water shortages (https://en.wikipedia.org/wiki/Sawla-Tuna-Kalba_District).

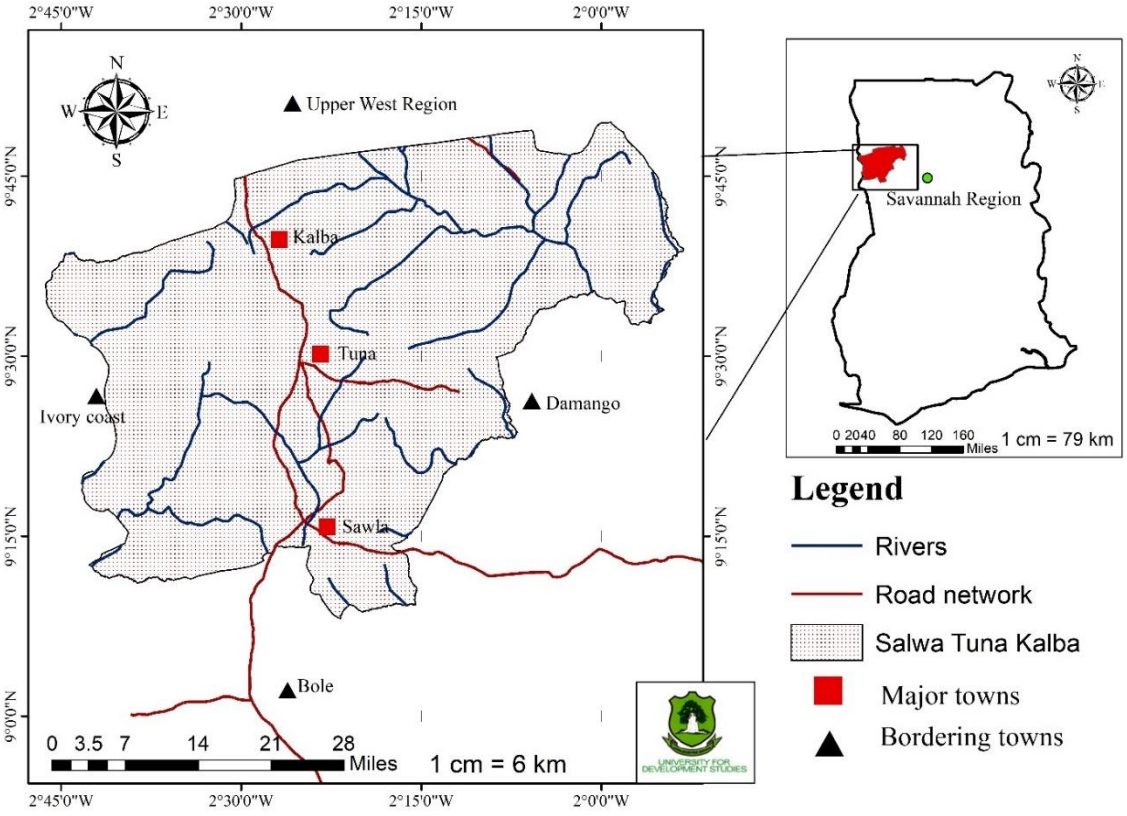

Figure 3.1: District Map of Sawla Tuna Kalba (Source; Author construct, 2021)

3.1.3 Geology and Hydrogeology

The Savannah Region falls within the Birimain and Voltaian basin which covers more than a third of the total area of Ghana. The Birimain formation is made up of Granitoids, Meta-

rocks, Phyllite, and many more while the Voltain formations consist of quartzite, shale, mudstone, siltstone, sandstone, and conglomerate or pebbly beds (William, 2013). Although there are areas of uniform lithology, interbedding of the different lithological units is a common geological feature of the basin as seen in figure 3.1.

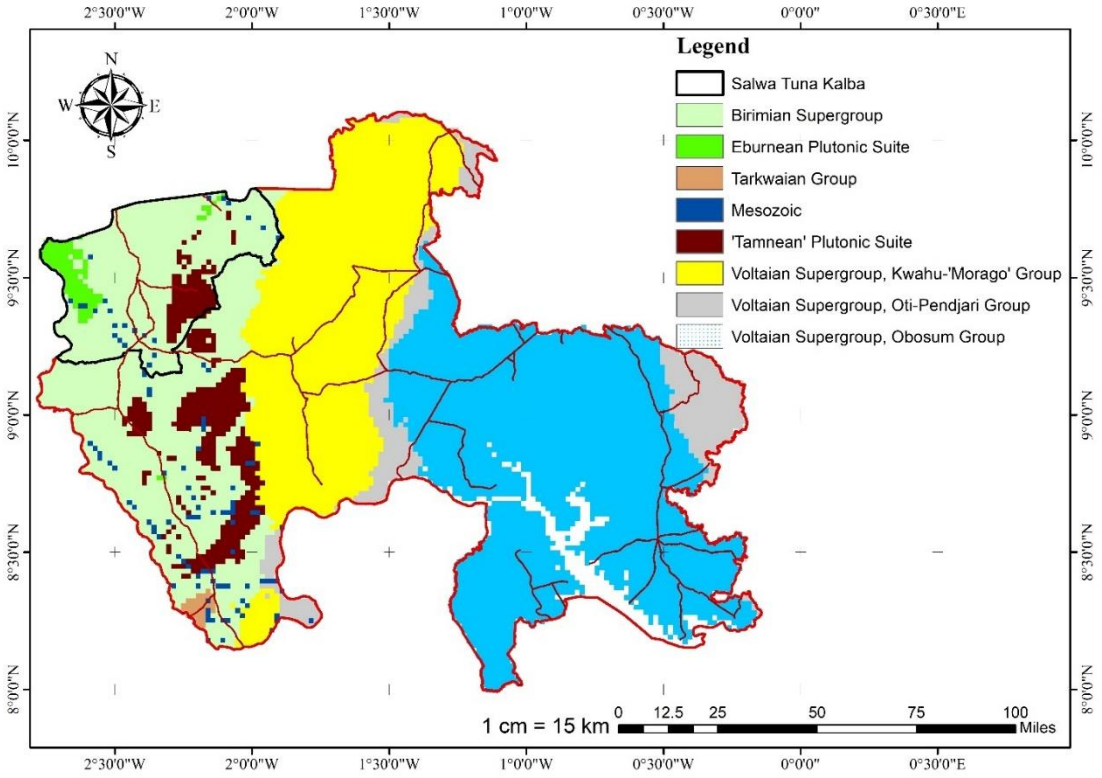

Figure 3.2: Geological map of the study area (Source; Author construct, 2021)

The study area encompasses more than one-third of Ghana's total land area, as seen in figure 3.1. The lithological cover within this basin is unique and distinct compared to other areas. The Birimian supergroup constitutes rocks of metavolcanics and metasediments but extends up to an area of 4047 Km^2. These very lithological units are evident in the towns of Damongo, Sawla, Laribanga, and Kulmasa along the major road linking the Savannah region to the Upper West region. The next geological unit after the Birimian supergroups in terms of the land area is the Eburnean plutonic suite, the Tarkwaian group, the Mesozoic,

and the Tamnean plutonic suite, which approximately have a land area of around 252 Km^2, 284 Km^2, 18 Km^2, and 3 Km^2 correspondingly. The latter combined units make up about 557 Km^2, which is more than the Obusum group. These units' ancestry is of volcanic activities and hence consist of metavolcanic units (Bruce *et al.*, 2009).

3.2 Materials and Methods

3.2.1 Field Data Collection

First and foremost, this research considered nine (9) communities for the assessment namely; Monah, Yipala, Sindaa, Korle No. 2, Cbaalyiri, Sawla yipala, Gbenyiri, Chanbalayiri, and Kaawie. These communities were selected based on groundwater potential and agricultural activities during the reconnaissance. The field data collected were primarily resistivity data using the the ABEM Terrameter. Vertical Electrical Sounding is a method used in determining a geolical medium as used in this study. The Schlumberger and the dipole-dipole arrays were often preferred for vertical soundings which were to measure variations in apparent resistivity with depth (Samouëlian *et al.*, 2005). In this research, two different arrays method were used in achieving the intended objectives (ie dipole-dipole and Schlumberger configuration array) as discussed sections 3.2.1.1 and 3.2.1.2.

3.2.1.1 Dipole-Dipole Configuration Array

The choice of a given array relied largely on the objective and accuracy of the results. Dipole-Dipole electrode array has proven to be an accurate groundwater-finder array (Yidana *et al.*, 2013) and hence was employed in this study. It was used in the delineation of groundwater points for future irrigation projects, studying aquifer properties and

describing the hydrogeological environment (Omolaiye *et al.,* 2020). The configuration depicts exactly the array arrangement used in the field (Figure 3.3) with the corresponding equation for calculating resistivity (Equation 3.1).

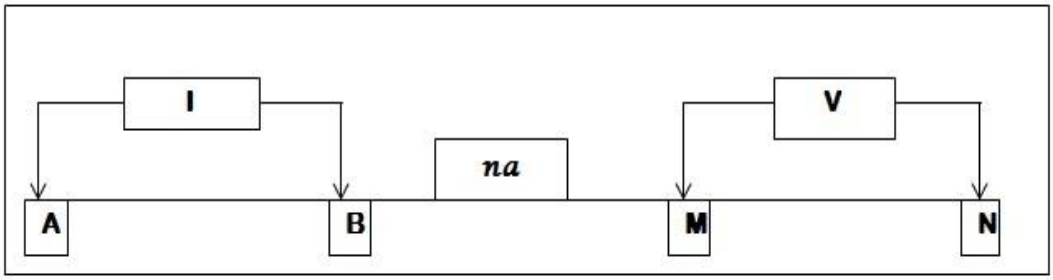

Figure 3.3: The Dipole-Dipole array configuration used for groundwater delineation (Source; Author construct, 2021)

$$R = n(n+1)(n+2)\alpha\frac{\Delta V}{I} \qquad (3.1)$$

MN = distance between potential electrodes (m), AB = distance between current electrodes (m), ΔV = Potential Difference (volts) and I = applied current, n = formation factor

For groundwater delineation, coordinates of high groundwater yields were picked and marked during the geophysical survey. The dipole-dipole array configuration showed in figure 3.3 was used in picking groundwater resistivity while the apparent resistivity was computed using the geometric factor (K). The survey was conducted at an average distance of about 1 Kilometer, readings was picked at 5 m to 10 m interval (profile interval). The data were analyzed using the Microsoft Excel sheet package; it was used to plot resistivity values against each profile interval. Areas of low resistivity and field experience played a huge role in choosing points for drilling purposes for future groundwater irrigation decision-making and other decision-making as well.

3.2.1.2 Schlumberger Configuration Array

The Schlumberger configuration and equation applied for the study are shown in figure 3.4 and equation 3.2. For each VES point, the length between potential electrodes MN was gradually increased in steps starting from 5 m to a suitable distance according to the geometrical factor (K). The half current electrodes separation (AB/2) was also increased in steps starting from 1 to 300 m and 400 m depending on the required depth of penetration. The essence of the Schlumberger configuration to study the geogical formation in the study area. This array was able to yield resistivity values stratigraphically to profile the regolith, lithological characterization, study clay-panning, consolidated sediments, and waterlogging (Gebbers & Lück, 2005; Ismailia & Rode, 2017).

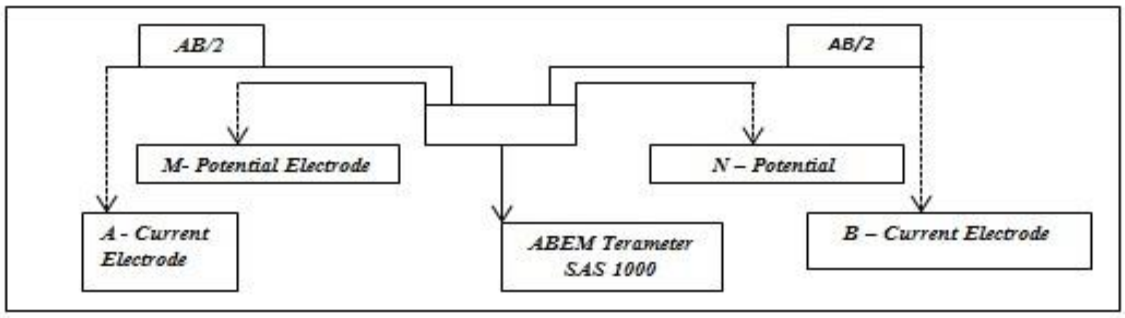

Figure 3.4: The Schlumberger configuration used for the VES(Source; Author construct, 2021)

$$\rho = \left\{ \frac{\frac{(AB)^2}{2} - \frac{(MN)^2}{2}}{MN} \right\} \Delta \frac{V}{I} \qquad (3.2)$$

MN = distance between potential electrodes (m), AB = distance between current electrodes (m), ΔV = Potential Difference (volts) and I = applied current

3.3.1 Geophysical Analysis and Presentation

In this context, resistivity data were modeled to generate 1-D and 2-D curves with the use of the inversion model in IPI2wins and IPI_res3 software packages respectively. This software produces a diagrammatic lithological and regolith profiles describing and naming each profile with its respective resistivity value. Furthermore, data collected to the Vertical Electrical Sounding (VES) were imported into the software package; the spreadsheet containing the data includes depth of investigation, resistivity, and apparent resistivity. The lithological profiles that were produced were compared to the lithological diagram (resistivity versus geology) for naming as seen in figure 3.5. The lithological profile in combination with the resistivity graph shows variation in apparent resistivity.

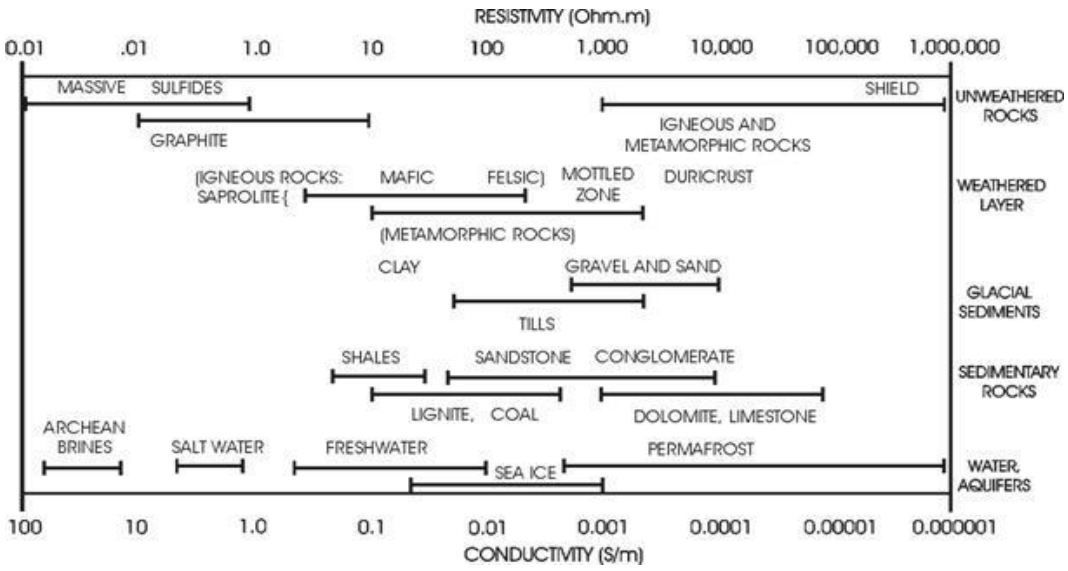

Figure 3.5: Resistivity versus geology (Gunn et al., 2015)

3.3.2 Groundwater potential mapping

Remote sensing and GIS data from Earth Explorer, Soil Grids, and Earthdata were used collaboratively to obtain data on past, present, and future activities such as vegetation, weather patterns, water resources, land use, and natural vegetation. This data was gathered

to provide a more thorough explanation of the land use pattern and its relationship to groundwater (Elmahdy *et al.,* 2020). Data obtained from the United States Geological Survey (USGS) department website (www.usgs.earthexplorer.gov) included Landsat 8 (OLI) imagery with a resolution of 30 m × 30 m and a Digital Elevation Model (DEM) with a resolution of 30 m. Soil information was downloaded at a resolution of about 250 m from the SoilGrid website (ISRIC.ORG), and lithology was processed from an existing geological shapefile. Data on rainfall was obtained from the Earthdata website (www.nasa.gov). The data covered a three-year period, from 2017 to 2019. Using the arctool box in Arcmap 10.3, the individual images were composited into a single image and masked using the shapefile of the study area. For this study, Landsat 8 (OLI) was used to generate a Land Use Land Cover thematic map (LULC) and a Lineament density map. A slope and drainage density map was created using the DEM dataset.

A supervised classification algorithm in ArcGIS was used to identify and classify the image into forest areas, vegetation, settlements, agricultural lands, wetland, and waterbody. In this perspective, forest areas are classified premised on trees that grow very close together and form a very thick canopy, where most lumbering and hunting takes place. Vegetation fills in areas where different plant species grow in the absence of a tree canopy. Over time, some of these areas may develop into farmland or settlements. Settlements are areas where people live in either urban, rural, or farming settlements. Wetland includes waterlogged areas and flood-prone areas, whereas agricultural land includes farmland, irrigational land, and animal stocking. Waterbodies include rivers, streams, dams, and dugouts.

The lineament map was created in ArcGIS 10.3 using the hillshade function and the Azuthimal combinations (315-45), (200-50), (160-60), and (50-90). After hillshading, the fractures become more readily apparent. The fractures are then drawn with the editor keys, and the fracture density was then developed. The total length of lineaments per unit area in Kilometer square (Km/Km^2) is simply the lineament density (Magesh *et al.,* 2012). To generate the appropriate density map, the study area was modeled based on flow direction, stream accumulation, stream feature, and stream order. Also, using the shapefile of the study area and the extraction tool in ArcMap 10.3, the soil map was masked from downloaded data to fit the study area. For further analysis, the individual thematic maps were reclassified into five (5) classes using equal internals. Overlay analysis and ranking were performed on these reclassified thematic maps using the weighted overlay tool in ArcGIS 10.3. The end product was a map showing the groundwater potential within the study area. Figure 3.6 indicates the source of data and the processes involved in developing groundwater potential map.

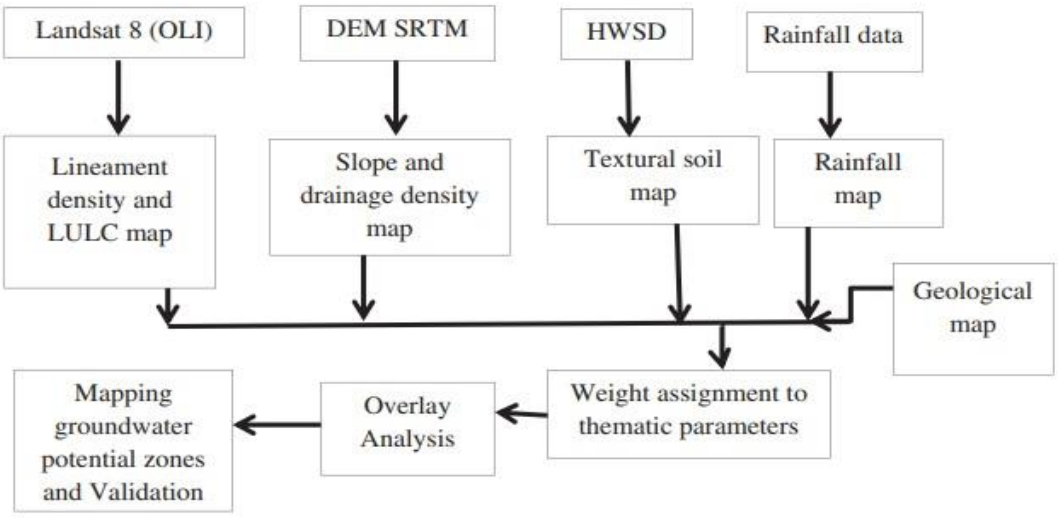

Figure 3.6: Flowchart for developing groundwater potential map (Adapted from Tolche, 2020)

3.4 Groundwater Storage Estimation

Groundwater storage estimation was done by taking stratigraphic samples from each drilling process every 5 meters of depth into the rock. The procedure facilitated the investigation and correlation of rock types with geophysical survey results. The stratigraphic samples assisted in detecting the aquifer's structure as well as any aquifer-related properties. Groundwater drilling equipment and methodologies range by desired purposes, geotechnical state of the studied region, and producer (Abdul-ganiyu & Prosper, 2020). Air drilling is the predominant way of boring in Northern Ghana, hence the Indian Drill Rigs (Ashok) and German Rigs are specifically developed for this. The data collected during the drilling phase were important in calculation of some parameters for characterizing the groundwater in the study area. This equation has been used recently by (Anornu *et al.,* 2009; Abdul-Ganiyu & Prosper, 2021) to calculate the storage capacity in the Northern Region of Ghana. Fundamentally, the data collected includes; the number of successful and unsuccessful boreholes, water depth, depth of water-strike, and many more.

Equations 3.3a and 3.3b (Schoeller, 1967) were employed to simulate water storage capacity and recoverable storage inside the reservoir.

$$Q_s = (P - \%) \times \emptyset \times H \times A \qquad 3.3a$$

Where Total Groundwater Storage (Q_s) = Percentage of Groundwater Coverage (P-%) x Effective Porosity (Ø) x Saturation Depth (H) x Extent of Study Area (A)

But Porosity $(\emptyset) = {}^{V_t}/_{V_v}$ *; V_v is the void volume and V_t is the total volume of unconsolidated material (Bear, 1979).*

$$Q_e = (P - \%) \times S_y \times H \times A \qquad 3.3b$$

Extractable Groundwater (Q_e) = Percentage Groundwater Coverage (P-%) x Specific Yield (S_y) x Saturation Depth (H) x Extent of Study Area (A).

Where, $S_y = {}^{V_{wd}}/_{V_t}$ *, Where V_{wd} is the volume of water drained and V_T is the total rock or material volume (Bear, 1979).*

3.5 Crop Water Requirements

This element is frequently computed in the presence of climatic data, crop data, and soil data, but in the absence of climatic data, empirical equations can be used to approximate the water requirements of the crops (Hargreaves *et al.*, 1985). The product of reference crop evapotranspiration and crop coefficient yields is the generally accepted equation for computing Crop Water Requirements (CWR) as in equation 3.4.

$$CWR = ET_0 \times Kc \qquad 3.4$$

Allen *et al.* (1994) developed an empirical equation that is now widely accepted and used by researchers. The equation was created by assuming a well-defined hypothetical reference crop with a crop height of 0.12 m, a canopy resistance of 70 sm^{-1}, and albedos of

0.23. As stated previously the lack of reliable meteorological information prompted Hargreaves et al. (1985) and Hargreaves (1994) to derive a function that is based on mean daily maximum and mean daily minimum, humidity and precipitation shown in equation 3.5.

$$ET_0 = 0.0023 \times 0.0408RA \times (T_{avg} + 17.8).TD^{0.5} \qquad 3.5$$

Where RA is extraterrestrial radiation expressed in ($MJm^{-2}d^{-1}$), T_{avg} is the average daily temperature (^{O}C) which is the average of the mean daily maximum and mean daily minimum temperature, and TD is the temperature range.

However, the use of CWR as the main parameter in computing the available irrigable area using the groundwater storage capacity was not fully appreciated due to overestimation during the period of cultivation. The irrigation water requirement was introduced to realistically ascertain the total irrigable area. Equation 3.6 depicts the relationship between CWR and IR

$$IR = CWR - (Effective\ rainfall + Groundwater\ contribution) \qquad 3.6$$

Moving forward, the absence of climatic data prompted the use of 20 % additional CWR to upscale the current CWR to represent IR to appreciate the quantity of water that can be abstracted for irrigating tomatoes and maize.

3.6 Determination of water quality

3.6.1 Water Sample collection

To determine the quality of water for domestic and agricultural purposes, water samples were taken from 120 boreholes in the study area for quality tests and analysis. During sample collection, the sampling protocols proposed by Loh *et al.* (2020) and Pandey *et al.*

(2020) were adopted. Acid-washed high-density linear polyethylene (HPDE) vials of 100 ml were used to collect water samples. Purification with a Sartorius polycarbonate filtering apparatus and a 0.45-m cellulose acetate filter membrane was used to remove contaminants from samples. After filtration, the samples for cation studies were promptly acidified to a pH of 2 using sodium acetate, whereas those for anion assays were not preserved. The samples were collected and GPS coordinates of the boreholes were taken with a GPS (GPSMAP 64s).

3.6.2 Laboratory Analysis of water samples

All major ions (Na^+, K^+, Ca^{2+}, Mg^{2+}, HCO_3^-, Cl^-, SO_4^{2-}), as well as minor elements, such as NO_3^-, and F^-, were analyzed using Dionex DX-120 ion chromatograph at the water quality laboratory (World Vision Ghana). The difference between the optimal analysis results and the cation-anion difference should be less than 5% (Appelo and Postma 2005). Following that, any sample that did not meet the Ion Balance Error (IBE) norm of 5% was ruled out of consideration for this study. This was computed using equation 3.7. Fortunately, all hundred and twenty samples fell within the IBE's tolerance of 5%.

$$IBE = \frac{\sum cations - \sum anions}{\sum cations + \sum anions} \times 100 \ldots\ldots\ldots\ldots\ldots (3.7)$$

The groundwater quality parameters investigated included potential hydrogen (pH), electrical conductivity (EC), sodium absorption ratio (SAR), total dissolved solids (TDS), total hardness (TH), magnesium hazard (MH), and residual sodium carbonate (RSC). Sodium (Na), potassium (K), magnesium (Mg), and calcium (Ca) are major cations, while chloride (Cl), sulfate (SO4), and chloride (Cl) are major anions (HCO3). An atomic absorption spectrophotometer (AAS) was used to measure major cations, while an

ultraviolet spectrophotometer (UV) was used to measure major anions, and titration process was used to measure bicarbonate. Based on previous research, various water quality measurements were performed to assess and classify the quality of groundwater suitability for domestic and agricultural (especially irrigation) purposes (Todd & Mays 2005; Anku *et al.*, 2009; Arumugam & Elangovan, 2009; Yidana *et al.*, 2012). Equations 3.8 to 3.12 were used to calculate various irrigation water quality parameters.

$$Sodium\ absorption\ ratio\ (SAR) = \frac{Na^{+}}{\sqrt{\frac{1}{2}\ [Ca^{2+} + Mg^{2+}}} \ldots\ldots\ldots\ldots\ldots (3.8)$$

$$Residual\ sodium\ carbonate(RSC) = [CO_3^{2-} + HCO_3^{-}] - [Ca + Mg] \ldots\ldots\ldots\ldots.. (3.9)$$

$$Potential\ Salinity\ (PS) = Cl^{-} + \sqrt{SO_4^{2-}}. \ldots\ldots\ldots\ldots. (3.10)$$

$$Kelly\ Ratio\ (KR) = \frac{Na^{+}}{[Ca^{2+} + Mg^{2+}]} \ldots\ldots\ldots\ldots. (3.11)$$

$$Magnesium\ Hazard\ (MH) = \frac{Mg^{+}}{[Ca^{2+} + Mg^{2+}]} \times 100 \ldots\ldots\ldots\ldots. (3.12)$$

3.7 Geospatial modeling of groundwater quality for agriculture

Several interpolation methods have been used by various authors to create groundwater suitability maps for agricultural use (Chaudhary & Satheeshkumar, 2018; Chegbeleh *et al.*, 2020; Rawat *et al.*, 2018; Tolche, 2020). In this study, the Inverse Distance Weight (IDW) and kriging methods were used. ArcGIS 10.8 was the primary analysis package used to perform IDW and kriging. These models provide the opportunity to visualize the various quality parameters spatially.ArcGIS 10.8 software was used to create spatial distribution maps for TDS, SAR, RSC, EC, MH, PS, and Kelly's Ratio (KR). These thematic maps

were superimposed onto a single map using the weighted overlay model to create an irrigation suitability map. Individual thematic maps, on the other hand, were reclassified into five equal interval classes and then used for the overlay analysis. Following that, thematic layers were ranked by assigning a weight to each layer that added up to a total of 100 %. The science behind ranking is the weighting of the most influential water quality parameter that ascertains the functionality of an irrigation scheme that uses groundwater as its source.

CHAPTER FOUR

RESULTS AND DISCUSSION

4.0 Overview

The findings from this study are presented in this chapter. The results of this research are presented in a figure and tables followed by interpretation and discussions.

4.1 Vertical Electrical Sounding (VES) in the Sawla Tuna Kalba District

The underlying geological formation around the Sawla catchment (Monah, Yipala, Sindaa, Korle No. 2, Cbaalyiri, Sawla yipala, Gbenyiri, Chanbalayiri, and Kaawie) was investigated using geophysical techniques, specifically Schlumberger configuration. The Schlumberger configuration was purposely deployed on the field to study the lateral variation within the near-surface geology. The communities in the next subsections below were where the survey was conducted and the results are presented based on these communities.

4.1.1 Geological formation of Korle No. 2

This survey was conducted in Korle No.2 (09.27659 ^{o}N, 02.55633 ^{o}W). From the pseudo-sectioning (Figure 4.1 and 4.1.1), it was revealed that the VES was up to 600 m (profile length) and had a probing depth of up to 100 m. The first layer of 5 m showed a resistivity range of 1166 Ωm – 1585 Ωm indicating a thin layer of gravel or preferable laterite. This layer is characterised as the overburden or the regolith containing the loose materials in the formation. The apparent resistivity dropped to 251 m – 464 m in the formation's second layer, which had a depth thickness of 35 m. The range of resistivity may suggest the presence of felsic rocks which may be in the form of shale and partly sandstone in nature

which may indirectly impact the quality (acidic) of groundwater (Yidana *et al.,* 2012). Zones of low resistivity are often footprints of groundwater occurrence (K *et al.,* 2020; Mesbah *et al.,* 2017; Riwayat *et al.,* 2018); hence the third layer had the lowest resistivity ranging from 29.3 Ωm – 39.8 Ωm which is similar to Abidin *et al.* (2017) findings in the work reveal that apparent resistivity ranging from 10 – 100 Ωm show presence of groundwater and clay deposit in Peninsular Malaysia. The bedrock is 40 m thickness with an apparent resistivity between 5412 Ωm – 7356 Ωm indicating the presence of metamorphic rocks. This kind of rock has undergone compaction and cementation through heating over geologic time (Abidin *et al.,* 2017). These results are however consistent with studies of (Vanella *et al.,* 2021; Ganiyu *et al.,* 2020)

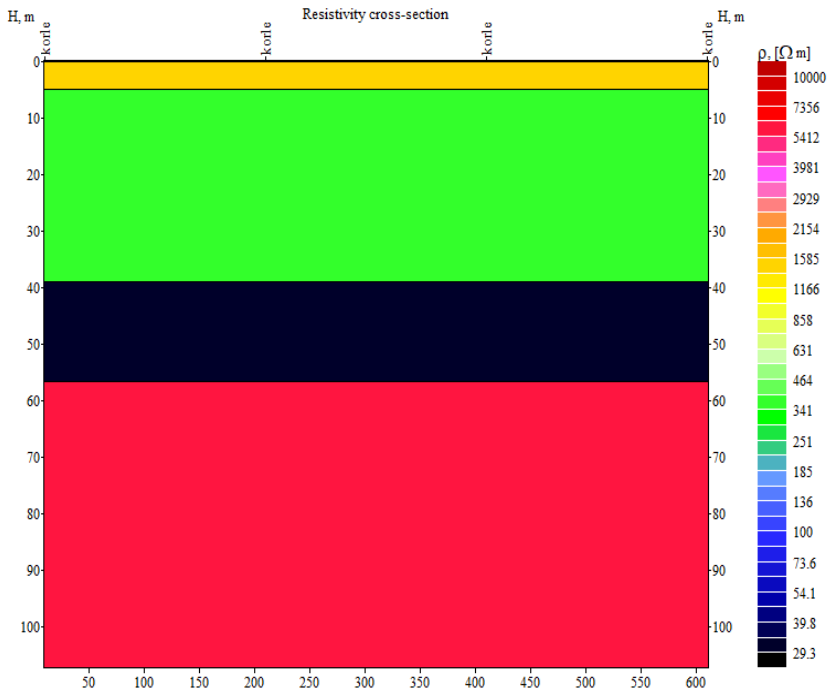

Figure 4.1 Pseudo-section of lithology at Korle No.2

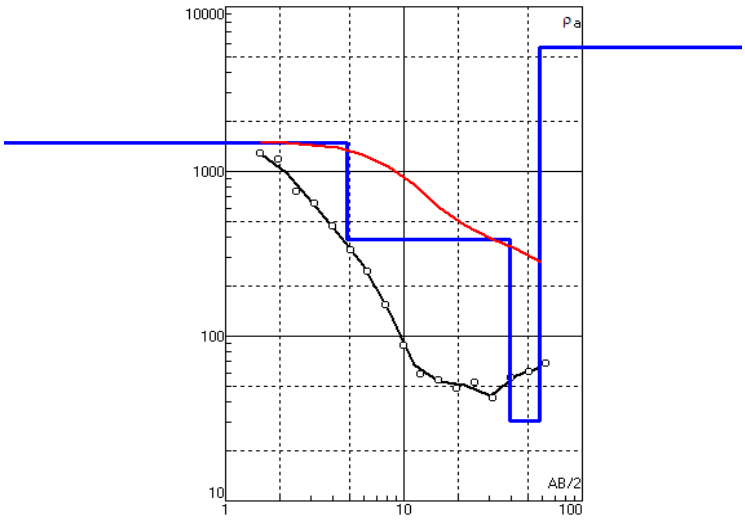

Figure 4.1.1 apparent resistivity curve of Korle No.2

4.1.2 Geological formation of Chanbalayiri

The pseudo-section for Changbalayiri (09.26754 ^{O}N 02.42383 ^{O}W) locality is displayed in Figures 4.2 and 4.2.1. The VES survey was carried out within 100 m (probing depth). The first geo-electric layer is a thin lithology of laterite with an overburdened thickness of about 4 m and resistivity around 6579 Ωm. A thin layer of laterite usually indicates that it has been formed as a result of deposition (Manyu *et al.,* 2018). The apparent resistivity for the second geo-electric layer runs from 100 Ωm-231Ωm which may suggest the existence of mafic to felsic rock (either sandstone or shale) as reported in the study by Cheng *et al.* (2019) in a study in the karst regions of southwest China reveal that apparent resistivity ranging from 150 Ωm – 300 Ωm suggest the presence of shale. The third layer has a thickness of 10 m with a resistivity between 5.34 Ωm – 12.3 Ωm confirming the zone of groundwater occurrence (Abdul-Ganiyu & Prosper, 2021; Riwayat et al., 2018). It is, however, not surprising that the Sawla Tuna Kalba district has an average water strike and hence, it is possible that at a depth of 12 m, groundwater exploration can take place. The

fourth layer has a thick bedrock of resistivity around 6579 Ωm, which could be 37 m of igneous rock like granite, according to Sikandar & Christen, (2012).

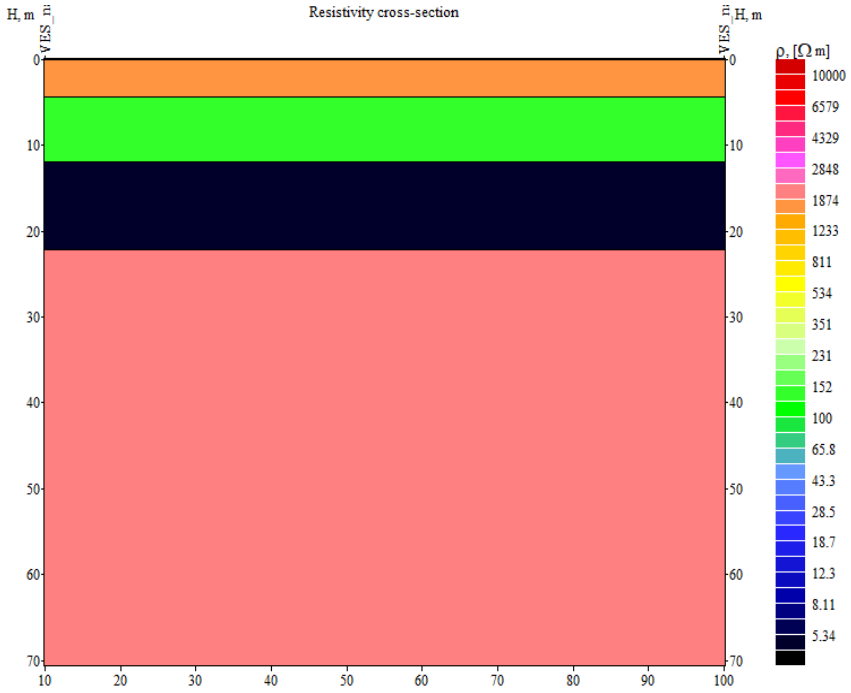

Figure 4.2 pseudo-section of lithology at Chanbalayiri

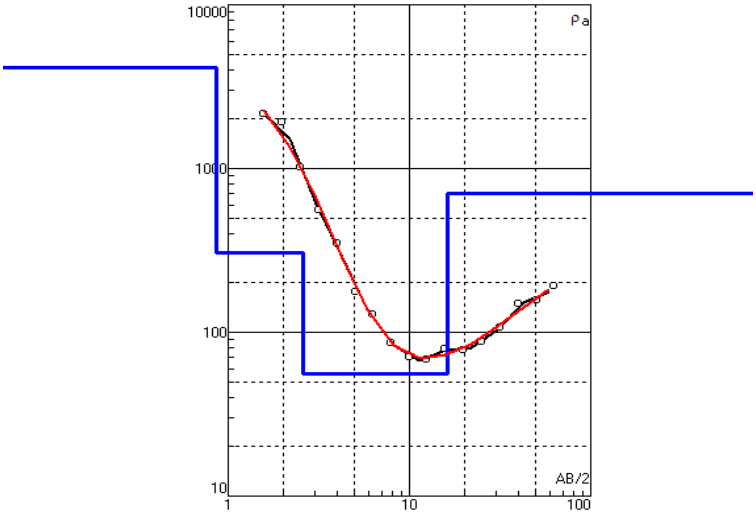

Figure 4.2.1 apparent resistivity curve of Chanbalayiri

4.1.3 Geological formation of Cbaalyiri

Cbaalyiri located on 09.47072 ^{o}N, and 02.6155 ^{o}W is one of the communities where the VES survey was carried out. The lithological variation can be described in four geoelectric layers (Figure 4.3 and 4.3.1). The first layer being the loose material (overburden) with a thickness of 5 m and an apparent resistivity between 351 Ωm – 811 Ωm which might be a cover of lateritic material (Cheng *et al.,* 2019). The preceding geo-electric layer had an apparent resistivity around 65.8 Ωm which showed a shale formation of about 4.5 m thickness. The third layer has a thickness of 6.5 m and a resistivity between 5.43 m – 28.5 m, which still forms part of the shale formation. This kind of formation does not exist in the province of a confined aquifer but shows the presence of a perched aquifer (Sahu & Sikdar, 2008). The final geo-electric layer thickness is about 13 m and has an apparent resistivity of 1874 Ωm. The apparent resistivity for the fourth layer is metamorphic, accounting for the thin covering of shale around the second and third layers. This analysis suggests that metamorphic formation may contain high pressured groundwater because of high atmospheric conditions, it will pose a good quality of metamorphic rocks that are impervious and hence unsusceptible to contamination (Anornu *et al.,* 2009).

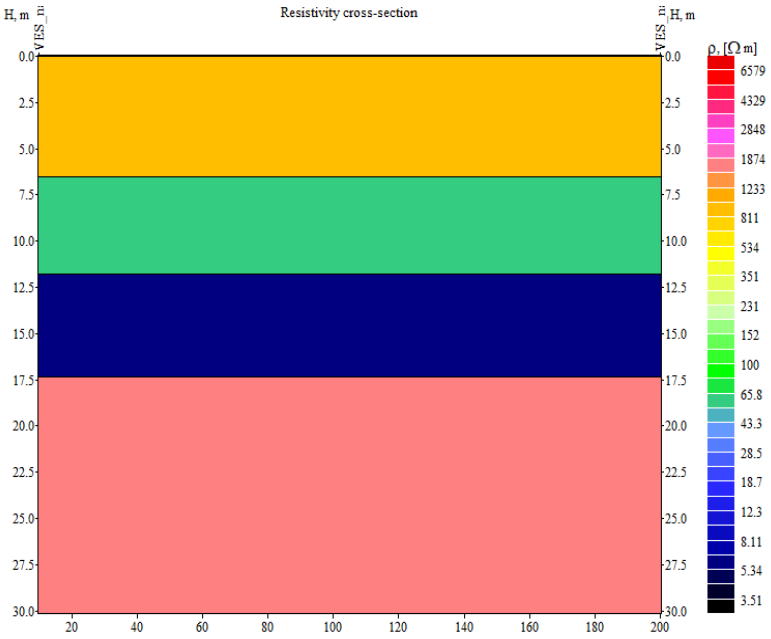

Figure 4.3 pseudo-section of lithology at Cbaalyiri

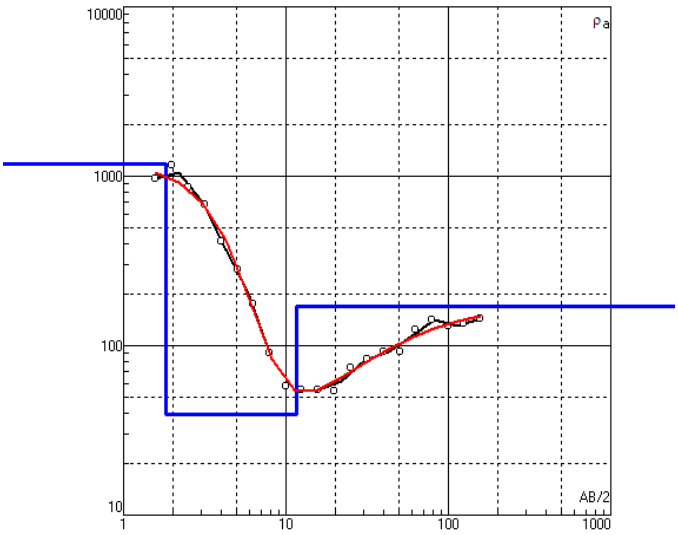

Figure 4.3.1 apparent resistivity curve of Cbaalyiri

4.1.4 Geological formation of Monah

The profile length for Monah (09.32197 ^{O}N, 02.43130 ^{O}W) was 240 m. This comprised four sounding points (VES) as seen in Figures 4.4 and 4.4.1. This was because the surface within the profile line has a massive rocky layer. That is why part of the pseudo-section

appears to be the same color throughout the formation. The other pseudo-sections showed the same formation but are different from the massive rock surface. The first geo-electric layer is a thin cover of lateritic material having an apparent resistivity between 390 Ωm – 593 Ωm and a thickness of 3.5 m which is similar to the findings of Sikandar & Christen. (2012) and Manyu *et al.* (2018). The layer is made up of semi-thick metamorphic rock rocks which might constitute shale or sandstone. This metamorphosed rock has a thickness of about 7.5 m and an apparent resistivity between 1369 Ωm – 1688 Ωm. The third geo-electric layer has a resistivity values range of 39.0 Ωm – 48.1 Ωm and a depth thickness of 18.5 m. Considering the range of resistivity values, this could be considered as a water-bearing formation (shale formation) which is consistent with studies of Swileam *et al.* (2019) and Vanella *et al.* (2021).

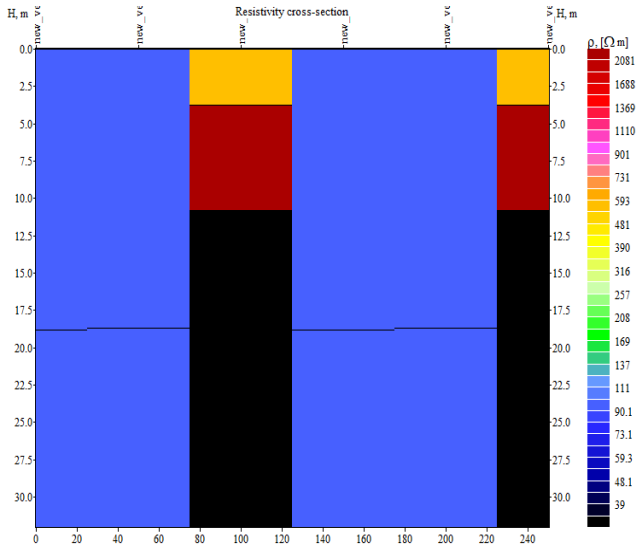

Figure 4.4 pseudo-section of lithology at Monah

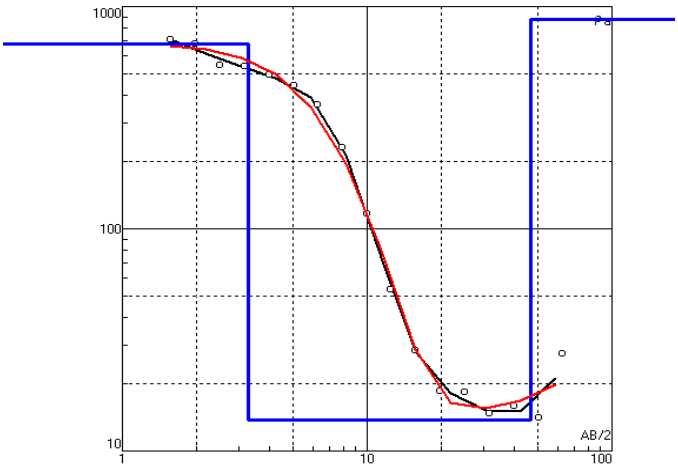

Figure 4.4.1 apparent resistivity curve of Monah

4.1.5 Geological formation of Kaawie

Kaawie located on 09.28683 ^{O}N and 02.5839 ^{O}W is among the communities in which the VES was carried out. The pseudo-section produced is shown in figures 4.5 and 4.5.1. The first geo-electric layer has apparent resistivity between 1179 Ωm-1638 Ωm with a thin cover of either lateritic or gravel of 3 m. The second geo-electric layer shows an apparent resistivity which runs from 316 Ωm – 439 Ωm and has a thickness of 11 m similarly to that found by Vanella *et al.* (2021) in a study Italy found that apparent resistivity from 300 Ωm to 500 Ωm may indicate the occurrence of groundwater in the upper layer of the geological formation. The range of resistivity indicates that the formation constitutes mafic to felsic rock materials. Even though the overlying layer might be hard, the underlying might be a fractured water-bearing rock with a thickness of 10.5 m (Duc Vu et al., 2021; El-Gawad et al., 2018; Kpiebaya *et al.,* 2021). The apparent resistivity of this water-bearing formation is 31.6 Ωm – 43.9 Ωm (Sahu & Sikdar, 2008). This zone of possible groundwater occurrence may be either high or low yielding depending on the fractures available. Therefore, an in-depth geophysical investigation may be required to harness the resource. The final layer has a thick and hard bedrock with an apparent resistivity of 4394 Ωm –

8483 Ωm and a thickness of 25 m - 80 m. The bedrock might be a metamorphosed rock considering the range of resistivity indicating the possibility of good quality groundwater and high groundwater occurrence. Results from this research are in accordance with the results of a study by Ganiyu *et al*. (2020) in Abeokuta, Nigeria.

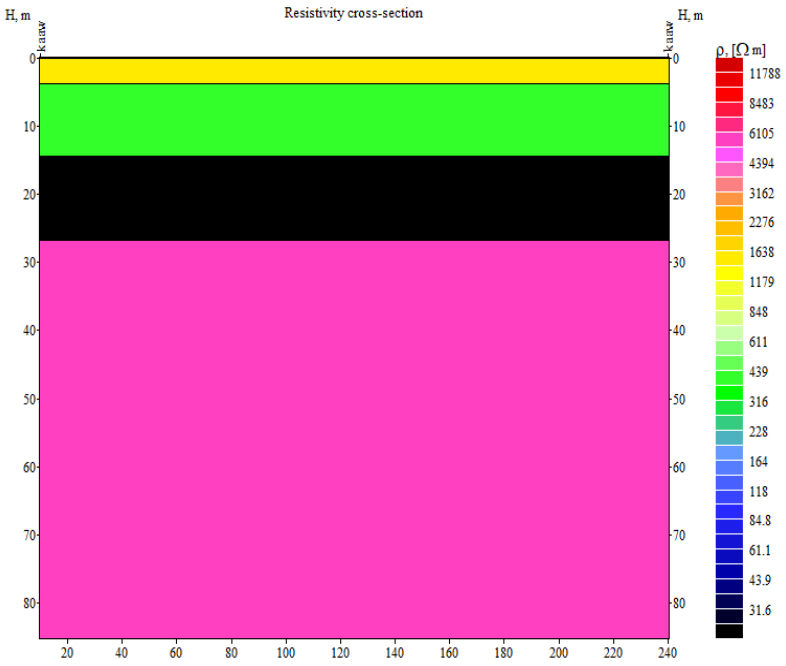

Figure 4.5 pseudo-section of lithology at Kaawie

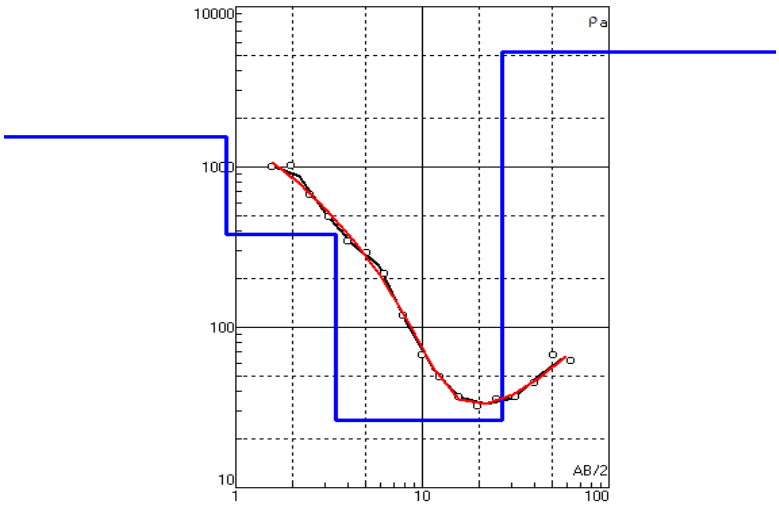

Figure 4.5.1 apparent resistivity curve of Kaawie

4.1.6 Geological formation of Yipala

The VES was conducted at Yipala (09.573084 ^{O}N, 02.4144 ^{O}W) but within this pseudo-section there exist two distinct sounding points clearly illustrated in figure 4.6 and 4.6.1. The first VES point has a thick overburden of about 45 m while the second VES point has a thin overburden of less than 5 m. The apparent resistivity ranges from 100 Ωm – 172 Ωm of a probable mixture of gravel, loose sand, or laterite. The geo-electric layer for the first VES is a semi-thick layer of mafic to felsic rock materials. The second geo-electric layer in the second VES point is also a thick layer of metamorphic strata of less than 2.5 m with an apparent resistivity of about 1968 Ωm. The third layer is of thick nature (31 m) with resistivity ranging from 296 Ωm – 508 Ωm which might contain shale, sandstone, siltstone, or mudstone. The fourth geo-electric layer may be the water-bearing formation with low apparent resistivity of about 19.7 Ω. This pseudo-section demonstrates why two wells were drilled at 20 m intervals and one has high yielding while the other was completely dry in the area. These findings are not completely different from previous studies by others (Swileam *et al.*, 2019; Ganiyu *et al.*, 2020).

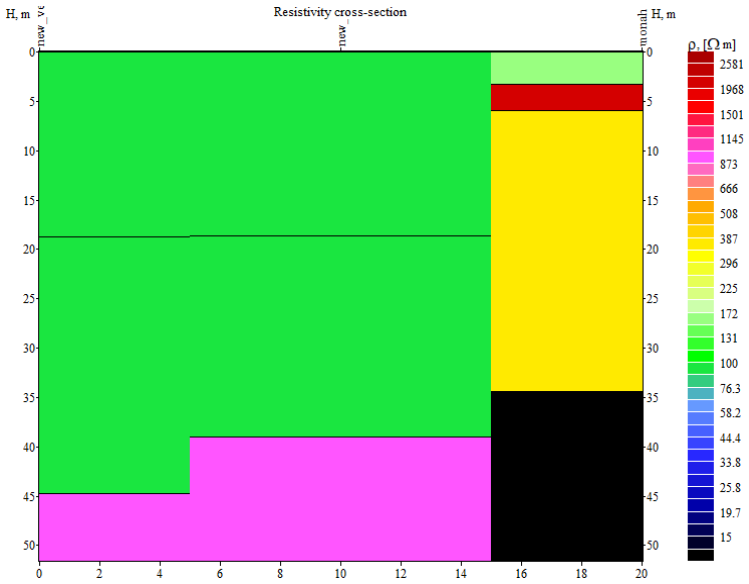

Figure 4.6 pseudo-section of lithology at Yipala

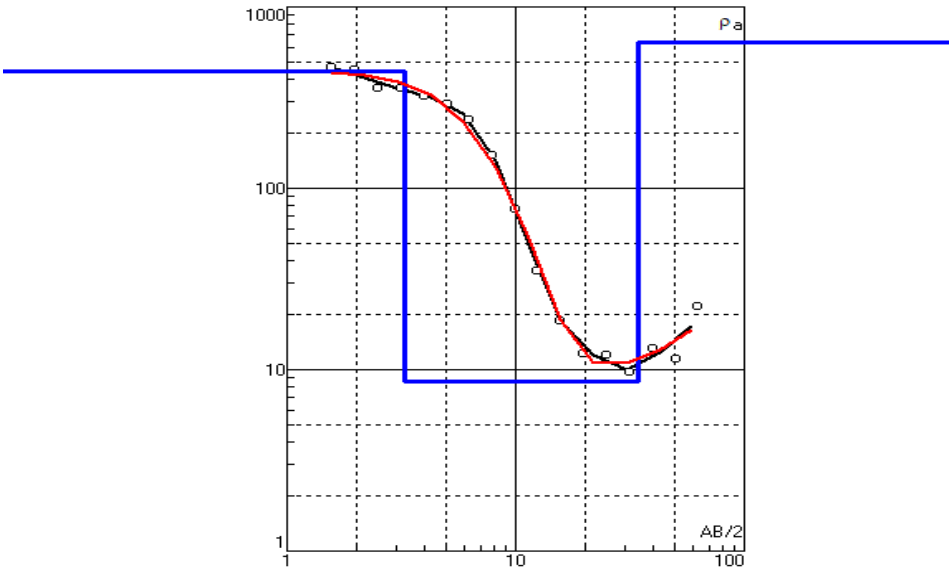

Figure 4.6.1 apparent resistivity curve of Yipala

4.1.7 Geological formation of Sindaa

The profile length for the survey in Sindaa (09.47001 ^{O}N, 02.61527 ^{O}W) was 200 m as shown in figures 4.7 and 4.7.1. This community shows a high surface water table (Sahu & Sikdar, 2008; Bayewu *et al.*, 2018). That is why the IPI2wins produced a pseudo-section

of 5.5 m. The first and second geo-electric layers of about 3.75 m with a resistivity of 178 Ωm – 316 Ωm are suspected to be of clay and weathered formation which is consistent with (Manyu *et al.*, 2018). The third and fourth geo-electric layers are also suspected to be loosed and weathered formations that might be of metamorphose or felsic origin. That is why it records low resistivity of about 31.6 Ωm. The indication of low resistivity brings to light the occurrence of groundwater hence the surface water table.

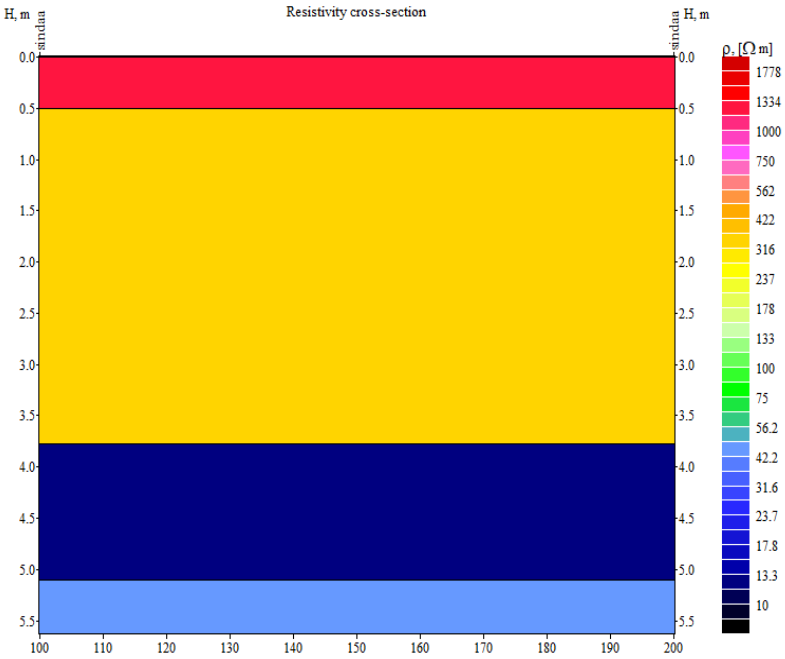

Figure 4.7 pseudo-section of lithology at Sindaa

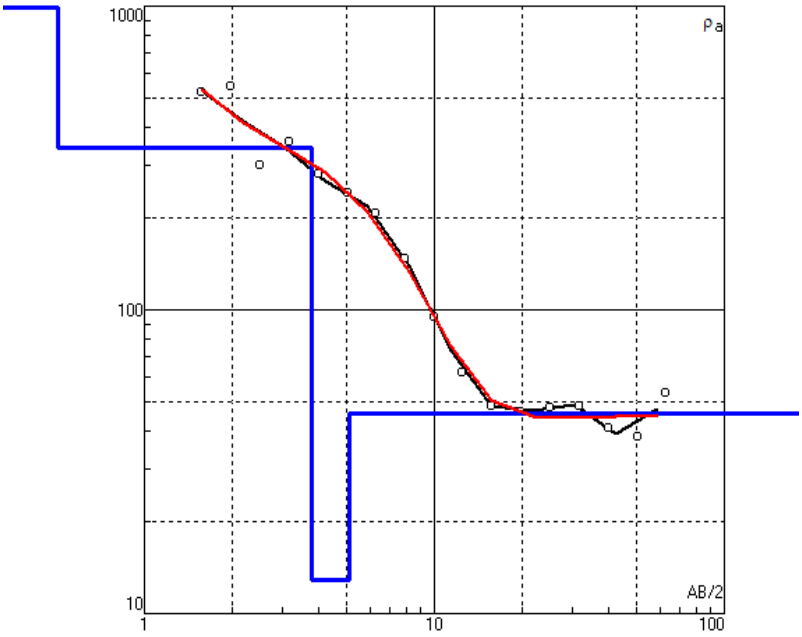

Figure 4.7.1 apparent resistivity curve of Sindaa

4.1.8 Geological formation of Gbenyiri

Gbeniyiri (09.26180 ^{O}N, 02.42663 ^{O}W) had a profile length of 200 m with a probed depth of 32.5 m as shown in Figures 4.8 and 4.8.1. The first of three geo-electric layers in this pseudo-section is a 5 m layer of lateritic material with apparent resistivity ranging from 1540 m to 2738 m (Manyu *et al.*, 2018). The second geo-electric layer has a thickness of about 11.5 m and apparent resistivity varying from 86.6 Ωm-154 Ωm and is suspected to be either of clay or shale (Ganiyu *et al.*, 2020). The final and third geo-electric layer has a thickness of about 30 m of saturated water-bearing formation with an apparent resistivity of 20.5 Ωm – 48.7 Ωm.

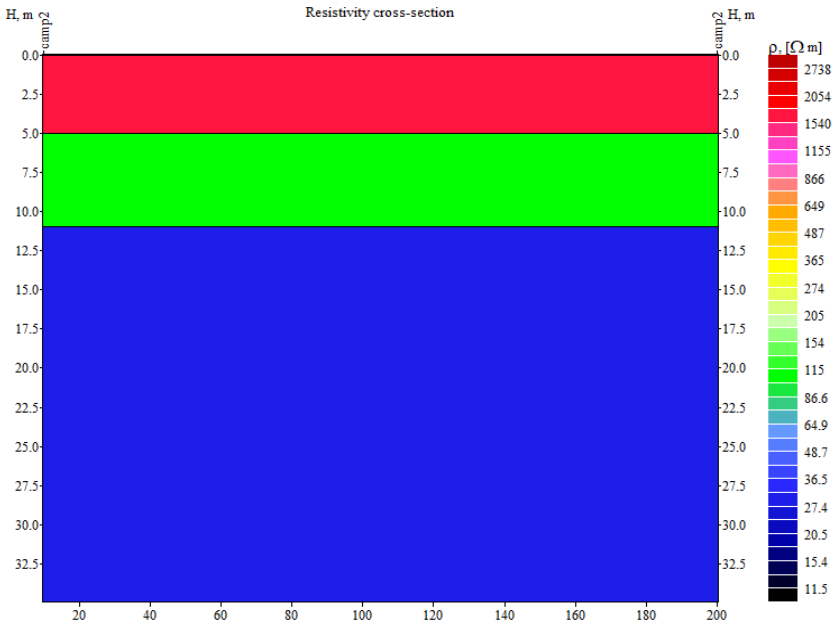

Figure 4.8 pseudo-section of lithology at Gbenyiri

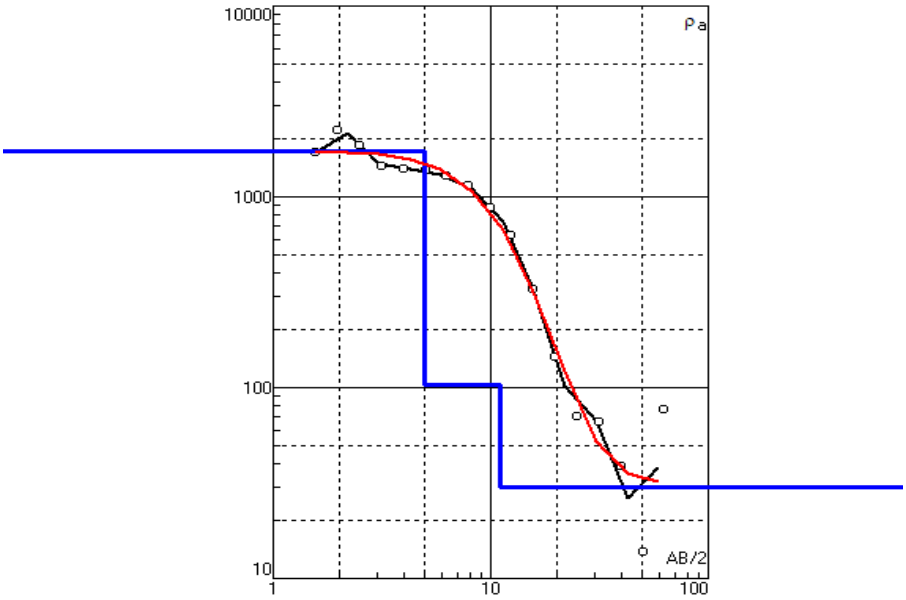

Figure 4.8.1 apparent resistivity curve of Gbenyiri

4.1.9 Geological formation of Sawla Yipala

For Sawla Yipala, the profile length for the VES was about 200 m with a probed depth of 30 m (Figures 4.9 and 4.9.1). The first geo-electric layer is about 2.5 m thin and has an

apparent resistivity which runs from 562 Ωm – 825 Ωm and might be from the transported lateritic family (Bayewu *et al.,* 2018). The second geo-electric layer is probably made up of mafic to felsic of about 13 m thick, accounting for the resistivity values between 121 Ωm – 178 Ωm. The third geo-electric layer has a resistivity range of 8.25 Ωm – 26.1 Ωm with a thickness of about 22 m which is likely to bear groundwater (Sahu & Sikdar, 2008). Within this zone, groundwater may exist in fractures and joints. The fourth geo-electric layer considered to be the bedrock is thin of about 2.5 m. It has an apparent resistivity between 1212 Ωm – 1778 Ωm with probable suspicion of underlying metamorphic rock materials. These findings are similar to previous research by others (Cheng *et al.,* 2019; Vanella *et al.*, 2021).

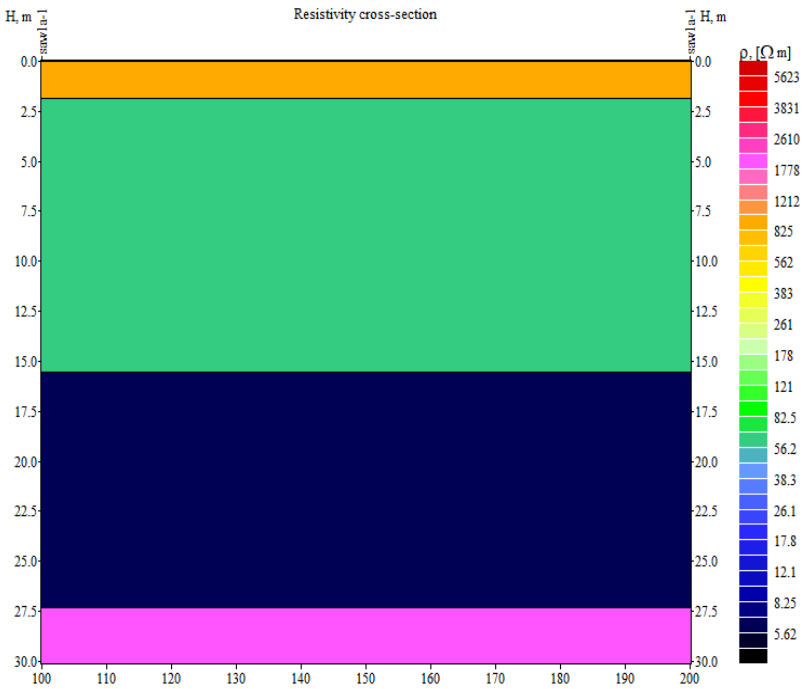

Figure 4.9 pseudo-section of lithology at Sawla Yipala

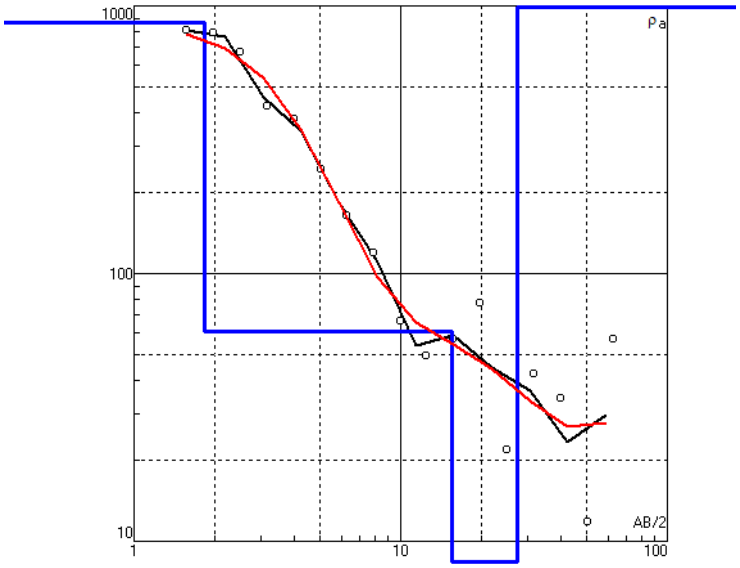

Figure 4.9.1 apparent resistivity curve of Sawla Yipala

4.2 Deterministic factors for groundwater availability and occurrence

In this study, the factors that influence groundwater occurrence include land use and land cover, soil, slope, rainfall, geological lineament, drainage, and lithology. These factors were thoroughly investigated to determine the spatial availability of groundwater in the area.

4.2.1.1 Lithology of the Sawla Tuna Kalba District

In terms of infiltration and lateral inflows, lithological units are the primary indicators of groundwater distribution. Even though infiltration and lateral inflows are contributing factors to the existing reservoir, the Sawla Tuna Kalba district's current lithology may have an impact on groundwater reclamation. The geological map (Figure 4.10) shows that the Birimain supergroup accounts for approximately 85 % of the area, Voltaian units account for 2 %, while the Mesozoic was, Eburnean, and the Tamnean units account for the remaining 13% of the area. The study area consists primarily of metamorphic and sedimentary rocks, which are reported to have a high groundwater yield (Chernet, 1993). The regolith and fractured rocks, on the other hand, are the primary groundwater holding and transmitting zones for this type of lithological unit. Sedimentary rocks are made up of alluvium deposits (sand, silt, and clay), river gravel, and travertine. Alluvial signature zones have high potential due to their high permeability rate and porosity, which influence groundwater productivity (Kebede, 2013). Furthermore, areas with good fractured rock system may contain massive amounts of water. As a result, the geological map is intended to provide insight into the potential of groundwater within the Sawla Tuna Kalba district.

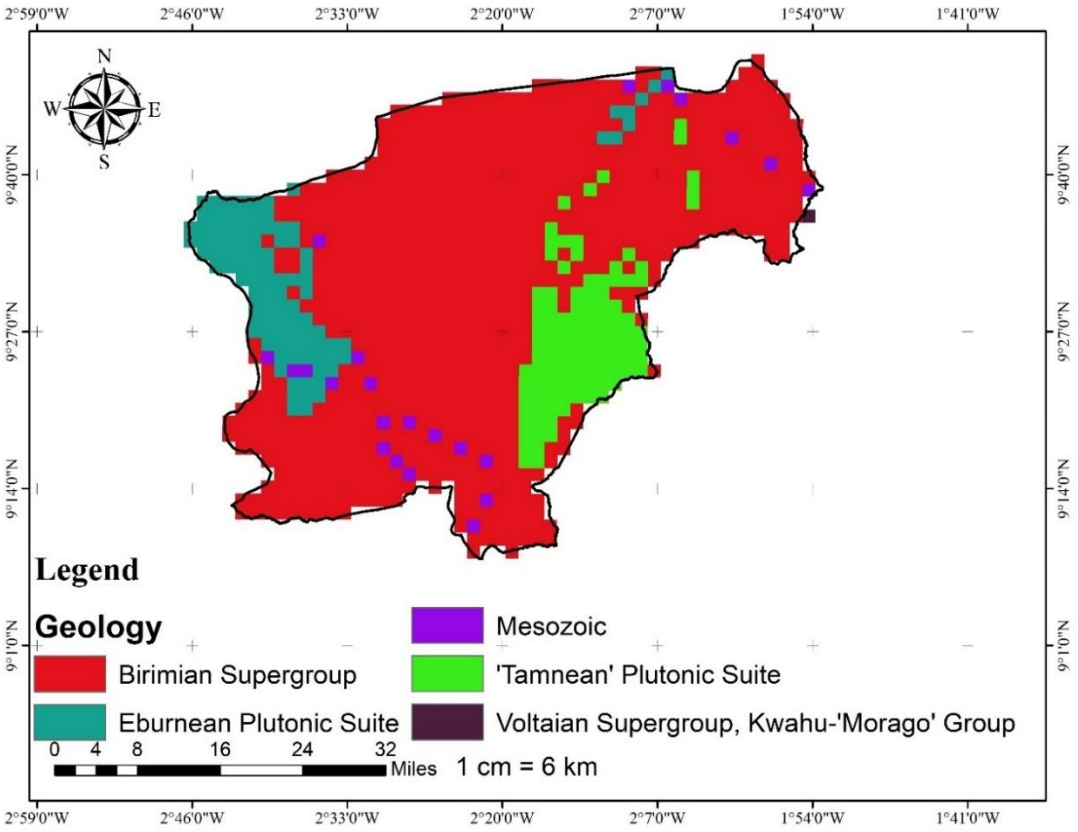

Figure 4.10 Lithology of the study area

4.2.1.2 Soils in the Sawla Tuna Kalba District

The dominant soil types in the study area are depicted in Figure 4.11. They include Dystric Regosols, Gleyic Luvisols, Lithosols, Eutric Nitsols, and Ferric Acrisols. Averagely, all the listed soil types have equal representation in the area (Table 4.0) However, Lithosols occupied the highest percent in the area (18.1%) while Ferric Acrisols occupied the least (6.8 %).

Table 4.0 Soil type with area percentage

Soil Types	Percentage

Lithosols	18.1
Dystric Regosols	17.1
Eutric Nitsols	16.7
Gleysols	11.2
Gleyic Luvisols	10.3
Orthic Ferralsols	10.1
Phinthic Acrisols	9.7
Ferric Acrisols	6.8

Apart from Lithosols, Regosols are the most common soil type in the study area and are generally suitable for irrigation (Water Resources Commission of Ghana, 2011). Knowing the soil type in the study area is critical in controlling the rate of infiltration, which is necessary for groundwater replenishment (Abdalla *et al.,* 2020; Tolche, 2021). Furthermore, soil types influence crop suitability, water holding capacity, and soil nutrients in the context of irrigation (Water Resources Commission of Ghana, 2011). Weathered soils (sandy) have high porosity and permeability, which is good for infiltration, whereas clayey soils have low infiltration. For these reasons, soil type is regarded as a controlling factor in defining zones of good groundwater potential (David Ndegwa Kuria, 2012; Kumar *et al.,* 2016).

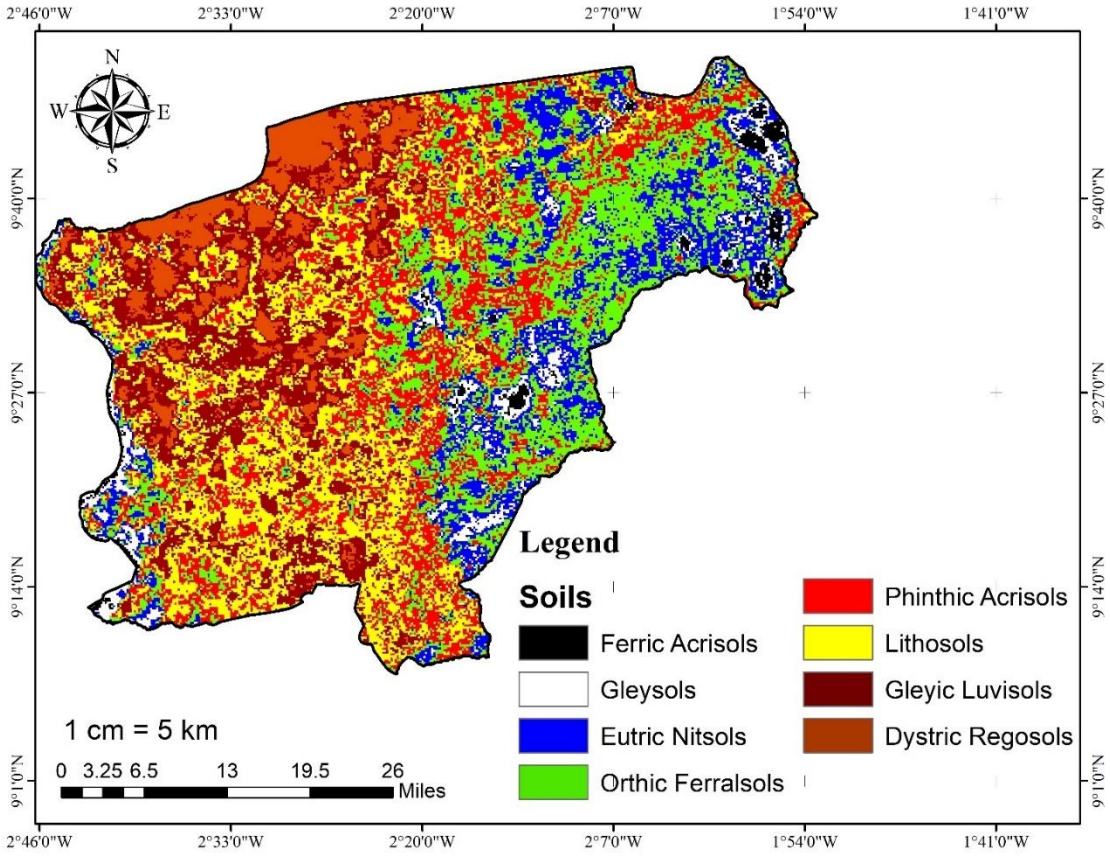

Figure 4.11 Distribution of soil types in the study area

4.2.1.3 Land Use Land Cover (LULC) map

The LULC classification yielded six classes in the study area (Figure 4.12). The six (6) LULC types were: agricultural land (1282.7 Km^2), vegetation (883 Km^2), urban settlements (690.6 Km^2), thick forest (1080.6 Km^2), water body (553.2 Km^2), and farming communities (300.78 Km2). The vegetation and dense forest land cover in the area may have a direct relationship with groundwater occurrence. Thus, deep-rooted trees will tap into the immediate groundwater reserve and also serve as cover/mulch to reduce groundwater losses through evaporation. Prabhakar & Tiwari, (2015) discovered in a study in Madhya Pradesh near the Indira Sagar Canal Command Area reported that areas with high settlements have low groundwater potentials due to industrialization and urbanization,

whereas areas with thick forest and vegetation have high groundwater potential due to high infiltration and percolation of rainfall. Findings from this study are consistent with previous research, which has identified vegetation and forest as an important LULC class for groundwater occurrence (Elmahdy *et al.*, 2020; Liaqat *et al.*, 2021).

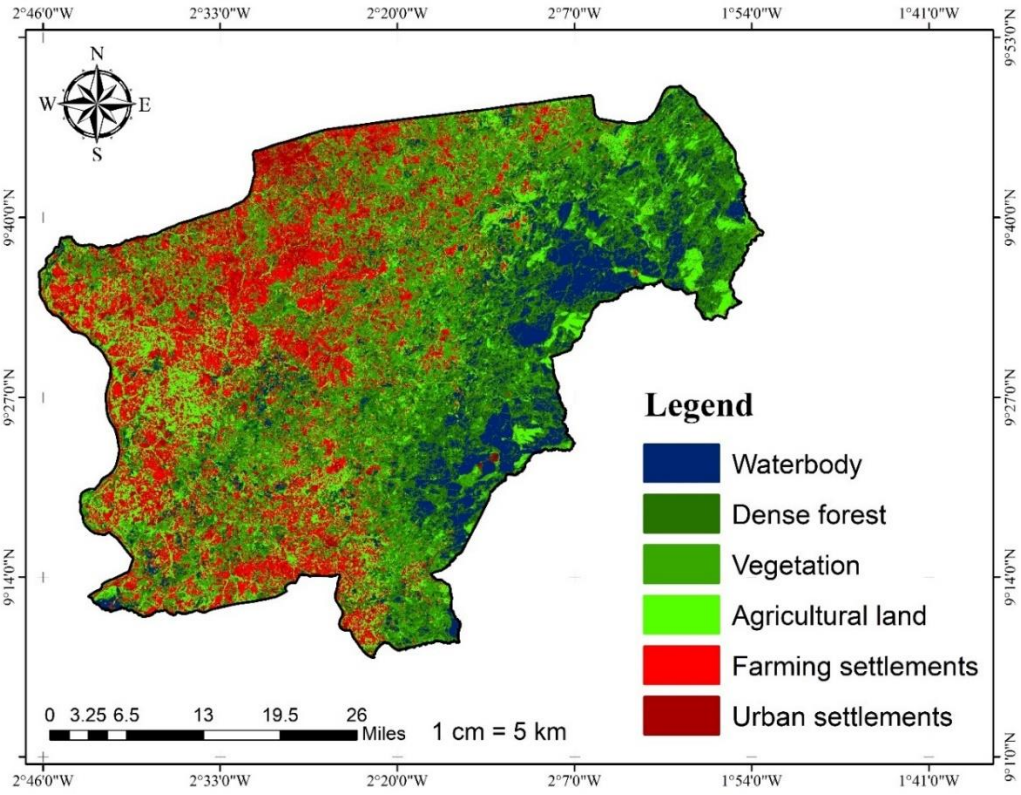

Figure 4.12 Land use Land cover of the research area

4.2.1.4 Lineament Density

The geological lineament in the study area ranges from 0.1567 to 0.7847 Km/Km2, as shown in figure 4.13. Geological lineaments are displays of possible deeper earth structures (fractures, faults, joints, fractures with obvious displacements, ruptures with no fractured displacements that are not visible with the naked eye (Hussein *et al.*, 2018). Areas with lineament density ranging from 0.314 to 0.7847 Km/Km2 indicate the presence of high fracturing and are potential groundwater occurrence zones. The study area is generally

underlain by crystalline hard rock, and groundwater can only exist in this type of environment if there are numerous fractures (Adam & Appiah-Adjei, 2019). Most studies ranked lithology higher because it is the major determinant of groundwater occurrence and hence this study goes contrary to previous studies (Tolche, 2020; Abdalla *et al.*, 2020). In this study, geological lineament was ranked higher because groundwater in the study area is primarily defined by fractures which were consistent with our thorough field works in the area. This observation can also be attributed to some drill wells which showed artesian properties as a result of high fracturing systems and high atmospheric pressure (Yusof *et al.*, 2011).

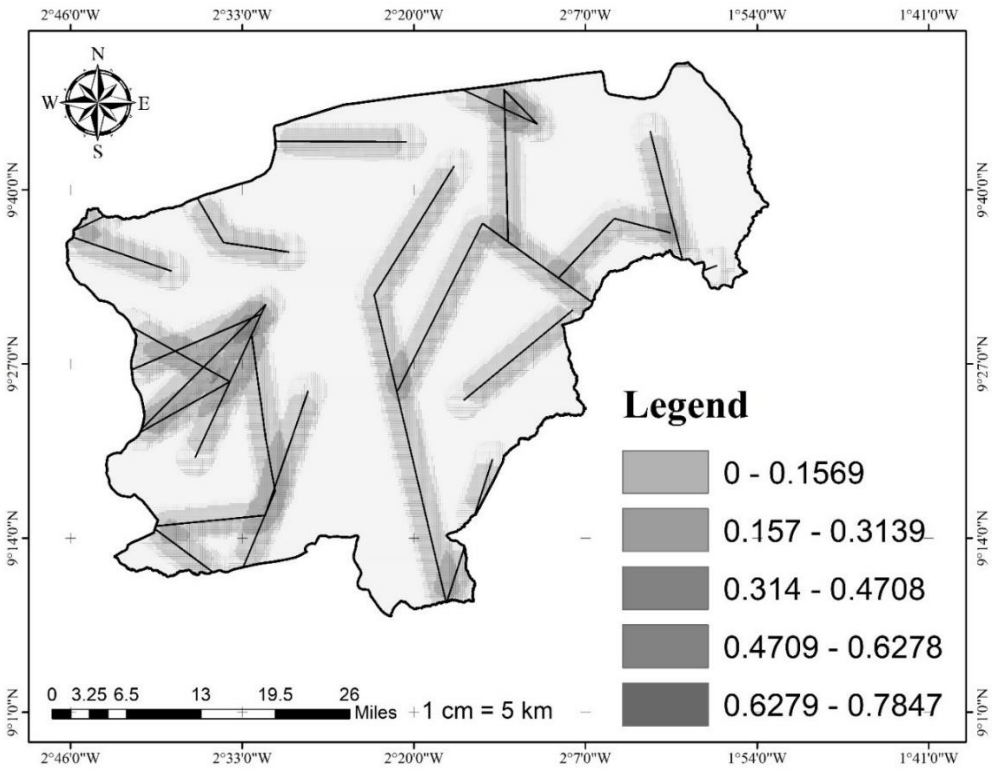

Figure 4.13 Lineament density in the study area

4.2.1.5 Rainfall

Rainfall plays an important role in defining groundwater potential zones. It is the primary source of natural recharge, which results in aquifer productivity. Figure 5 depicts the annual rainfall range for the area. It ranges from 725 mm/year to 1750 mm/year. However, in some cases, the study area may experience extremely heavy rainfall (Loh *et al.*, 2020). Areas with high rainfall and significant vegetative cover indicate high infiltration and deep percolation, resulting in natural replenishment of groundwater, whereas areas with low rainfall indicate less infiltration, influencing groundwater recharge (Murthy & Mamo,2009; Prabhakar & Tiwari, 2015; Liaqat *et al.*, 2021a). Figure 4.14 shows that the southwestern part receives more rainfall than areas other areas, indicating that the Southwestern part will have higher infiltration.

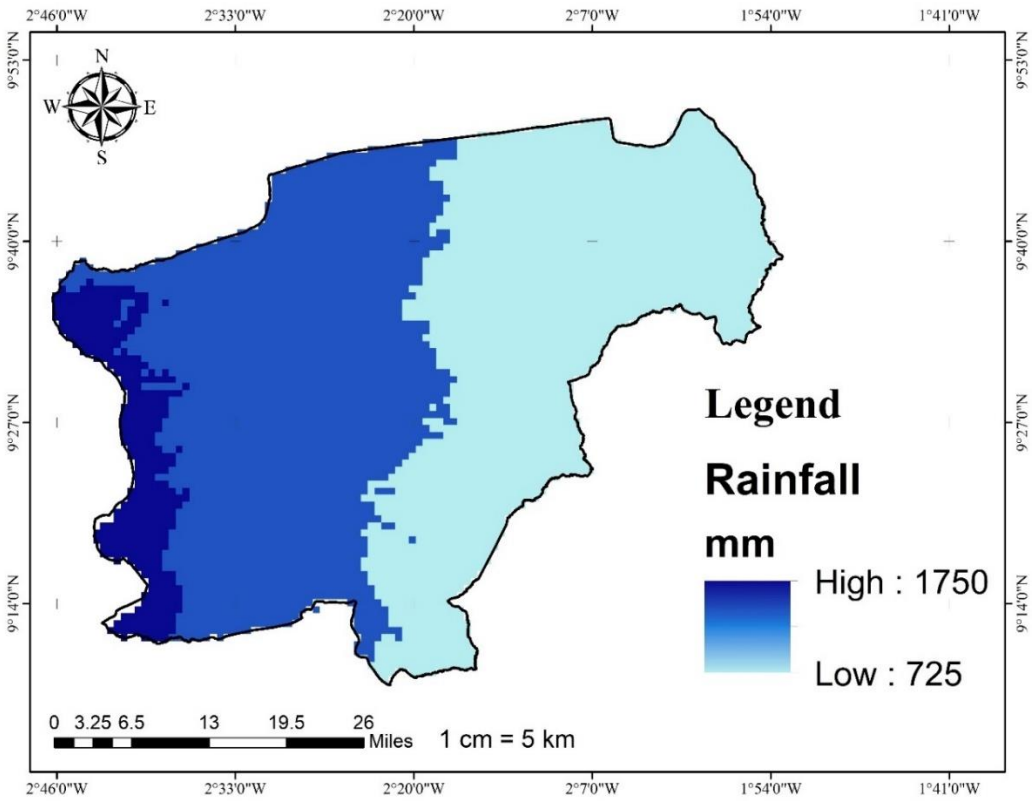

Figure 4.14 Rainfall pattern in the Study area

4.2.1.6 Drainage Density

Figure 4.15 shows that the drainage density within the study area ranges from 0.041 to 0.492 Km/Km^2, indicating that the entire Area of Interest (AOI) is reasonably drained and thus a good zone of groundwater occurrence. The total length of all streams, rivers, and drainage systems within the basin per unit area of the basin is referred to as drainage density (Abdalla *et al.*, 2020). The stream channel is commonly used to assess how good or bad a watershed is. This property is important in investigating groundwater potential zones because a good drainage system influences percolation and leads to groundwater replenishment. Areas with drainage densities ranging from 0.1134 to 0.5669 Km/Km^2 have a dense drainage system and, as a result, are potential groundwater occurrence zones. A similar study by Tolche, (2020) in Dhungeta-Ramis sub-basin, Ethiopia reported drainage density values ranging from 0.3410 to 0.5669 Km/Km^2. The values found for the current study are rather lower than that of Tolche's. This could be due to the underlying geology in the research area. The underlying geology in the study area is crystalline hard rock, making drainage very slow or impossible.

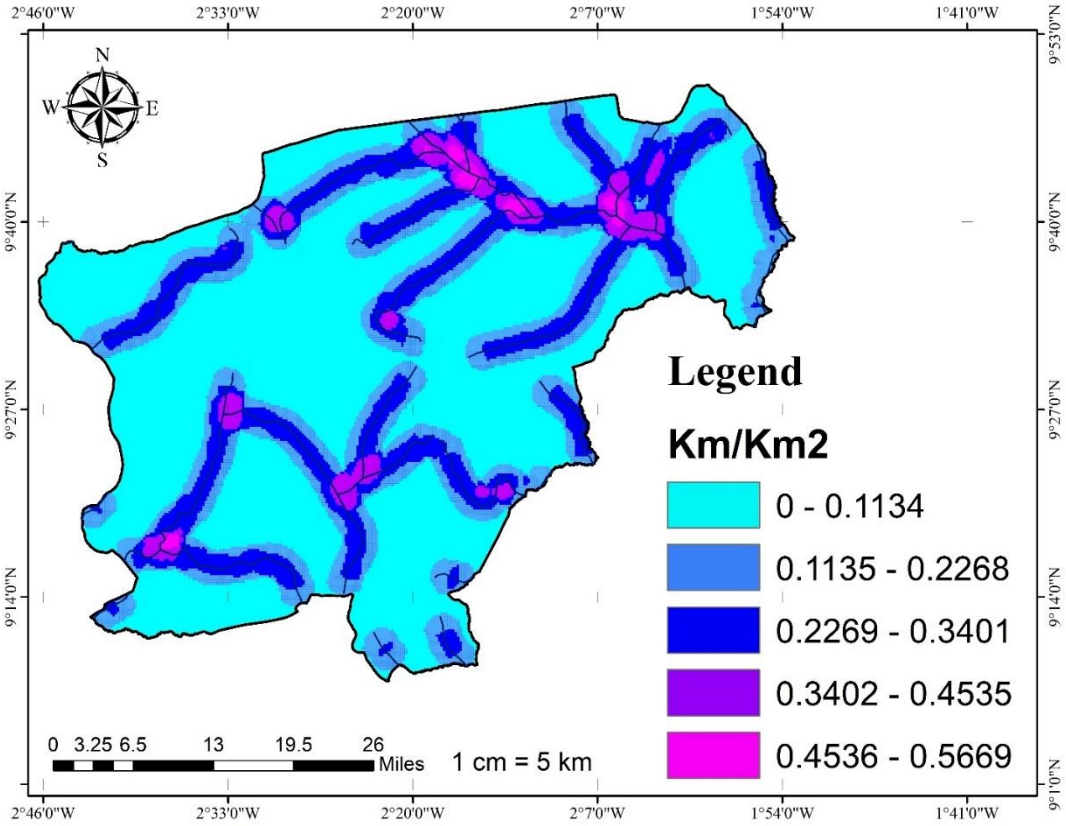

Figure 4.15 Drainage density of the study area

4.2.1.7 Slope

The slope in the study area was expressed in percentage, as shown in figure 4.16. The slope ranges range from 1.7 to 36.1 %. It is perceived that areas with high slopes are likely to have a high potential for groundwater occurrence than areas with low slopes. Drilling on top of a hill, for example, may not yield the desired quantity of water. Low-lying (flat) areas may be good groundwater zones. Drilling down a hill has revealed high-yielding aquifers (Wei *et al.*, 2019). This could be due to the affinity of gentle slopes to holding rainfall for a period to facilitate groundwater recharge and also serve as reservoirs to contain groundwater. The study showed high degree slopes that are mostly undulating in a valley, with slope values of 36.1 %. The gradient of the slope in any area is an important factor in determining the movement of groundwater (Oh *et al.*, 2011; Adeyeye *et al.*, 2019;

Tolche, 2020; Abdalla *et al.*, 2020). The nature of topography may influence rainfall infiltration directly or indirectly and may be regarded as a promising factor in determining groundwater availability (Al Saud, 2018). The slope can indicate the direction of groundwater recharge or flow in a specific basin (Gupta and Srivatava, 2010) and this is very useful in groundwater harvesting.

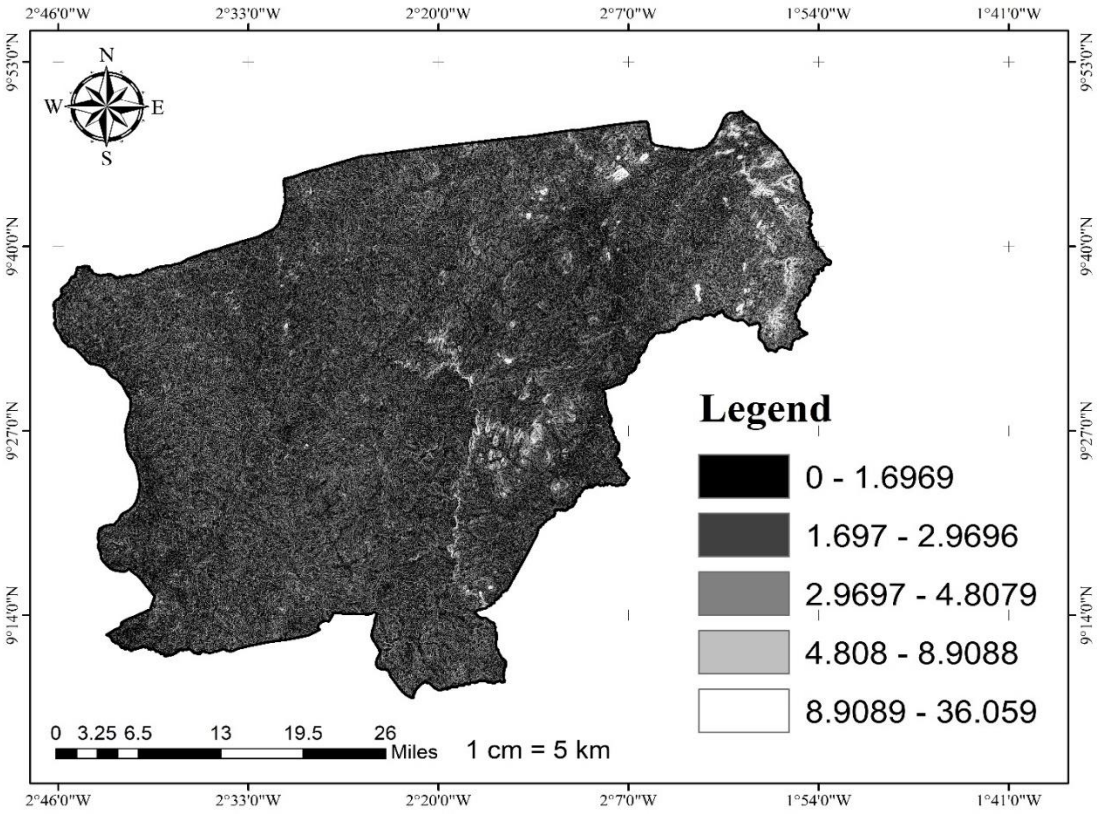

Figure 4.16 Slope of the study area

4.2.1.8 Groundwater potential zone

Figure 4.17 depicts the different zones of possible occurrences and quantities of groundwater in the area. The potential quantities are classified into low, moderate, and high potentials. The zone of occurrences is also classified based on ariel coverage in terms of

land stretch viz low zones comprise 1614 Km^2, moderate zones comprise 2786 Km^2 (the largest in terms of land stretch), and high zones comprise 201 Km^2.

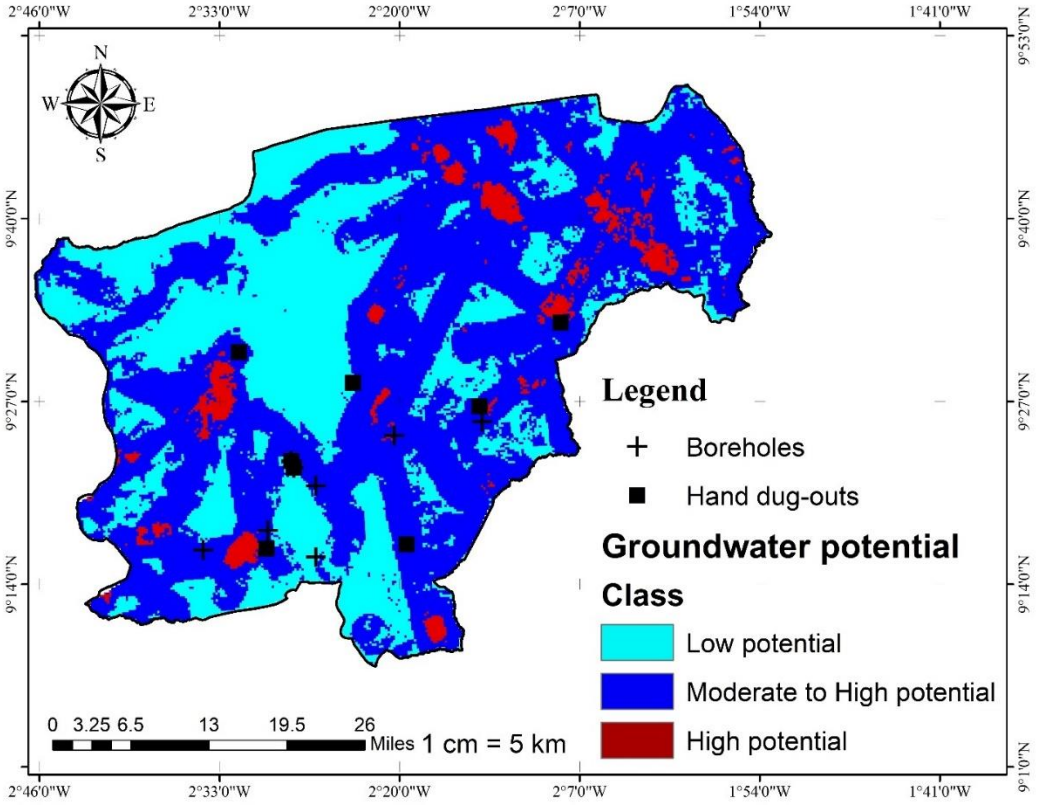

Figure 4.17 Groundwater potential of the Sawla Tuna Kalba

This study is consistent with (Oh *et al.,* 2011; Kuria, 2012; Magesh *et al.,* 2012; Rahmati *et al.,* 2015; Kumar *et al.,* 2016; Adeyeye *et al.,* 2019; Díaz-Alcaide & Martínez-Santos, 2019; Hassan & Khalaf, 2020; Abdalla *et al.,* 2020; Tolche, 2020). In separate studies, they reported groundwater potential ranges from low to high potential with high potential being the least in ariel coverage. Figure 4.17 shows that the Sawla Tuna Kalba has a high groundwater potential which may be exploited for future domestic and agricultural (especially irrigational) activities. The majority of this resource falls within the moderate to high groundwater zones. The cross-validation results showed that areas with moderate-

high potential are suitable for deep-seated wells such as boreholes, whereas areas with low potential are dominated by shallow and hand-dug wells, which yield enough during the rainy season but dry up during the dry season. Existing boreholes and hand dugouts yields confirmed that the Study area has a high groundwater yield.

4.2.2 Groundwater Storage Capacity Estimation

Computations of total groundwater storage and extractable storage capacity have been done using different datasets and the Schoeller equation. Table 4 shows a summary of the data used for the estimation of groundwater extractable storage capacity.

Table 4.1 Summary of Borehole Loggings in the Sawla Tuna Kalba District

Parameters	Granites	Meta-Volcanic	Mean values
Total Weathered Depth (D) m	30.5	28.5	29.5
Depth of water strike (h) m	22.5	11.5	17.0
Saturated Depth (H=D-h) m	16.27	13.79	12.5
Number of Boreholes (N)	83	46	129
Number of successful (S)	74	39	113
Number of unsuccessful (U)	9	7	16
Groundwater Coverage (P - %) = S/N	0.89	0.84	0.86

*Granites and *Meta-Volcanics are geological zones where the studied boreholes are located

The quantification of Groundwater Storage Capacity was based on the data gathered from the 129 borehole logs using equations 3.3a and 3.3b. Taking Effective Porosity (well-interconnected –pores) to be 5% and Specific Yield to be 2% respectively (Acworth, 1987 and Asomaning, 1993) with an area of 4601 km² (Extent of Study Area). The Groundwater Coverage was attained by rationing the number of successful boreholes to the number of boreholes studied [(P - %) = S/N]. After thorough computation, the Total Groundwater

Storage and Extractable Groundwater were approximately 24.7 × 10^6 km³ and 9.8 × 10^6 Km³ respectively. The purpose of calculating the Extractable Groundwater Amount is to avoid over-abstraction while also preventing aquifer damage, contamination, and stress. The computation reflects areas with high groundwater yield to make these sites suitable and financially beneficial for irrigated agriculture.

4.2.3 Crop Water Requirement Estimation

During the dry season, the most commonly cultivated crops in the study area are vegetables and cereals. Tomatoes (***Solanum lycopersicum)***and maize (***Zea mays***) are the crops commonly irrigated during the dry season. These crops are planted during the same season, from November to February, but with different coefficients. Hargreaves equation was used to calculate the reference crop evapotranspiration, as shown in equation (3.5). The summary of climatic information analyzed using remote sensing is shown in Table (4.2), with temperatures ranging from 20.2 ^{O}C to 38.5 ^{O}C during May, with a mean temperature of 29.35 ^{O}C. Temperature variation together with its means can also be seen in Table (4.2) with the highest and lowest being in May per the analysed data. Based on the temperature data, the crop water requirements for tomatoes and maize were computed.

Table 4.2 Summary of Climatic data in the Sawla Tuna Kalba District

S/N	Month	Tmin	Tmax	T.D	Tavg	RA
1	November	20.2	38.5	18.3	29.35	4.5
2	December	22.1	35.3	13.4	28.7	4.5
3	January	21.6	34.8	13.2	27.9	4.5
4	February	21.8	29.0	8.7	25.4	4.5

*Minimum Temperature *Maximum Temperature *Temperature Difference *Average Temperature *Extraterrestrial Radiation

4.2.3.1 Crop Water Requirements for Tomato and Maize

The crop coefficient was calculated using the curve depicted in figure 4.18a, and the Crop Water Requirements (CWR) was estimated using the CWR equation. Tables 4.3a depicts the Crop Water Requirements (CWR) computed from the tomato's growing stage in November to the maturity stage in February. The highest evapotranspiration is 8.5 mm/day in November, and the lowest is 5.3 mm/day in February.

Table 4.3a Computed Values of Evapotranspiration and Crop Water Requirements for Tomato

S/N	Month/Variables	November	December	January	February
1	Reference crop Evapotranspiration- ET_0 (mm)	8.5	7.3	6.8	5.3
2	Crop Coefficient - K_C	0.7	1.15	1.15	0.7
3	Crop Water Requirements – CWR (mm/month)	208.25	303.86	214.2	35.78

Previous research has shown that the crop water requirement for tomatoes is between 400 mm/period and 800 mm/period, which is similar to studies of (Xue *et al.*, 2020; Ewaid *et al.*, 2019). The total amount of water required from planting to maturity in this study is 762.09 mm/groeing season and the average CWR for the period is 190.52 mm/growing season and these are consistent with Gong *et al.*, (2020). The quantity of water required by the crop in November is 208.25 mm, which is the initial stage of tomato growth after transplanting and hence requires an appreciable amount of water to survive. The CWR in December is 303.86 mm, which is the development stage of the tomato and as such demands a substantial amount of water. In January, the CWR was found to be 214.2 mm, which is the mid-stage of the tomato, and hence there would be a decline in water demand

compared to the development stage. Finally, the CWR in February was found to be 35.78 mm, which is the late stage of the tomato and as such may demand less or no amount of water. Thus, at the late stage, the tomato is at a harvesting stage where even some of the leaves are drying and dropping. Photosynthetic activities are completed and less water is required (Ewaid *et al.,* 2019).

Furthermore, the crop water requirements for maize were calculated using the same cropping period as in November to February. The total CWR for maize for the growth period was 695.93 mm/growing season. These findings are reconcilable with the results of Ewaid *et al.* (2019) and Gong *et al.* (2020) who reported similar values for maize in their studies.

Table 4.3b Computed Values of Evapotranspiration and Crop Water Requirements for Maize

S/N	Month/Variables	November	December	January	February
1	Reference crop Evapotranspiration- ET_0 (mm)	8.5	7.3	6.8	5.3
2	Crop Coefficient - K_C	0.35	1.2	1.2	0.35
3	Crop Water Requirements – CWR (mm/month)	74.38	226.3	260.1	135.15

4.2.2.2 The potential total irrigable land in the area

The intent of developing a Land Use Land Cover (LULC) map is to provide information on the available land its nature and use pattern within the area. LULC is an unmistakable factor that influences groundwater movement, availability, and recharge (Hussein *et al.*, 2018). The land use land cover portrays the availability of agriculture in the study area,

which is approximately 1282.7 Km^2 (128,270 Hectares). The presence of vegetation and water bodies (figure 4.12) in the area can serve as markers to map irrigational land. Conversely, the vegetation stretch is roughly 883 Km^2 (88,300 Hectares), which can also be used as available land for possible irrigation. Though vegetated areas may be suitable irrigable lands, the prevalence of deforestation coupled with the effects of climate change may render such areas non-suitable as there are protected for the above and other reasons. These assessments are consistent with the Ministry of Food and Agriculture's (MoFA), which estimated the total irrigable land available to be approximately 1,945.3 km^2 (MOFA, 2019). The 1,945.3 Km^2 may contain bare soils, forest areas, vegetation, and/or wetlands that are irrigable.

4.2.2.3 Total Land area that can be irrigated using groundwater in the study area

In a perfect scenario, a hectare of tomato can contain 16,000 plant populations (pp) if they are spaced about 300 – 500 mm apart, and a hectare of maize can contain around 25,000 pp (Japanse International Cooperation Agency, 2020). The total area that can be irrigated, however, is 1,282.7 Km^2 (128,270 Hectares). Further to that, the total crop water requirement for tomato and maize over the entire season was estimated to be 762.09 mm/growing season and 695.93 mm/growing season respectively. The irrigation water requirements for tomato and maize were found to be 914.508 mm/growing season and 835.116 mm/growing season. Hence, the total irrigation water required for a hectare of tomato and maize is approximately 5,097 m^3/ha/growing season and 5,960 m^3/ha/growing season respectively. Consequently, the available groundwater storage was found to be approximately 24.7×10^6 Km^3, and the usable storage was estimated to be 9.8×10^6 Km^3. From the above, the total land area that can be allocated to irrigated tomato with usable

storage groundwater as the source is approximately 143.6 Km^2 (14,360 ha), which is approximately, and the total land area that can also be irrigated maize land with groundwater is approximately 196.2 Km^2 (19,620 ha).

4.3 Hydro-chemical Analysis and Evaluation of Groundwater Quality for Irrigation

Groundwater quality is an important component in evaluating its suitability for drinking, domestic, agricultural, and industrial purposes (Subramani *et al.,* 2005; Mohammad *et al.,* 2018). However, this evaluation is for irrigation on a possible large scale in the future. Physiochemical variables showing statistical measures such as minimum, maximum, average, and standard deviation are given in Table (4.4).

Parametrically, it was noticed that most of the groundwater samples analysed fell within the allowable standards for domestic and agricultural use. The table also depicts a decreasing order of cations in the groundwater samples ($Ca^{2+} > Na^{+} > K^{+} > Mg^{2+}$) and that of anions is $NO_3^- > Cl^- > SO_4 > HCO_3^- > F^-$ which suggest that the groundwater may be Ca^{2+}, Na^{+}, and NO_3^-, Cl^- in nature. This agrees with the ionic pattern for most tropical freshwaters (Karikari & Ansa-Asare, 2009). Figure 4.18 indicates that Cl is the prevalent anion while SO_4, HCO_3, and F^- occur in minor concentrations indicating the possibility of chlorite groundwater in nature.

Table 4.4 Summary of physio-chemical parameters in the study area

S/N	Parameter	Units	Max	Min	Mean	Media	STD	Kurt	Skew	WHO PL
1	EC	µS/m	1.9	0.1	0.5	0.4	0.3	4.3	1.9	14.0
2	TH	mg/l	294.0	41.3	87.3	126.1	44.9	1.0	0.6	500.0
3	pH		8.1	6.1	7.1	7.1	0.4	0.6	0.0	6.5 - 8.5

4	Temp	°C	33.9	27.4	29.9	29.8	1.2	0.9	31.7	
5	TDS	mg/l	1256.2	82.3	272.7	213.3	200.7	7.9	2.6	1000.0
6	Ca^{2+}	mg/l	133.1	3.8	25.8	20.7	22.1	5.9	2.3	200.0
7	Mg^{2+}	mg/l	33.9	2.1	25.0	18.2	18.9	10.3	2.8	150.0
8	Na^{+}	mg/l	70.0	8.7	26.4	23.0	13.1	1.1	1.2	200.0
9	K^{+}	mg/l	56.6	1.6	5.6	4.5	6.0	54.8	6.9	30.0
8	F^{-}	mg/l	1.5	0.0	0.5	0.3	0.6	31.1	4.7	1.5
9	Cl^{-}	mg/l	210.3	0.6	23.6	10.6	34.2	9.7	2.8	250.0
10	SO_4	mg/l	139.9	0.4	13.7	4.1	20.9	14.3	3.3	250.0
11	NO_3	mg/l	587.3	0.0	55.0	6.8	100.8	9.4	2.8	50.0
12	HCO_3	mg/l	10.5	0.0	1.6	0.9	2.5	4.3	2.1	250.0
13	SAR		2.3	0.3	930.0	0.9	0.4	1.7	1.1	

*STD- Standard Deviation **Kurt- Kurtosis ***Skew- Skewness ****PL- Permissible Limit

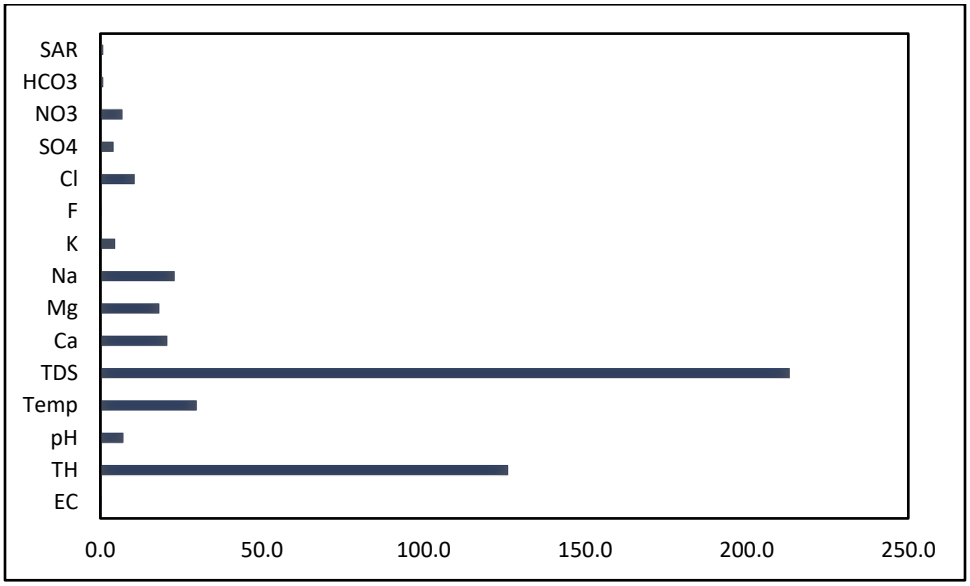

Figure 4.18 Median concentration of chemical constituents in the study area

The pH values of groundwater in the research area run from 6.1 to 8.1 with an average value of 7.1 suggesting that the groundwater is likely alkaline within the area. The EC

values range from 1.9 to 0.1 µS/m with a mean value of 0.5 µS/m, on the other hand, the TDS ranges from 82.3 to 1256.2 mg/l with an average of 272.7 mg/l with most of the samples not exceeding the desirable WHO limit of TDS (1000mg/l) (WHO, 2003). Concentrations of Ca^{2+}, Mg^{2+}, HCO_3^- and Cl^- range from 3.8 to 133.1, 2.1 to 33.9, 0 to 10.5 and 0.6 to 210 mg/l respectively (Table 4.4). Some comparisons of these concentrations are recommendable for drinking purposes indicating that the concentrations of Ca^{2+} and Mg^{2+} are within the acceptable limits whereas those for Cl^- and HCO_3^- are higher than the acceptable limits in some areas. The concentrations of SO_4^{2-} and NO_3^- are respectively within the limits of 250 mg/l and 50 mg/l (WHO, 2003) as prescribed for drinking waters.

4.3.1 Classification of Groundwater in the area

To evaluate the efficacy of groundwater for a certain purpose, it is necessary to classify the groundwater based on its hydro-chemical properties. Olusola (2020) and George et al., (2009) proposed a classification technique that was based on total dissolved solids (TDS) and was adopted for this study. The results of the classification are presented in Table 4.5. The groundwater samples are classified as fresh (TDS1,000 mg/l) or brackish (TDS>1,000 mg/l) using the standard TDS classification (George *et al.,* 2009).

Table 4.5 Groundwater classificationbased on TDS

Total Dissolved Solids (mg/l)	Classification	Number of samples	Percentage
0 - 1000	Fresh water Type	116	94
1000 - 10000	Brackish water Type	3	6
10000 - 100000	Saline water Type	0	0

The study found that 94.0 percent of the samples had a concentration of less than 1000 mg/l, implying that they could be used for irrigation. Plant growth is slowed by high TDS concentrations because they reduce water uptake, resulting in wilting and low yield (George *et al.*, 2009; Singh *et al.*, 2012; Ram *et al.*, 2021).

Table 4.6 also shows groundwater classes in the area based on Electrical conductivity (EC). Generally, 92 percent of the samples fall within the permissible limit (WHO; 2003), while 8 percent are above the permissible limit, indicating that they are marginally poor in quality according to the WHO (2003).

Table 4.6 Groundwater classifications based on EC levels

Electrical conductivity (µS/m)	Classification	Number of samples	Percentage
<1500	Permissible	115	92
1500 - 3000	Not permissible	4	8
>3000	Hazardous	0	0

Groundwater classes with a slight salinity hazard (EC) may be harmful to salt-sensitive plants like peanuts and cowpeas (Tschakert & Singha, 2007) and should be used with caution for crop growth. Human and anthropogenic factors may have exacerbated the concentration increase in the 8% of samples that exceeded the desirable limits (Prasood *et al.*, 2021). These findings are consistent with those of Nagaraju et al. (2014) in the Bandalamottu lead mining area, Guntur District, Andhra Pradesh, South India, and Varol and Davraz in (2015) the Tefenni plain (Burdur/Turkey).

Table (4.7) shows Total Hardness (TH) values running from 41.3 to 294 mg/l, with a mean value of 87.3 mg/l. The results showed that the majority of the experimented samples fell

in the soft to moderately hard water category. The sodium adsorption ratio (SAR) is directly related to total hardness. Because it quantifies the alkali/sodium hazard to crops.

Table 4.7 Groundwater classifications of all groundwater samples (Olusola, 2020)

Total Hardness (mg/l)	Classification	Number of samples	Percentage
<75	Soft	53	44
75 - 150	Moderately Hard	54	46
150 - 300	Hard	7	6
>300	Very Hard	5	4

4.3.2 Hydro-chemical Evaluation of groundwater

Güler & Thyne (2004) indicated that to understand the variation of groundwater ionic concentration, the geochemical variations must be plotted on an X–Y coordinate. Figures 4.19 and 4.20 showed scatter diagrams for the most important parameters (Na^+, Cl^-, and Ca^{2+}, NO_3^-) which define the type of groundwater present. The sample distribution in Figure 4.20 does not attribute the Na+ content of the water to halite. More samples plot above the equiline in Figure 4.20, indicating that sodium chloride cannot account for all of the sodium in the study area. Furthermore, only a few data samples plot near the equiline, indicating that halite dissolution is not the primary source of Na+ ion in groundwater from the study area. The trend observed in Fig 4.20 suggests silicate mineral weathering and ion exchange processes as the probable sources of Na^+ enrichment in groundwater from the study area. This is consistent with the findings from similar rocks in the Afram Plains area by Yidana *et al.* (2012). In the inclusion of montmorillonite and other adsorption surfaces in the system, Na+ and K+ play a key role in chemical bonding.

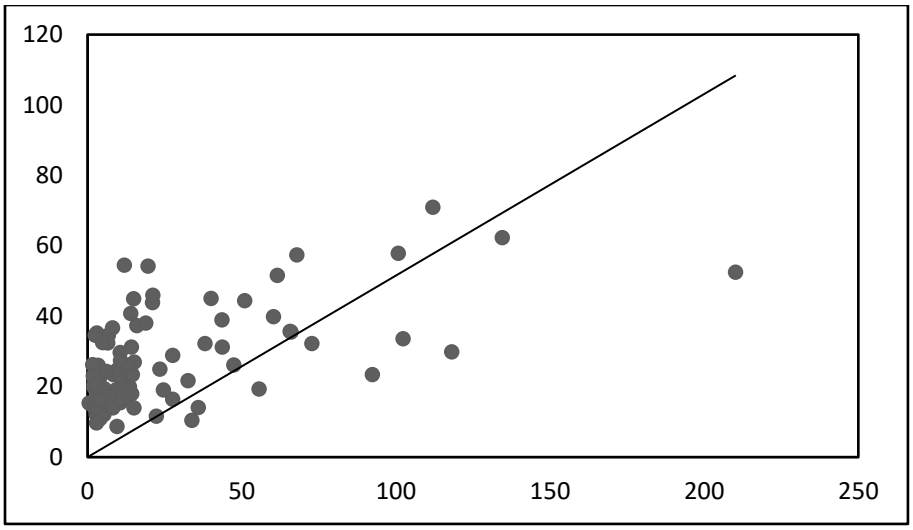

Figure 4.19 The relationship between the variations in the concentrations of sodium and chloride

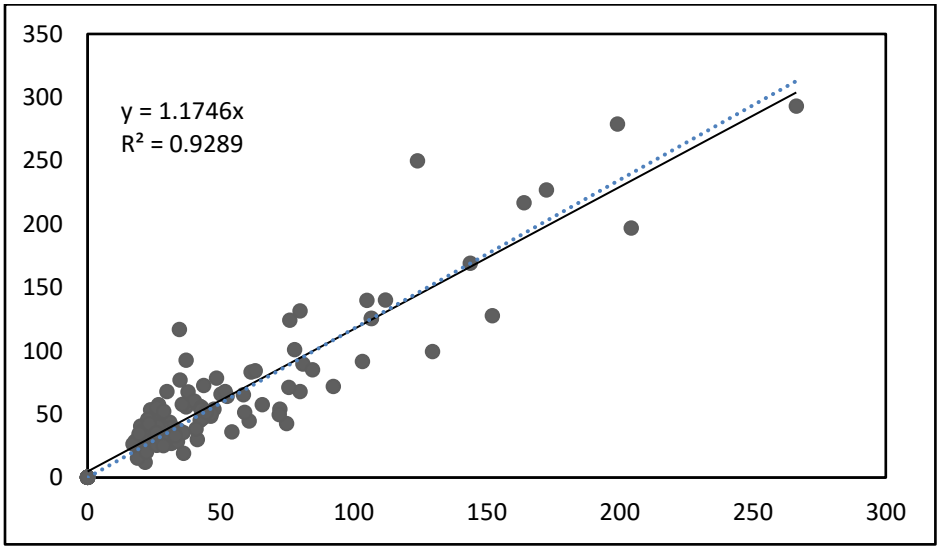

Figure 4.20 Influence of cation exchange in the hydrochemistry of groundwater in the study area

4.3.3 Modelling irrigation quality water in the study area

The overlay model was used to examine groundwater suitability for irrigation purposes. Total dissolved solids (TDS), Kelly's ratio (KR), Potential Salinity (PS), Sodium Absorption Ratio (SAR), Electrical Conductivity (EC), Magnesium Hazard (MH), and Residual Sodium Carbonate (RSC) were variables considered as the main influential

factors in determining the suitability of the groundwater for this purpose in the study area. SAR was ranked higher (16) in the ranking analysis, signifying that SAR is one of the major determinants among the selected variables. These parameters were visualized in thematic maps as shown in appendix A. Before running the overlay model, the thematic maps were reclassified into five classes with equal intervals, as shown in figure 4.21. Magnesium Hazard is the excess Magnesium ions in water resources that slow plant utilization of water in the soils. Thus if the sample is less than 50 (MH<50), it is suitable for irrigation; if it exceeds 50 (MH>50), it should be treated or not used for crops' irrigation. Appendix 6 showed that 12 samples (14.64 %) were above the 50 (MH>50) and the remaining 70 samples (85.36 %) were below the 50 (MH<1) and thus wholesome for irrigation. Potential Salinity (PS) is another water quality parameter-based index (Rawat *et al.*, 2018) for categorizing agricultural water. PS values ranging from 23 to 233 indicate the suitability of water for irrigation. Equation 3.10 was used to generate the temporal distribution of PS in the study area for both dry and rainy seasons. About 56% of the groundwater samples were within the prescribed limit, while the remaining 44% were not eligible for irrigation use. Figure 4.22 illustrates a suitability map for groundwater irrigation in terms of quality, which is divided into five categories: Excellent areas, very good areas, good areas less restricted areas, and extremely restricted areas. The zones of excellent groundwater irrigation have a land area of (507.88 Km^2), the zones of a very good class have a land area of (3277.99 Km^2), good areas were found to have an area of (790.21 Km^2), the restricted areas constituted an area of (24,21 Km2) and the zones of poor (extremely restricted) irrigation water have a land area of (1.11 Km^2).

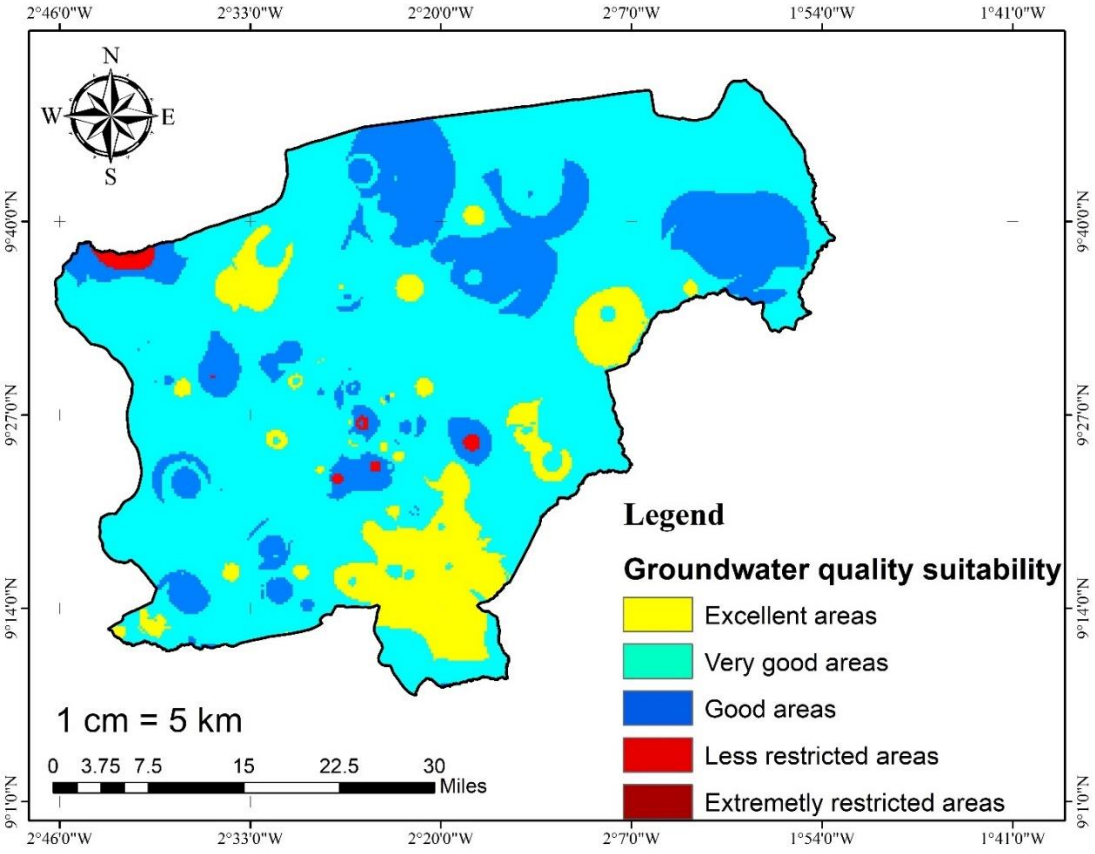

Figure 4.21 Spatial variation of Groundwater quality suitability in the study area

4.4 Prospecting for groundwater points for future irrigation schemes

4.4.1 Gbeniyiri

Table 4.8 and Figure 4.22 show resistivity information generated on the field during the Electrical Resistivity survey using the ABEM Terameter SAS 4000. The graph and table showed promising points for drilling. This is because areas of low resistivity are reported to have high yields of groundwater (Zainal Abidin *et al.*, 2017).

Table 4.8 summary of resistivity results at Gbenyiri

S/N	[1]a	[2]n	Electrode inner	Electrode out	Depth (m)	[3]Ls/m	Resistivity	[4]K	App Resistivity
1	2	1	1	3	2	0	264	1900	501600

2	2	3	3	5	4	10	214	1900	406600
3	2	5	5	7	6	20	224	1900	425600
4	4	3	6	10	8	30	177	1900	336300
5	4	5	10	14	12	40	187	1900	355300
6	4	7	14	18	16	50	198	1900	376200
7	10	3	15	25	20	60	232	1900	440800
8	10	4	20	30	25	70	215	1900	408500
9	10	5	25	35	30	80	174	1900	330600
10	10	6	30	40	35	90	177	1900	336300
11	10	7	35	45	40	100	190	1900	361000
12	10	8	40	50	45	110	40	1900	76000
13	20	4	40	60	50	120	153	1900	290700
14	20	5	50	70	60	130	167	1900	317300

[1]a = current electrodes [2]n = potential electrodes [3]Ls/m = profile intervals [4]K = geometric constant

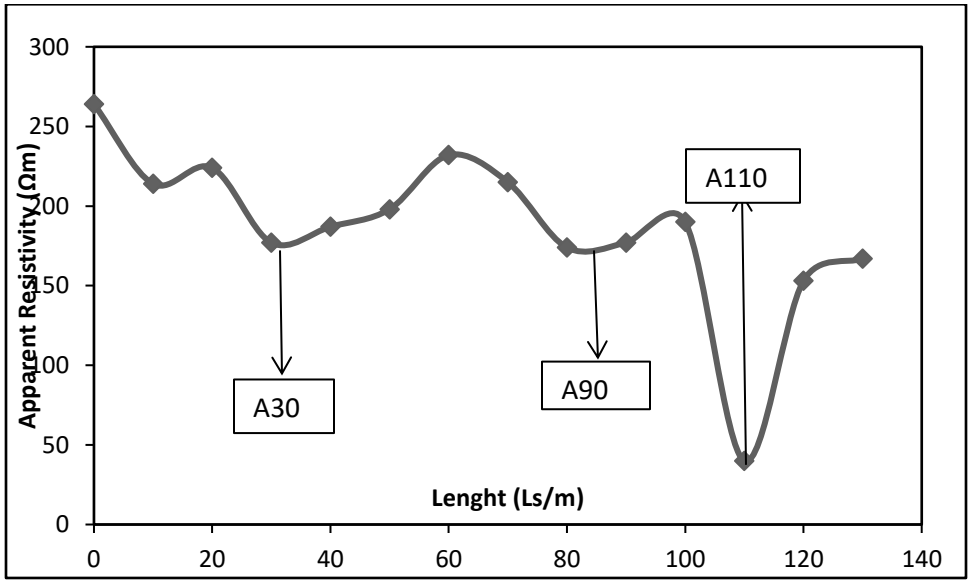

Figure 4.22 graph showing drilling points at Gbenyiri

From the graph, points marked A30 (09.26180 ºN, 02.42663 ºW, Elevation 346m) A90 (09.26211, 02.42618, Elevation 345m), and A110 (09.26230, 02.42603, Elevation 344m)

showed low resistivity areas with apparent resistivity values of 336300 Ωm, 76000 Ωm, and 336300 Ωm respectively which are comparable to results of Omolaiye *et al,* (2020) and Bayewu *et al.* (2018). In situations where resistivity starts to increase and decrease, it can also be considered suitable for groundwater exploration (Chegbeleh *et al.,* 2009).

4.4.2 Changbalayiri

At Changbalayiri, the field survey suggested that a good occurrence of groundwater can be extracted for irrigation schemes now or in the near future as shown in table 4.9.

Table 4.9 summary of resistivity results at Changbalayiri

S/N	[1]a	[2]n	Electrode inner	Electrode out	Depth (m)	[3]Ls/m	Resistivity	[4]K	App Resistivity
1	2	1	1	3	2	0	157	1.9	298.3
2	2	3	3	5	4	10	145	1.9	275.5
3	2	5	5	7	6	20	147	1.9	279.3
4	4	3	6	10	8	30	181	1.9	343.9
5	4	5	10	14	12	40	197	1.9	374.3
6	4	7	14	18	16	50	180	1.9	342
7	10	3	15	25	20	60	165	1.9	313.5
8	10	4	20	30	25	70	164	1.9	311.6
9	10	5	25	35	30	80	181	1.9	343.9
10	10	6	30	40	35	90	176	1.9	334.4
11	10	7	35	45	40	100	156	1.9	296.4
12	10	8	40	50	45	110	155	1.9	294.5
13	20	4	40	60	50	120	123	1.9	233.7
14	20	5	50	70	60	130	85	1.9	161.5
15	20	5	50	70	60	140	114	1.9	216.6
16	20	6	60	80	70	150	106	1.9	201.4

[1]a = current electrodes [2]n = potential electrodes [3]Ls/m = profile intervals [4]K = geometric constant

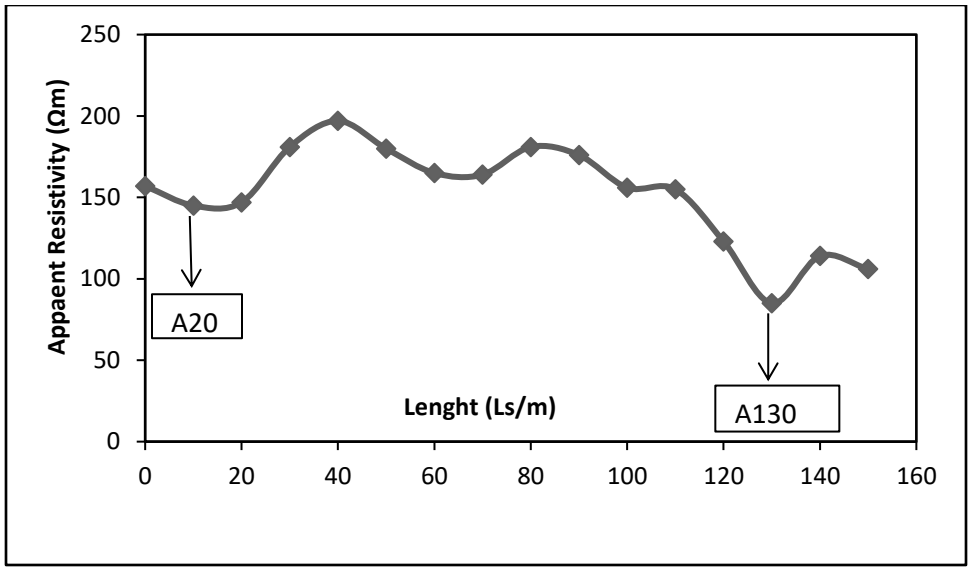

Figure 4.23 resistivity graph showing drill points at Changbalayiri

Two major groundwater points were discovered based on low apparent resistivity and field experience. These reference points were; A20 (09.26754, 02.42383, Elevation 328m) and A130 (09.26844 ºN, 02.42396 ºW, Elevation 328m) as in figure 4.23. For drilling purposes, it would be recommended to drill up to a depth of 80 m because the expected water strike is around 50 m - 60 m but the primary drilling point is A130. Results from this survey are in line with (John, 2014) and (Chegbeleh *et al.*, 2009).

4.4.3 Kaawie

The results of the survey at Kaawie are presented in table 4.10 and figure 4.24. Three groundwater points were discovered for a future irrigation scheme. The resistivity ranges from 0.038 Ωm – 100.7 Ωm but areas of low resistivity were considered for drilling and exploration as depicted in table 4.10 and figure 4.24. The groundwater points were A10, A130, and A280 with low resistivity of 19 Ωm, 0.14 Ωm, and 0152 Ωm respectively. The primary drilling point for A130 is closely related to previous research (Bayewu *et al.*, 2018; Seidu *et al.*, 2019). The GPS coordinates for these groundwater points are; A10 (09.28683,

02.5839, Elevation 237 m), A130 (09.28611, 2.58464, Elevation 238 m), and A280 (09.28325, 02.58358, Elevation 239 m).

Table 4.10 summary of resistivity results at Kaawie

S/N	[1]a	[2]n	Electrode inner	Electrode out	Depth (m)	[3]Ls/m	Resistivity	[4]K	App Resistivity
1	2	1	1	3	2	0	11	1.9	20.9
2	2	3	3	5	4	10	10	1.9	19
3	2	5	5	7	6	20	26	1.9	49.4
4	4	3	6	10	8	30	36	1.9	68.4
5	4	5	10	14	12	40	34	1.9	64.6
6	4	7	14	18	16	60	21	1.9	39.9
7	10	3	15	25	20	80	15	1.9	28.5
8	10	4	20	30	25	100	16	1.9	30.4
9	10	5	25	35	30	120	0.02	1.9	0.038
10	10	6	30	40	35	140	11	1.9	20.9
11	10	7	35	45	40	160	36	1.9	68.4
12	10	8	40	50	45	180	44	1.9	83.6
13	20	4	40	60	50	200	24	1.9	45.6
14	20	5	50	70	60	220	48	1.9	91.2
15	20	6	60	80	70	240	36	1.9	68.4
16	20	7	70	90	80	260	14	1.9	26.6
17	20	8	80	100	90	280	0.08	1.9	0.152
18	20	9	90	110	100	300	53	1.9	100.7

[1]a = current electrodes [2]n = potential electrodes [3]Ls/m = profile intervals [4]K = geometric constant

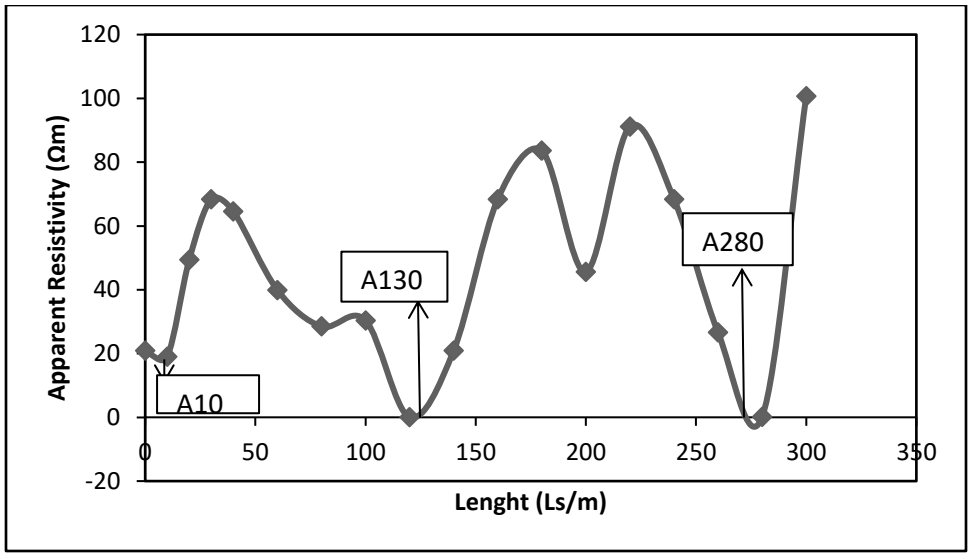

Figure 4.24 resistivity graph showing drilling points at Kaawie

4.4.4 Korle No.2

Table 4.11 and Figure 4.25 showed two different profiles adjacent to each other with the same profile length. The first profile indicates the possibility of groundwater about 10 m to 20 m away and for this reason, another profile was conducted 10 m away from the first profile. The essence of two separate profiles was to get more precision since the groundwater may be used on a larger scale. Figure 4.26 indicated overlapping of precision (have close resistivity) and hence the groundwater points discovered were A30 suggesting profile A and B130 suggesting profile B. The coordinates for the drill points were recorded as A30 (09.27663, 02.55705, Elevation 255 m) and B130 (09.27659, 02.55633, Elevation 256 m). Findings from this survey are in accordance with the literature (Riwayat *et al.*, 2018; Hasan *et al.*, 2019).

Table 4.11 summary of resistivity results at Korle No.2

S/N	a	n	Electrode inner	Electrode out	Depth (m)	Ls/m	Resis 1	Resis 2	K	App Resis 1	App Resis 2

1	2	1	1	3	2	0	654	846	1900	1242600	1607400
2	2	3	3	5	4	10	638	544	1900	1212200	1033600
3	2	5	5	7	6	20	548	492	1900	1041200	934800
4	4	3	6	10	8	30	423	617	1900	803700	1172300
5	4	5	10	14	12	40	499	709	1900	948100	1347100
6	4	7	14	18	16	50	615	877	1900	1168500	1666300
7	10	3	15	25	20	60	660	1.56	1900	1254000	2964
8	10	4	20	30	25	70	702	2.14	1900	1333800	4066
9	10	5	25	35	30	80	821	1.07	1900	1559900	2033
10	10	6	30	40	35	90	799	1.13	1900	1518100	2147
11	10	7	35	45	40	100	758	720	1900	1440200	1368000
12	10	8	40	50	45	110	801	744	1900	1521900	1413600
13	20	4	40	60	50	120	840	788	1900	1596000	1497200

[1]a = current electrodes [2]n = potential electrodes [3]Ls/m = profile intervals [4]K = geometric constant

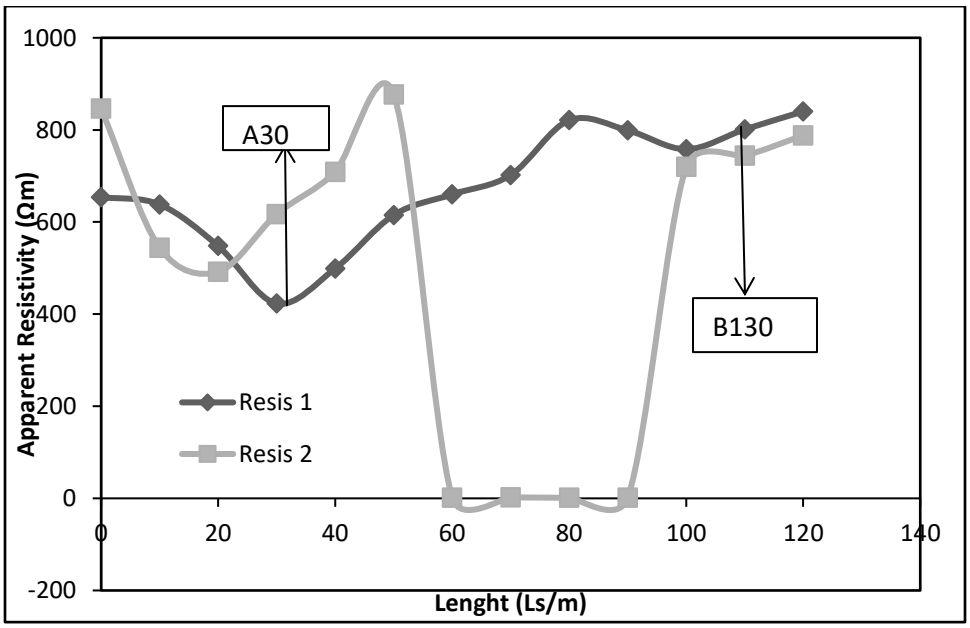

Figure 4.25 resistivity graph showing drilling points at Korle No.2

4.4.5 Monah

At Monah, three groundwater points were discovered based on low resistivity and field experience. The points A50, A70, and A170 on the graph are areas of low resistivity which indicate fractured and weathered zones, implying the presence of groundwater accordingly as in table 4.12 and figure 4.26. The low resistivity values for these points are 385.7 Ωm, 361 Ωm, and 155.8 Ωm respectively, with the primary drill point being A170 which is familiar with the study of Omolaiye *et al*. (2020) and Sahu & Sikdar (2008). The reference coordinates were A50 (09.32197, 02.43130, Elevation 304 m, A70 (09.32204, 02.43113, Elevation 305 m), and A170 (09.32067, 02.43253, Elevation 307 m).

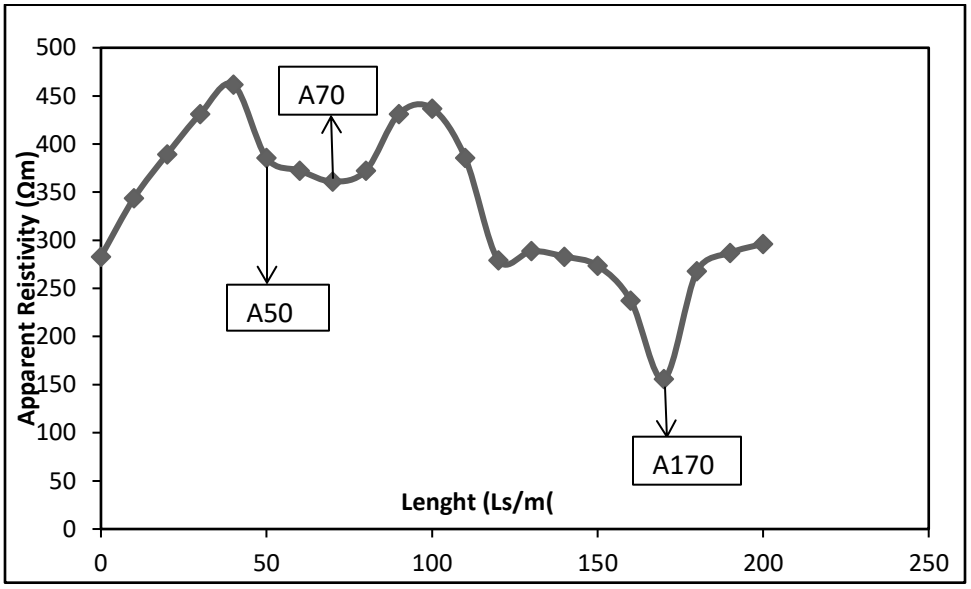

Figure 4.26 resistivity graph showing drilling points at Monah

Table 4.12 summary of resistivity results at Monah

S/N	[1]a	[2]n	Electrode inner	Electrode out	Depth (m)	[3]Ls/m	Resistivity	[4]K	App Resistivity
1	2	1	1	3	2	0	149	1.9	283.1
2	2	3	3	5	4	10	181	1.9	343.9
3	2	5	5	7	6	20	205	1.9	389.5
4	4	3	6	10	8	30	227	1.9	431.3
5	4	5	10	14	12	40	243	1.9	461.7
6	4	7	14	18	16	50	203	1.9	385.7
7	10	3	15	25	20	60	196	1.9	372.4
8	10	4	20	30	25	70	190	1.9	361
9	10	5	25	35	30	80	196	1.9	372.4
10	10	6	30	40	35	90	227	1.9	431.3
11	10	7	35	45	40	100	230	1.9	437
12	10	8	40	50	45	110	203	1.9	385.7
13	20	4	40	60	50	120	147	1.9	279.3
14	20	5	50	70	60	130	152	1.9	288.8
15	20	6	60	80	70	140	149	1.9	283.1
16	20	7	70	90	80	150	144	1.9	273.6
17	20	8	80	100	90	160	125	1.9	237.5
18	20	9	90	110	100	170	82	1.9	155.8
19	20	11	110	130	120	180	141	1.9	267.9
20	20	13	130	150	140	190	151	1.9	286.9
21	20	15	150	170	160	200	156	1.9	296.4

[1]a = current electrodes [2]n = potential electrodes [3]Ls/m = profile intervals [4]K = geometric constant

4.4.6 Yipala

Unlike Korle No.2 the distance between the two profiles at the Yipala was far apart and there was no correlation in values (see table 4.13a and figure 4.27a). The first profile (A)

showed one point promising to be of high yield, which is A60 with reference coordinates of 09.573084 ºN, 02.4144 ºW, Elevation 313 m). Also, two (2) groundwater points were discovered on the second profile (B) as in table 4.13b and figure 4.27b, which were B100 and B150 with GPS coordinates of (09.57398 ºN, 02.41244 ºW, Elevation 316m) and (09.57380 ºN, 02.41326 ºW, Elevation 316m). Results from this study are however in line with previous research (Chegbeleh *et al.*, 2009; Mohamaden *et al.*, 2016).

Table 4.13a Summary of resistivity results at Yipala (A)

Profile A

S/N	[1]a	[2]n	Electrode inner	Electrode out	Depth (m)	[3]Ls/m	Resis	[4]K	App Resis
1	2	1	1	3	2	0	718	1900	1364200
2	2	3	3	5	4	10	499	1900	948100
3	2	5	5	7	6	20	467	1900	887300
4	4	3	6	10	8	30	541	1900	1027900
5	4	5	10	14	12	40	627	1900	1191300
6	4	7	14	18	16	50	590	1900	1121000
7	10	3	15	25	20	60	414	1900	786600
8	10	4	20	30	25	70	419	1900	796100
9	10	5	25	35	30	80	647	1900	1229300
10	10	6	30	40	35	90	739	1900	1404100
11	10	7	35	45	40	100	775	1900	1472500
12	10	8	40	50	45	110	1.08	1900	2052
13	20	4	40	60	50	120	1.232	1900	2340.8
14	20	5	50	70	60	130	0.984	1900	1869.6
15	20	6	60	80	70	140	0.832	1900	1580.8

[1]a = current electrodes [2]n = potential electrodes [3]Ls/m = profile intervals [4]K = geometric constant

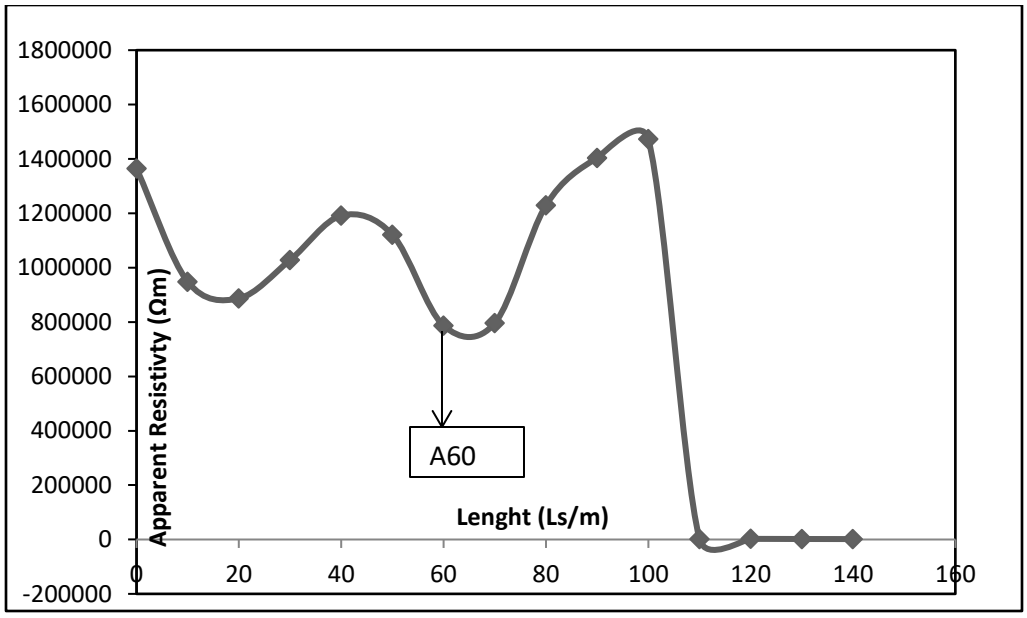

Figure 4.27a resistivity graph showing drilling points at Yipala (A)

Table 4.13b Summary of resistivity results at Yipala (B)

Profile B

S/N	[1]a	[2]n	Electrode inner	Electrode out	Depth (m)	[3]Ls/m	Resis	[4]K	App Resis
1	2	1	1	3	2	0	519	1900	986100
2	2	3	3	5	4	10	471	1900	894900
3	2	5	5	7	6	20	882	1900	1675800
4	4	3	6	10	8	30	951	1900	1806900
5	4	5	10	14	12	40	602	1900	1143800
6	4	7	14	18	16	50	601	1900	1141900
7	10	3	15	25	20	60	560	1900	1064000
8	10	4	20	30	25	70	688	1900	1307200
9	10	5	25	35	30	80	941	1900	1787900
10	10	6	30	40	35	90	720	1900	1368000
11	10	7	35	45	40	100	374	1900	710600
12	10	8	40	50	45	110	534	1900	1014600
13	20	4	40	60	50	120	542	1900	1029800
14	20	5	50	70	60	130	302	1900	573800

15	20	6	60	80	70	140	102	1900	193800
16	20	7	70	90	80	150	53	1900	100700
17	20	8	80	100	90	160	98	1900	186200

[1]a = current electrodes [2]n = potential electrodes [3]Ls/m = profile intervals [4]K = geometric constant

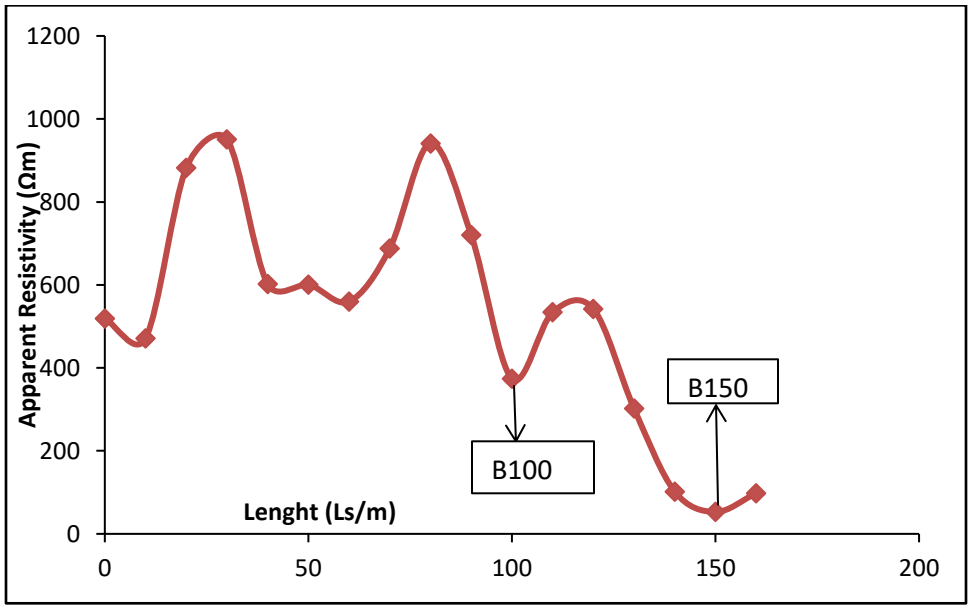

Figure 4.27b resistivity graph showing drilling points at Yipala (B)

4.4.7 Sindaa

At Sindaa three groundwater points were found based on low resistivity as seen in figure 4.28 and table 4.14. The groundwater points found were A60, A130, and A160 with low resistivity values of 2017 Ωm, 1.16 Ωm, and 244 Ωm respectively which are consistent with past studies (Bayewu *et al.*, 2018; Riwayat *et al.*, 2018). The reference coordinates for the drill points are; A60 (09.5784 ºN, 02.21641 ºW, Elevation 203 m), A130 (09.5749 ºN, 02.4209 ºW, Elevation 203 m), and A160 (09.5756 ºN, 02.4211 ºW, Elevation 204 m) with A60 as the primary drill point similar to of John (2014).

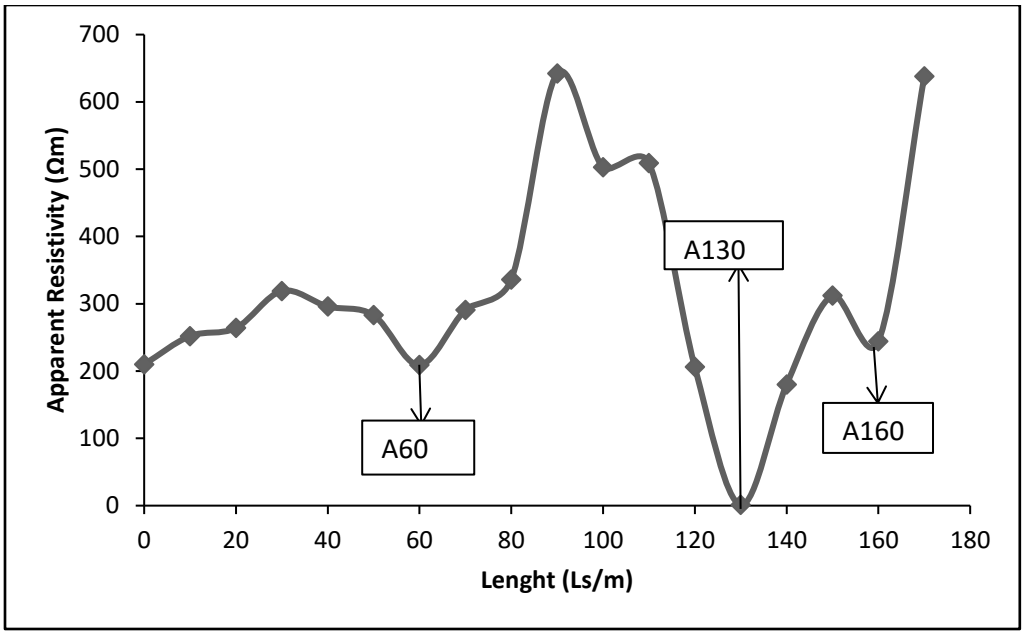

Figure 4.28 resistivity graph showing drilling points at Sindaa

Table 4.14 Summary of resistivity results at Sindaa

S/N	[1]a	[2]n	Electrode inner	Electrode out	Depth (m)	[3]Ls/m	Resis	[4]K	App Resis
1	2	1	1	3	2	0	210	1900	399000
2	2	3	3	5	4	10	252	1900	478800
3	2	5	5	7	6	20	264	1900	501600
4	4	3	6	10	8	30	319	1900	606100
5	4	5	10	14	12	40	296	1900	562400
6	4	7	14	18	16	50	283	1900	537700
7	10	3	15	25	20	60	209	1900	397100
8	10	4	20	30	25	70	291	1900	552900
9	10	5	25	35	30	80	336	1900	638400
10	10	6	30	40	35	90	642	1900	1219800
11	10	7	35	45	40	100	503	1900	955700
12	10	8	40	50	45	110	509	1900	967100
13	20	4	40	60	50	120	206	1900	391400
14	20	5	50	70	60	130	1.16	1900	2204

15	20	6	60	80	70	140	180	1900	342000
16	20	7	70	90	80	150	312	1900	592800
17	20	8	80	100	90	160	244	1900	463600
18	20	9	90	110	100	170	638	1900	1212200

[1]a = current electrodes [2]n = potential electrodes [3]Ls/m = profile intervals [4]K = geometric constant

4.4.8 Sawla Yipala

The resistivity results in figure 4.29 and table 4.15 suggest that A120 will be a promising point for groundwater exploration for irrigation with a low value of 457.9 Ωm. This point was picked and pegged with GPS coordinates of A120 (09.28305 ºN, 02.41360 ºW, Elevation 326 m) consistently with (Chegbeleh *et al.*, 2009). It is strongly advised to drill during the dry season because the community roads deteriorate slightly during heavy rains.

Table 4.15 summary of resistivity results at Sawla Yipala

S/N	[1]a	[2]n	Electrode inner	Electrode out	Depth (m)	[3]Ls/m	Resis	[4]K	App Resis
1	2	1	1	3	2	0	0.43	1900	817
2	2	3	3	5	4	10	0.374	1900	710.6
3	2	5	5	7	6	20	0.749	1900	1423.1
4	4	3	6	10	8	30	1.45	1900	2755
5	4	5	10	14	12	40	1.4	1900	2660
6	4	7	14	18	16	50	0.35	1900	665
7	10	3	15	25	20	60	0.93	1900	1767
8	10	4	20	30	25	70	0.418	1900	794.2
9	10	5	25	35	30	80	0.415	1900	788.5
10	10	6	30	40	35	90	2.33	1900	4427
11	10	7	35	45	40	100	0.817	1900	1552.3
12	10	8	40	50	45	110	0.271	1900	514.9
13	20	4	40	60	50	120	0.241	1900	457.9

14	20	5	50	70	60	130	0.355	1900	674.5
15	20	6	60	80	70	140	0.278	1900	528.2
16	20	7	70	90	80	150	0.212	1900	402.8
17	20	8	80	100	90	160	0.322	1900	611.8

[1]a = current electrodes [2]n = potential electrodes [3]Ls/m = profile intervals [4]K = geometric constant

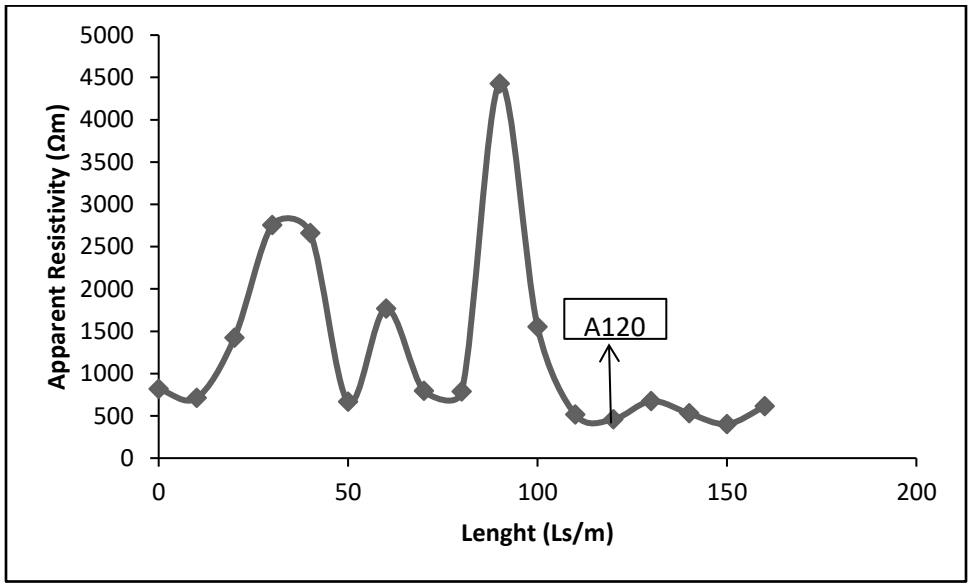

Figure 4.29 resistivity graph showing drilling point at Sawla Yipala

4.4.9 Cbaalyiri

Table 4.16 and figure 4.30 show two different profiles adjacent to each other with the same profile lengths. The reason for the two profiles (A and B) was that the first profile indicated the possibility of groundwater about 5 m to 15 m away; thus, another profile was conducted 10 m away from the first profile. The primary purpose for this was to delineate a zone that is high yielding while comparing to the first profile. Figure 4.30 indicates overlapping of precision (have close resistivity) and hence the groundwater points were A20 (for profile A) and B60 (for profile B) which is following John (2014) in a study around the Sunyani areas. The coordinates for the drill points were recorded as A20 (09.98447 ºN, 02.12811

ºW, Elevation 314 m) and B60 (09.8996 ºN, 02.1293 ºW, Elevation 315 m). The study reflects the similarity in results of previous research works (Hasan *et al.*, 2019; Seidu *et al.*, 2019).

Table 4.16 summary of resistivity results at Cbaalyiri

[1]a	[2]n	Electrode inner	Electrode out	Depth (m)	[3]Ls/m	Resis 1	Resis 2	[4]K	App Resis 1	App Resis 2
2	1	1	3	2	0	7	13	1900	13300	24700
2	3	3	5	4	10	7	15	1900	13300	28500
2	5	5	7	6	20	6	7	1900	11400	13300
4	3	6	10	8	30	7	9	1900	13300	17100
4	5	10	14	12	40	8	10	1900	15200	19000
4	7	14	18	16	50	9	13	1900	17100	24700
10	3	15	25	20	60	10	11	1900	19000	20900
10	4	20	30	25	70	11	14	1900	20900	26600
10	5	25	35	30	80	12	14	1900	22800	26600
10	6	30	40	35	90	12	15	1900	22800	28500
10	7	35	45	40	100	11	12	1900	20900	22800
10	8	40	50	45	110	11	11	1900	20900	20900
20	4	40	60	50	120	11	10	1900	20900	19000

[1]a = current electrodes [2]n = potential electrodes [3]Ls/m = profile intervals [4]K = geometric constant

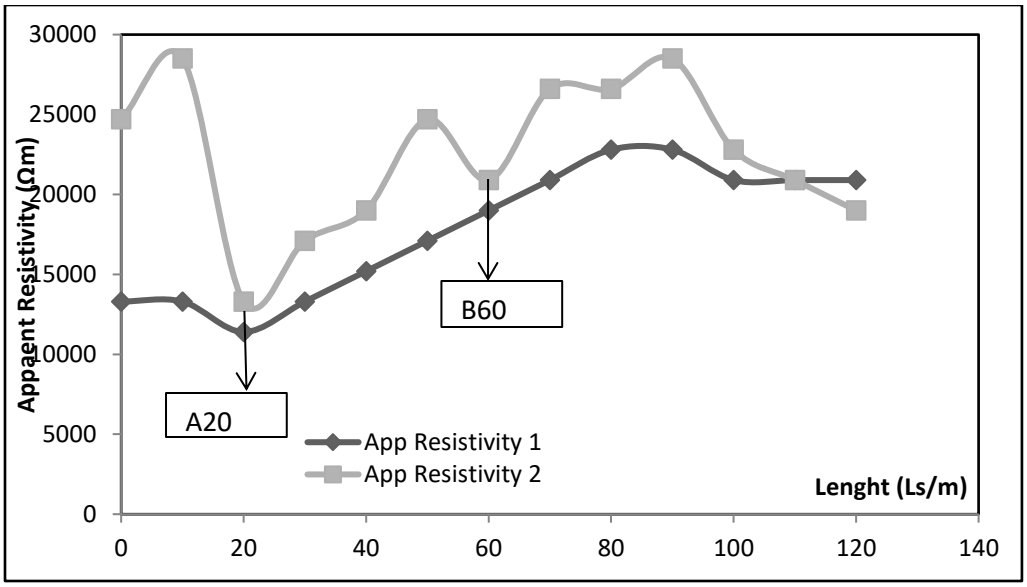

Figure 4.30 resistivity graph showing drilling points at Cbaalyiri

CHAPTER FIVE

CONCLUSION AND RECOMMENDATIONS

5.0 Overview

This chapter presents the conclusion and recommendations of the study.

5.1 Conclusion

The resistivity results from the Sawla Tuna Kalba District revealed that the lithological structure is predominantly Precambrian and Paleozoic units. The Precambrian units were metamorphic rocks, granites, meta-sedimentary rock, and others, while the Paleozoic units consisted of shales, volcanic rocks, mudstones, siltstones, and others. The groundwater potential of the area showed that about 90% of the study area has groundwater and can be explored for irrigation purposes. The storage capacity and extractable capacity of groundwater (24.7×10^3 Km^3 and 9.8×10^3 Km^3) in the study area indicates a high untapped resource and hence can support irrigation using tomato and maize. Also, the computed Irrigation Water Requirements suggests that the extractable groundwater storage can irrigate up to 143.6 Km^2 (14,360 ha) of land for tomatoes and 19.6 Km^2 (19,620 ha) for maize respectively. A large portion of the study area (3277.99 Km^2) shows good groundwater quality. In this context, it shows that the quality of groundwater in the study area meets the acceptable limits of the World Health Organization (WHO, 2003), hence recommendable for irrigation. The groundwater points picked for future exploration were discovered and geographically referenced. These points can guide and inform decision-makers in terms of groundwater exploration for irrigation in the area.

5.2 Recommendations

Based on the findings of this research, the following are recommended:

I. An in-depth hydro-geophysical survey should be carried out for the remaining communities to get a general perspective of the geological units of the Sawla Tuna Kalba District.

II. The cost of groundwater exploration is considered expensive and therefore different methodologies should be used in producing the groundwater potential maps for a better assessment. Some of these methodologies include; fuzzy logic (gamma overlay), Analytic Hierarchy Process (AHP), Multi-criteria Decision Analysis, and many more.

III. Groundwater quality in the study area should be monitored regularly to ensure early detection and intervention of any pollution or contamination that may occur due to the susceptibility of the regional aquifer system to pollution (weedicides, pesticides, etc.).

IV. It will be important to cross-validate the groundwater points discovered with other geophysical methods like the magnetic and seismic methods in the future for groundwater exploration

V. Further research should be conducted to estimate the safe yield of the aquifer in the study area to know the volume of water that can be abstracted and readily available for irrigation and its sustainability.

VI. Further research should be conducted in developing a groundwater model to integrate all variables into the determination of outputs such as crop and irrigation water requirements and the irrigable area.

REFERENCE

Abanyie, S. K., Sunkari, E. D., Apea, O. B., Abagale, S., & Korboe, H. M. (2020). Assessment of the quality of water resources in the Upper East Region, Ghana: a review. *Sustainable Water Resources Management*, *6*(4). https://doi.org/10.1007/s40899-020-00409-4

Abd El-Gawad, A. M. S., Helaly, A. S., & Abd El-Latif, M. S. E. (2018). Application of geoelectrical measurements for detecting the ground-water seepage in clay quarry at Helwan, southeastern Cairo, Egypt. *NRIAG Journal of Astronomy and Geophysics*, *7*(2), 377–389. https://doi.org/10.1016/j.nrjag.2018.04.003

Abdalla, F., Moubark, K., & Abdelkareem, M. (2020). Groundwater potential mapping using GIS, linear weighted combination techniques and geochemical processes identification, west of the Qena area, Upper Egypt. *Journal of Taibah University for Science*, *14*(1), 1350–1362. https://doi.org/10.1080/16583655.2020.1822646

Abdul-ganiyu, S., & Prosper, K. (2020). *Hydrogeological Study of Groundwater for Dry Season Farming in Northern Region of Ghana*.

Abdul-Ganiyu, S., & Prosper, K. (2021). Estimating the groundwater storage for future irrigation schemes. *Water Supply*, 1–15. https://doi.org/10.2166/ws.2021.041

Abdul-ganiyu, S., Prosper, K., & Africa, W. (2020). *Groundwater Resources as a Resilient Alternative for Irrigation in the Upper West Region of Ghana – A Study of Groundwater Potential*. *5*(6).

Abidin, M. H. Z., Saad, D. R., Ahmad, F., Wijeyesekera, D. C., & Baharuddin, E. M. F. T. (2011). Application of Geophysical Methods in Civil Engineering. *International Conference on Engineering & Technology, November 2015*, 1–12.

Abudulawal, L., Amidu, S. A., & Adeagbo, O. A. (2017). *Overburden Thickness and Potential Tonnage Estimate of Olode-Gbayo Pegmatite Deposit , Southwestern Nigeria , Using Electrical Resistivity Method*. https://doi.org/10.9734/JGEESI/2017/32811

Adam, A. B., & Appiah-Adjei, E. K. (2019). Groundwater potential for irrigation in the Nabogo basin, Northern Region of Ghana. *Groundwater for Sustainable Development*, *9*(August),

100274. https://doi.org/10.1016/j.gsd.2019.100274

Adamo, N., Al-ansari, N., Sissakian, V., & Laue, J. (2020). *Geophysical Methods and their Applications in Dam Safety Monitoring*. *11*(1), 291–345.

Adeyeye, O. A., Ikpokonte, E. A., & Arabi, S. A. (2019). GIS-based groundwater potential mapping within Dengi area, North Central Nigeria. *Egyptian Journal of Remote Sensing and Space Science*, *22*(2), 175–181. https://doi.org/10.1016/j.ejrs.2018.04.003

Africa, S., Development, S. A., Acyl, F., Free, T., Area, T., Summit, T., Committee, T. S., Tfta, T., Community, E. A., African, S., Community, D., Market, C., Africa, S., Africa, S., Union, A., Tfta, T., Fta, G., Summit, T., Secretary, C., … Summary, E. (2020). No 主観的健康感を中心とした在宅高齢者における　健康関連指標に関する共分散構造分析Title. *Human Relations*, *3*(1), 1–8. http://search.ebscohost.com/login.aspx?direct=true&AuthType=ip,shib&db=bth&AN=92948285&site=eds-live&scope=site%0Ahttp://bimpactassessment.net/sites/all/themes/bcorp_impact/pdfs/em_stakeholder_engagement.pdf%0Ahttps://www.glo-bus.com/help/helpFiles/CDJ-Pa

Aizebeokhai, A. P. (2010). 2D and 3D geoelectrical resistivity imaging: Theory and field design. *Scientific Research and Essays*, *5*(23), 3592–3605.

Allred, B., & Redman, J. D. (2009). Assessment of agricultural drainage pipe conditions using ground penetrating radar. *Proceedings of the Symposium on the Application of Geophyics to Engineering and Environmental Problems, SAGEEP*, *2*, 932–947. https://doi.org/10.4133/1.3176785

Anku, Y. S., Banoeng-Yakubo, B., Asiedu, D. K., & Yidana, S. M. (2009). Water quality analysis of groundwater in crystalline basement rocks, Northern Ghana. *Environmental Geology*, *58*(5), 989–997. https://doi.org/10.1007/s00254-008-1578-4

Anornu, G. K., Kortatsi, B. K., & Saeed, Z. M. (2009). Evaluation of groundwater resources potential in the Ejisu-Juaben district of Ghana. *African Journal of Environmental Science and Technology*, *3*(10), 332–340. https://doi.org/10.5897/AJEST09.048

Arabi, J., Judson, M. L. I., Deharveng, L., Lourenço, W. R., Cruaud, C., & Hassanin, A. (2012). Nucleotide composition of CO1 sequences in Chelicerata (arthropoda): Detecting new mitogenomic rearrangements. *Journal of Molecular Evolution*, *74*(1–2), 81–95. https://doi.org/10.1007/s00239-012-9490-7

Arjwech, R., Everett, M. E., Saengchomphu, S., Somchat, K., & Pondthai, P. (2021). *Geophysical mapping of gypsum for exploration of reserves in the Nong Bua area of Thailand*. *54*.

Arumugam, K., & Elangovan, K. (2009). Hydrochemical characteristics and groundwater quality assessment in Tirupur region, Coimbatore District, Tamil Nadu, India. *Environmental Geology*, *58*(7), 1509–1520. https://doi.org/10.1007/s00254-008-1652-y

At, P., & Fields, O. V. (2020). *APPLICATION OF GEOPHYSICAL METHODS IN FOUNDATION INVESTIGATION FOR CONSTRUCTION*. *8*(3), 121–147.

Bahri, F., & Saibi, H. (2010). Characterisation, classification, and evaluation of some groundwater samples in the Mostaganem area of northwestern Algeria. *Arabian Journal of Geosciences*, *3*(1), 79–89. https://doi.org/10.1007/s12517-009-0062-0

Bayewu, O. O., Oloruntola, M. O., Mosuro, G. O., Laniyan, T. A., Ariyo, S. O., & Fatoba, J. O. (2018). Assessment of groundwater prospect and aquifer protective capacity using resistivity method in Olabisi Onabanjo University campus, Ago-Iwoye, Southwestern Nigeria. *NRIAG Journal of Astronomy and Geophysics*, *7*(2), 347–360. https://doi.org/10.1016/j.nrjag.2018.05.002

Belkhiri, L., Boudoukha, A., Mouni, L., & Baouz, T. (2010). Multivariate statistical characterization of groundwater quality in Ain Azel plain, Algeria. *African Journal of Environmental Science and Technology*, *4*(8), 526–534. https://doi.org/10.5897/AJEST10.003

Benoit, S., Ghysels, G., Gommers, K., Hermans, T., Nguyen, F., & Huysmans, M. (2019). Characterization of spatially variable riverbed hydraulic conductivity using electrical resistivity tomography and induced polarization. *Hydrogeology Journal*, *27*(1), 395–407. https://doi.org/10.1007/s10040-018-1862-7

Birkenholtz, T. (2017). Assessing India's drip-irrigation boom: efficiency, climate change and groundwater policy. *Water International*, *42*(6), 663–677. https://doi.org/10.1080/02508060.2017.1351910

Bodrud-Doza, M., Islam, S. M. D. U., Rume, T., Quraishi, S. B., Rahman, M. S., & Bhuiyan, M. A. H. (2020). Groundwater quality and human health risk assessment for safe and sustainable water supply of Dhaka City dwellers in Bangladesh. *Groundwater for Sustainable Development*, *10*. https://doi.org/10.1016/J.GSD.2020.100374

Bruce, B. Y., Yidana, S. M., Anku, Y., Akabzaa, T., & Asiedu, D. (2009). Water quality characterization in some birimian aquifers of the Birim Basin, Ghana. *KSCE Journal of Civil Engineering*, *13*(3), 179–187. https://doi.org/10.1007/s12205-009-0179-4

Chaudhary, V., & Satheeshkumar, S. (2018). Assessment of groundwater quality for drinking and irrigation purposes in arid areas of Rajasthan, India. *Applied Water Science*, *8*(8), 1–17. https://doi.org/10.1007/s13201-018-0865-9

Chegbeleh, L. P., Akurugu, B. A., & Yidana, S. M. (2020). Assessment of Groundwater Quality in the Talensi District, Northern Ghana. *Scientific World Journal*, *2020*. https://doi.org/10.1155/2020/8450860

Cheng, Q., Tao, M., Chen, X., & Binley, A. (2019). Evaluation of electrical resistivity tomography (ERT) for mapping the soil–rock interface in karstic environments. *Environmental Earth Sciences*, *78*(15), 1–14. https://doi.org/10.1007/s12665-019-8440-8

Dahlin, T., & H. Loke, M. (2014). *Quasi-3D resistivity imaging - mapping of three dimensional structures using two dimensional DC resistivity techniques*. 3–6. https://doi.org/10.3997/2214-4609.201407298

Dampney, P. M. R., King, J. a., Lark, R. M., Wheeler, H. C., Bradley, R. I., & Mayr, T. R. (2004). Non-intrusive sensors for measuring soil physical properties. *HGCA Conference 2004: Managing Soil and Roots for Profitable Production*, 1–7.

David Ndegwa Kuria. (2012). Mapping groundwater potential in Kitui District, Kenya using geospatial technologies. *International Journal of Water Resources and Environmental*

Engineering, *4*(1), 15–22. https://doi.org/10.5897/ijwree11.119

Dehnavi, A. G. (2018). Hydrochemical assessment of groundwater using statistical methods and ionic ratios in Aliguodarz , Lorestan , west of Iran. *Journal of Advances in Environmental Health Research*, 193–201. https://doi.org/10.22102/JAEHR.2018.137767.1091

Díaz-Alcaide, S., & Martínez-Santos, P. (2019). Review: Advances in groundwater potential mapping. *Hydrogeology Journal*, *27*(7), 2307–2324. https://doi.org/10.1007/s10040-019-02001-3

Dong, C., Schoups, G., & Van de Giesen, N. (2013). Scenario development for water resource planning and management: A review. *Technological Forecasting and Social Change*, *80*(4), 749–761. https://doi.org/10.1016/j.techfore.2012.09.015

Duc Vu, M., Xayavong, V., Anh Do, C., Thanh Pham, L., Gómez-Ortiz, D., & Eldosouky, A. M. (2021). Application of the improved multi-electrode electrical exploration methods for groundwater investigation in Vientiane Province, Laos. *Journal of Asian Earth Sciences: X*, *5*, 100056. https://doi.org/10.1016/J.JAESX.2021.100056

Elmahdy, S., Mohamed, M., & Ali, T. (2020). Land use/land cover changes impact on groundwater level and quality in the northern part of the United Arab Emirates. *Remote Sensing*, *12*(11). https://doi.org/10.3390/rs12111715

Espindola Canata, R., Fonseca Ferreira, F. J., Rodrigues Borges, W., & Da Silva Salvador, F. A. (2020). Analysis of 2d and 3d gpr responses in the federal university of paranÁ forensic geophysics controlled site-a case study. *Revista Brasileira de Geofisica*, *38*(2), 1–19. https://doi.org/10.22564/rbgf.v38i2.2045

Etikala, B., Golla, V., Adimalla, N., & Marapatla, S. (2019). Factors controlling groundwater chemistry of Renigunta area, Chittoor District, Andhra Pradesh, South India: A multivariate statistical approach. *HydroResearch*, *1*, 57–62. https://doi.org/10.1016/j.hydres.2019.06.002

Ewaid, S. H., Abed, S. A., & Al-Ansari, N. (2019). Crop water requirements and irrigation schedules for some major crops in southern Iraq. *Water (Switzerland)*, *11*(4).

https://doi.org/10.3390/w11040756

Ewida, A. Y. I., Khalil, M., & Ammar, A. (2020). Impact of Domestic Wastewater Treatment Plants on the Quality of Shallow Groundwater in Qalyubia, Egypt; Discrimination of Microbial Contamination Source Using BOX-PCR. *Egyptian Journal of Botany*, *0*(0), 0–0. https://doi.org/10.21608/ejbo.2020.30986.1505

Faroque, S., & South, N. (2021). Water pollution and environmental injustices in Bangladesh. *International Journal for Crime, Justice and Social Democracy*, *10*(2). https://doi.org/10.5204/IJCJSD.2006

Fenta, M. C., Anteneh, Z. L., Szanyi, J., & Walker, D. (2020). Hydrogeological framework of the volcanic aquifers and groundwater quality in Dangila Town and the surrounding area, Northwest Ethiopia. *Groundwater for Sustainable Development*, *11*(April). https://doi.org/10.1016/j.gsd.2020.100408

Ganiyu, S. A., Olurin, O. T., Oladunjoye, M. A., & Badmus, B. S. (2020). Investigation of soil moisture content over a cultivated farmland in Abeokuta Nigeria using electrical resistivity methods and soil analysis. *Journal of King Saud University - Science*, *32*(1), 811–821. https://doi.org/10.1016/j.jksus.2019.02.016

Gebbers, R., & Lück, E. (2005). Comparison of geoelectrical methods for soil mapping. *Precision Agriculture 2005, ECPA 2005, May*, 473–479. https://doi.org/10.13140/RG.2.1.3435.9201

George, R., Branch, W. P., & Environment, A. (2009). *Overview*.

Giordano, M. (2006). Agricultural groundwater use and rural livelihoods in sub-Saharan Africa: A first-cut assessment. *Hydrogeology Journal*, *14*(3), 310–318. https://doi.org/10.1007/s10040-005-0479-9

Gong, X., Wang, S., Xu, C., Zhang, H., & Ge, J. (2020). Evaluation of several reference evapotranspiration models and determination of crop water requirement for tomato in a solar greenhouse. *HortScience*, *55*(2), 244–250. https://doi.org/10.21273/HORTSCI14514-19

Gracia-de-Rentería, P., Barberán, R., & Mur, J. (2020). The groundwater demand for industrial uses in areas with access to drinking publicly-supplied water: A microdata analysis. *Water (Switzerland)*, *12*(1), 1–16. https://doi.org/10.3390/w12010198

Grogan, D. S., Wisser, D., Prusevich, A., Lammers, R. B., & Frolking, S. (2017). The use and re-use of unsustainable groundwater for irrigation: A global budget. *Environmental Research Letters*, *12*(3). https://doi.org/10.1088/1748-9326/aa5fb2

Gunn, D. A., Chambers, J. E., Uhlemann, S., Wilkinson, P. B., Meldrum, P. I., Dijkstra, T. A., Haslam, E., Kirkham, M., Wragg, J., Holyoake, S., Hughes, P. N., Hen-Jones, R., & Glendinning, S. (2015). Moisture monitoring in clay embankments using electrical resistivity tomography. *Construction and Building Materials*, *92*(August), 82–94. https://doi.org/10.1016/j.conbuildmat.2014.06.007

Guo, Z. (2020). Electromagnetic methods for mineral exploration in China : A review Electromagnetic methods for mineral exploration in China : A review. *Ore Geology Reviews*, *118*(March), 103357. https://doi.org/10.1016/j.oregeorev.2020.103357

Hasan, M., Shang, Y. jun, Jin, W. jun, & Akhter, G. (2019). Investigation of fractured rock aquifer in South China using electrical resistivity tomography and self-potential methods. *Journal of Mountain Science*, *16*(4), 850–869. https://doi.org/10.1007/s11629-018-5207-8

HASRA HARTINA. (2017). нской организации по разделу «Эпидемиологическая безопасностьNo Title. *Manajemen Asuhan Kebidanan Pada Bayi Dengan Caput Succedaneum Di Rsud Syekh Yusuf Gowa Tahun*, *4*, 9–15.

Hassan, I., Kalin, R. M., White, C. J., & Aladejana, J. A. (2019). Hydrostratigraphy and hydraulic characterisation of shallow coastal aquifers, niger delta basin: A strategy for groundwater resource management. *Geosciences (Switzerland)*, *9*(11). https://doi.org/10.3390/geosciences9110470

Hassan Rashid, M. A. U., Manzoor, M. M., & Mukhtar, S. (2018). Urbanization and its effects on water resources: An exploratory analysis. *Asian Journal of Water, Environment and Pollution*, *15*(1), 67–74. https://doi.org/10.3233/AJW-180007

Hassan, W. H., & Khalaf, R. M. (2020). Optimum Groundwater use Management Models by Genetic Algorithms in Karbala Desert, Iraq. *IOP Conference Series: Materials Science and Engineering*, *928*(2). https://doi.org/10.1088/1757-899X/928/2/022141

Havril, T., Tóth, Á., Molson, J. W., Galsa, A., & Mádl-Szőnyi, J. (2018). Impacts of predicted climate change on groundwater flow systems: Can wetlands disappear due to recharge reduction? *Journal of Hydrology*, *563*, 1169–1180. https://doi.org/10.1016/j.jhydrol.2017.09.020

Hoover, J., Gonzales, M., Shuey, C., Barney, Y., & Lewis, J. (2017). Elevated arsenic and uranium concentrations in unregulated water sources on the Navajo Nation, USA. *Exposure and Health*, *9*(2), 113–124. https://doi.org/10.1007/s12403-016-0226-6

Huang, C. S., Wang, Z., Lin, Y. C., Yeh, H. Der, & Yang, T. (2020). New Analytical Models for Flow Induced by Pumping in a Stream-Aquifer System: A New Robin Boundary Condition Reflecting Joint Effect of Streambed Width and Storage. *Water Resources Research*, *56*(4). https://doi.org/10.1029/2019WR026352

Hussein, S. O., Kovács, F., Tobak, Z., & Abdullah, H. J. (2018). Spatial distribution of vegetation cover in Erbil city districts using high-resolution Pléiades satellite image. *Landscape & Environment*, *12*(1), 10–22. https://doi.org/10.21120/le/12/1/2

Ismailia, C., & Rode, D. (2017). *" Geoelectrical contribution for solving water logging in selected sites , kilometer*. *February*.

K, V., S, S., B, G., & K, S. (2020). Delineate Subsurface and Groundwater Investigation of Ongur Watershed, South India. *International Journal of Civil, Environmental and Agricultural Engineering*, *2*(1), 17–33. https://doi.org/10.34256/ijceae2012

Karikari, A., & Ansa-Asare, O. (2009). Physico-Chemical and microbial water quality assessment of Densu River of Ghana. *West African Journal of Applied Ecology*, *10*(1). https://doi.org/10.4314/wajae.v10i1.45701

Kowalczyk, S., Zukowska, K. A., Mendecki, M. J., & Łukasiak, D. (2017). Application of electrical resistivity imaging (ERI) for the assessment of peat properties: A case study of

the Całowanie Fen, Central Poland. *Acta Geophysica*, *65*(1), 223–235. https://doi.org/10.1007/s11600-017-0018-9

Krietsch, H., Doetsch, J., Dutler, N., Jalali, M., Gischig, V., Loew, S., & Amann, F. (2018). Comprehensive geological dataset describing a crystalline rock mass for hydraulic stimulation experiments. *Scientific Data*, *5*, 1–12. https://doi.org/10.1038/sdata.2018.269

Kumar, P., Thakur, P. K., Bansod, B. K. S., & Debnath, S. K. (2018). Groundwater: a regional resource and a regional governance. *Environment, Development and Sustainability*, *20*(3), 1133–1151. https://doi.org/10.1007/s10668-017-9931-y

Kundzewicz, Z. W., Mata, L. J., Arnell, N. W., DÖLL, P., Jimenez, B., Miller, K., Oki, T., ŞEN, Z., & Shiklomanov, I. (2008). The implications of projected climate change for freshwater resources and their management. *Hydrological Sciences Journal*, *53*(1), 3–10. https://doi.org/10.1623/hysj.53.1.3

Kwoyiga, L., & Stefan, C. (2018). Groundwater development for dry season irrigation in North East Ghana: The place of local knowledge. *Water (Switzerland)*, *10*(12). https://doi.org/10.3390/w10121724

Li, L., Tan, J., & Schwarz, B. (2020). *Recent Advances and Challenges of Waveform - Based Seismic Location Methods at Multiple Scales*. 1–47. https://doi.org/10.1029/2019RG000667

Liaqat, M. U., Mohamed, M. M., Chowdhury, R., Elmahdy, S. I., Khan, Q., & Ansari, R. (2021a). Impact of Land Use/Land Cover Changes on Ground Water Resources in Al Ain Region of the United Arab Emirates Using Remote Sensing and GIS Techniques. *Groundwater for Sustainable Development*, *14*(April), 100587. https://doi.org/10.1016/j.gsd.2021.100587

Liaqat, M. U., Mohamed, M. M., Chowdhury, R., Elmahdy, S. I., Khan, Q., & Ansari, R. (2021b). Impact of land use/land cover changes on groundwater resources in Al Ain region of the United Arab Emirates using remote sensing and GIS techniques. *Groundwater for Sustainable Development*, *14*, 100587. https://doi.org/10.1016/J.GSD.2021.100587

Lin, C. H., Lin, C. P., Hung, Y. C., Chung, C. C., Wu, P. L., & Liu, H. C. (2018). Application of geophysical methods in a dam project: Life cycle perspective and Taiwan experience. *Journal of Applied Geophysics*, *158*, 82–92. https://doi.org/10.1016/j.jappgeo.2018.07.012

Liu, Y., Habibi, D., Chai, D., Wang, X., Chen, H., Gao, Y., & Li, S. (2020). A comprehensive review of acoustic methods for locating underground pipelines. *Applied Sciences (Switzerland)*, *10*(3). https://doi.org/10.3390/app10031031

Loh, Y. S. A., Akurugu, B. A., Manu, E., & Aliou, A. S. (2020). Assessment of groundwater quality and the main controls on its hydrochemistry in some Voltaian and basement aquifers, northern Ghana. *Groundwater for Sustainable Development*, *10*(November 2019), 100296. https://doi.org/10.1016/j.gsd.2019.100296

Loke, M. H. (2001). *Constrained Time-Lapse Resistivity Imaging Inversion*. EEM7–EEM7. https://doi.org/10.4133/1.2922877

Lomazzi, M., Borisch, B., & Laaser, U. (2014). The Millennium Development Goals: Experiences, achievements and what's next. *Global Health Action*, *7*(SUPP.1), 1–9. https://doi.org/10.3402/gha.v7.23695

MacDonald, A. M., Carlow, R. C., MacDonald, D. M. J., Darling, W. G., & Dochartaigh, B. É. Ó. (2009). What impact will climate change have on rural groundwater supplies in Africa? *Hydrological Sciences Journal*, *54*(4), 690–703. https://doi.org/10.1623/hysj.54.4.690

MacDonald, A. M., & Davies, J. (2000). *A brief review of groundwater for rural water supply in sub-Saharan Africa. British Geological Survey Technical Report WC/00/33. BGS Keyworth UK*. 13.

MacDonald, G. M., & Case, R. A. (2005). Variations in the Pacific Decadal Oscillation over the past millennium. *Geophysical Research Letters*, *32*(8), 1–4. https://doi.org/10.1029/2005GL022478

Magesh, N. S., Chandrasekar, N., & Soundranayagam, J. P. (2012). Delineation of groundwater potential zones in Theni district, Tamil Nadu, using remote sensing, GIS and MIF techniques. *Geoscience Frontiers*, *3*(2), 189–196.

https://doi.org/10.1016/j.gsf.2011.10.007

Mall, R. K., Singh, R., Gupta, A., Srinivasan, G., & Rathore, L. S. (2006). Impact of climate change on Indian agriculture: A review. *Climatic Change*, *78*(2–4), 445–478. https://doi.org/10.1007/s10584-005-9042-x

MANYU, A., EKAWITA, R., JANI, S., ISMI, Y., & BAHRUM, Z. (2018). *Geoelectrical Sounding For Groundwater Interpretation In Oil Palm Plantation*. *August*, 17–23. https://doi.org/10.15224/978-1-63248-143-6-04

Martin, N., & van de Giesen, N. (2005). Spatial distribution of groundwater production and development potential in the volta river basin of ghana and burkina faso. *Water International*, *30*(2), 239–249. https://doi.org/10.1080/02508060508691852

Mcdowell, R., Us, F. L., Nelson, T., & Us, F. L. (2002). *s : 2*(12).

Mesbah, H. S., Ismail, A., Taha, A. I., Massoud, U., & Soilman, M. M. (2017). Electrical and electromagnetic surveys to locate possible causes of water seepage to ground surface at a quarry open pit near Helwan city, Egypt. *Arabian Journal of Geosciences*, *10*(10). https://doi.org/10.1007/s12517-017-2997-x

Mohamaden, M. I. I., Hamouda, A. Z., & Mansour, S. (2016). Application of electrical resistivity method for groundwater exploration at the Moghra area, Western Desert, Egypt. *Egyptian Journal of Aquatic Research*, *42*(3), 261–268. https://doi.org/10.1016/j.ejar.2016.06.002

Mohammad Amin Bhat, Sheeraz Ahmad Wani, Vijay Kant Singh, Jyotirmaya Sahoo, Dinesh Tomar, R. S. (2018). An Overview of the Assessment of Groundwater Quality for Irrigation. *Journal of Agricultural Science and Food Research*, *9*(1), 1–9.

Of, A., Quality, G., & Sunamganj, I. N. (2008). *Archive of SID ASSESSMENT OF GROUNDWATER QUALITY IN SUNAMGANJ OF Archive of SID*. *5*(3), 155–166.

Oh, H. J., Kim, Y. S., Choi, J. K., Park, E., & Lee, S. (2011). GIS mapping of regional probabilistic groundwater potential in the area of Pohang City, Korea. *Journal of Hydrology*, *399*(3–4), 158–172. https://doi.org/10.1016/j.jhydrol.2010.12.027

Olesen, J. E., Carter, T. R., Díaz-Ambrona, C. H., Fronzek, S., Heidmann, T., Hickler, T., Holt, T., Minguez, M. I., Morales, P., Palutikof, J. P., Quemada, M., Ruiz-Ramos, M., Rubæk, G. H., Sau, F., Smith, B., & Sykes, M. T. (2007). Uncertainties in projected impacts of climate change on European agriculture and terrestrial ecosystems based on scenarios from regional climate models. *Climatic Change*, *81*(SUPPL. 1), 123–143. https://doi.org/10.1007/s10584-006-9216-1

Olusola, F. O. (2020). Groundwater quality evaluation for drinking, domestic and irrigation uses in parts of ode irele local government area of Ondo state, Nigeria. *Water Conservation and Management*, *4*(1), 32–41. https://doi.org/10.26480/wcm.01.2020.32.41

Omolaiye, G. E., Oladapo, I. M., Ayolabi, A. E., Akinwale, R. P., Akinola, A. A., Omolaye, K. L., & Sanuade, O. A. (2020). Integration of remote sensing, GIS and 2D resistivity methods in groundwater development. *Applied Water Science*, *10*(6), 1–24. https://doi.org/10.1007/s13201-020-01219-x

Oseke, F. I., Anornu, G. K., Adjei, K. A., & Eduvie, M. O. (2021). Assessment of water quality using GIS techniques and water quality index in reservoirs affected by water diversion. *Water-Energy Nexus*, *4*, 25–34. https://doi.org/10.1016/J.WEN.2020.12.002

Pandey, H. K., Tiwari, V., Kumar, S., Yadav, A., & Srivastava, S. K. (2020). Groundwater quality assessment of Allahabad smart city using GIS and water quality index. *Sustainable Water Resources Management*, *6*(2). https://doi.org/10.1007/s40899-020-00375-x

Parnow, S., Oskooi, B., & Florio, G. (2021). Improved linear inversion of low induction number electromagnetic data. *Geophysical Journal International*, *224*(3), 1505–1522. https://doi.org/10.1093/gji/ggaa531

Peng, R., & Han, B. (2020). *Exploration of Seafloor Massive Sulfide Deposits with Fixed-O ff set Marine Controlled Source Electromagnetic Method : Numerical Simulations and the E ff ects of Electrical Anisotropy*. 1–15.

Piccoli, I., Furlan, L., Lazzaro, B., & Morari, F. (2020). Examining conservation agriculture soil profiles: Outcomes from northeastern Italian silty soils combining indirect geophysical and direct assessment methods. *European Journal of Soil Science*, *71*(6), 1064–1075.

https://doi.org/10.1111/ejss.12861

Prabhakar, A., & Tiwari, H. (2015). Land use and land cover effect on groundwater storage. *Modeling Earth Systems and Environment*, *1*(4), 1–10. https://doi.org/10.1007/s40808-015-0053-y

Prasood, S. P., Mukesh, M. V., Rani, V. R., Sajinkumar, K. S., & Thrivikramji, K. P. (2021). Urbanization and its effects on water resources: Scenario of a tropical river basin in South India. *Remote Sensing Applications: Society and Environment*, *23*, 100556. https://doi.org/10.1016/J.RSASE.2021.100556

Prosper, K., Abdul-ganiyu, S., Amadu, I., & Bismark, M. (2020). *Assessment of Groundwater for Dry Season Farming in the Upper East Region of Ghana-Determining the Storage Capacity*. *8*(7), 4147–4159.

Rahmati, O., Nazari Samani, A., Mahdavi, M., Pourghasemi, H. R., & Zeinivand, H. (2015). Groundwater potential mapping at Kurdistan region of Iran using analytic hierarchy process and GIS. *Arabian Journal of Geosciences*, *8*(9), 7059–7071. https://doi.org/10.1007/s12517-014-1668-4

Ram, A., Tiwari, S. K., Pandey, H. K., Chaurasia, A. K., Singh, S., & Singh, Y. V. (2021). Groundwater quality assessment using water quality index (WQI) under GIS framework. *Applied Water Science*, *11*(2), 1–20. https://doi.org/10.1007/s13201-021-01376-7

Rawat, K. S., Singh, S. K., & Gautam, S. K. (2018). Assessment of groundwater quality for irrigation use: a peninsular case study. *Applied Water Science*, *8*(8), 1–24. https://doi.org/10.1007/s13201-018-0866-8

Riwayat, A. I., Ahmad Nazri, M. A., & Zainal Abidin, M. H. (2018). Application of Electrical Resistivity Method (ERM) in Groundwater Exploration. *Journal of Physics: Conference Series*, *995*(1). https://doi.org/10.1088/1742-6596/995/1/012094

Robinson, D. A., Binley, A., Hubbard, S. S., & Huisman, J. A. (2015). *understanding of subsurface processes over multiple scales*. 3837–3866. https://doi.org/10.1002/2015WR017016.Received

Romero-Ruiz, A., Linde, N., Keller, T., & Or, D. (2018). A Review of Geophysical Methods for Soil Structure Characterization. *Reviews of Geophysics*, *56*(4), 672–697. https://doi.org/10.1029/2018RG000611

Rosenberg, D. M., McCully, P., & Pringle, C. M. (2000). Global-scale environmental effects of hydrological alterations: Introduction. *BioScience*, *50*(9), 746–751. https://doi.org/10.1641/0006-3568(2000)050[0746:GSEEOH]2.0.CO;2

Sadat-Noori, S. M., Ebrahimi, K., & Liaghat, A. M. (2014). Groundwater quality assessment using the Water Quality Index and GIS in Saveh-Nobaran aquifer, Iran. *Environmental Earth Sciences*, *71*(9), 3827–3843. https://doi.org/10.1007/s12665-013-2770-8

Saeedi, M., Abessi, O., Sharifi, F., & Meraji, H. (2010). Development of groundwater quality index. *Environmental Monitoring and Assessment*, *163*(1–4), 327–335. https://doi.org/10.1007/s10661-009-0837-5

Sahu, P., & Sikdar, P. K. (2008). Hydrochemical framework of the aquifer in and around East Kolkata Wetlands, West Bengal, India. *Environmental Geology*, *55*(4), 823–835. https://doi.org/10.1007/s00254-007-1034-x

Sajil Kumar, P. J., Elango, L., & James, E. J. (2014). Assessment of hydrochemistry and groundwater quality in the coastal area of South Chennai, India. *Arabian Journal of Geosciences*, *7*(7), 2641–2653. https://doi.org/10.1007/s12517-013-0940-3

Samouëlian, A., Cousin, I., Tabbagh, A., Bruand, A., & Richard, G. (2005). Electrical resistivity survey in soil science: A review. *Soil and Tillage Research*, *83*(2), 173–193. https://doi.org/10.1016/j.still.2004.10.004

Sanuade, O. A., Olaojo, A. A., Akanji, A. O., Oladunjoye, M. A., & Omolaiye, G. E. (2018). A Resistivity Survey of Phosphate Nodules in Oshoshun, Southwestern Nigeria. *Materials and Geoenvironment*, *65*(2), 103–114. https://doi.org/10.1515/rmzmag-2018-0006

Seidu, J., Ewusi, A., & Kuma, J. S. Y. (2019). Combined Electrical Resistivity Imaging and Electromagnetic Survey for Groundwater Studies in the Tarkwa Mining Area, Ghana. *Ghana Mining Journal*, *19*(1), 29–41. https://doi.org/10.4314/gm.v19i1.4

Shishaye, H. A. (2017). *Groundwater Exploration for Water Well Site Locations Using Geophysical Hydrology Current Research Groundwater Exploration for Water Well Site Locations Using Geophysical Survey Methods*. *August*. https://doi.org/10.4172/2157-7587.1000226

Siebert, S., Burke, J., Faures, J. M., Frenken, K., Hoogeveen, J., Döll, P., & Portmann, F. T. (2010). Groundwater use for irrigation – a global inventory. *Hydrology and Earth System Sciences Discussions*, *7*(3), 3977–4021. https://doi.org/10.5194/hessd-7-3977-2010

Siena, M., Guadagnini, A., Bouissonnié, A., Ackerer, P., Daval, D., & Riva, M. (2020). Generalized Sub-Gaussian Processes: Theory and Application to Hydrogeological and Geochemical Data. *Water Resources Research*, *56*(8), 1–20. https://doi.org/10.1029/2020WR027436

Sikandar, P., & Christen, E. W. (2012). Geoelectrical Sounding for the Estimation of Hydraulic Conductivity of Alluvial Aquifers. *Water Resources Management*, *26*(5), 1201–1215. https://doi.org/10.1007/s11269-011-9954-3

Subramani, T., Elango, L., & Damodarasamy, S. R. (2005). Groundwater quality and its suitability for drinking and agricultural use in Chithar River Basin, Tamil Nadu, India. *Environmental Geology*, *47*(8), 1099–1110. https://doi.org/10.1007/s00254-005-1243-0

Swileam, G. S., Shahin, R. R., Nasr, H. M., & Essa, K. S. (2019). Assessment of soil variability using electrical resistivitytechnique for normalalluvialsoils, Egypt. *Plant Archives*, *19*(1), 905–912.

Swileam, Gamal S., Shahin, R. R., Nasr, H. M., & Essa, K. S. (2019). Spatial variability assessment of nile alluvial soils using electrical resistivity technique. *Eurasian Journal of Soil Science*, *8*(2), 110–117. https://doi.org/10.18393/ejss.528851

Taha, A. I., Al Deep, M., & Mohamed, A. (2021). Investigation of groundwater occurrence using gravity and electrical resistivity methods: a case study from Wadi Sar, Hijaz Mountains, Saudi Arabia. *Arabian Journal of Geosciences*, *14*(5). https://doi.org/10.1007/s12517-021-06628-z

Tolche, A. D. (2020). Groundwater potential mapping using geospatial techniques: a case study of Dhungeta-Ramis sub-basin, Ethiopia. *Geology, Ecology, and Landscapes*, *00*(00), 1–16. https://doi.org/10.1080/24749508.2020.1728882

Tolche, A. D. (2021). Groundwater potential mapping using geospatial techniques: a case study of Dhungeta-Ramis sub-basin, Ethiopia. *Geology, Ecology, and Landscapes*, *5*(1), 65–80. https://doi.org/10.1080/24749508.2020.1728882

Tschakert, P., & Singha, K. (2007). Contaminated identities: Mercury and marginalization in Ghana's artisanal mining sector. *Geoforum*, *38*(6), 1304–1321. https://doi.org/10.1016/j.geoforum.2007.05.002

Umar, R., Ahmed, I., Alam, F., & Khan, M. M. (2009). Hydrochemical characteristics and seasonal variations in groundwater quality of an alluvial aquifer in parts of Central Ganga Plain, Western Uttar Pradesh, India. *Environmental Geology*, *58*(6), 1295–1300. https://doi.org/10.1007/s00254-008-1630-4

Vanella, D., Ramírez-Cuesta, J. M., Sacco, A., Longo-Minnolo, G., Cirelli, G. L., & Consoli, S. (2021). Electrical resistivity imaging for monitoring soil water motion patterns under different drip irrigation scenarios. *Irrigation Science*, *39*(1), 145–157. https://doi.org/10.1007/s00271-020-00699-8

Wada, Y., Van Beek, L. P. H., & Bierkens, M. F. P. (2012). Nonsustainable groundwater sustaining irrigation: A global assessment. *Water Resources Research*, *48*(1). https://doi.org/10.1029/2011WR010562

Wahyudi, F. R., & Moersidik, S. S. (2016). The Analysis of Ground Water Availability and Utility in DKI Jakarta. *Procedia - Social and Behavioral Sciences*, *227*, 799–807. https://doi.org/10.1016/j.sbspro.2016.06.148

Walsh, D. (2017). Environmental Geophysics. *Preview*, *2017*(186), 29–31. https://doi.org/10.1071/pvv2017n186p29

Water Resources Commission of Ghana. (2011). *Executive Report on the State of Groundwater Resources of the Northern Regions of Ghana*. *December*, 1–101. http://www.wrc-

gh.org/dmsdocument/89

Xue, J., Bali, K. M., Light, S., Hessels, T., & Kisekka, I. (2020). Evaluation of remote sensing-based evapotranspiration models against surface renewal in almonds, tomatoes and maize. *Agricultural Water Management*, *238*, 106228. https://doi.org/10.1016/j.agwat.2020.106228

Yeleliere, E., Cobbina, S. J., & Duwiejuah, A. B. (2018). Review of Ghana's water resources: the quality and management with particular focus on freshwater resources. *Applied Water Science*, *8*(3), 1–12. https://doi.org/10.1007/s13201-018-0736-4

Yidana, S. M., Banoeng-Yakubo, B., Aliou, A. S., & Akabzaa, T. M. (2012). Qualité des eaux souterraines des aquifères voltaÏque et birimien du nord Ghana - application de méthodes statistiques multivariées et de systèmes d'information géographique. *Hydrological Sciences Journal*, *57*(6), 1168–1183. https://doi.org/10.1080/02626667.2012.693612

Yidana, S. M., Fynn, O. F., Chegbeleh, L. P., Nude, P. M., & Asiedu, D. K. (2013). Hydrogeological conditions of a crystalline aquifer: Simulation of optimal abstraction rates under scenarios of reduced recharge. *The Scientific World Journal*, *2013*. https://doi.org/10.1155/2013/606375

Ylaya, V. J. V, Pongcol, D. P., & Gerasta, O. J. L. (2020). *Linear Frequency Modulated Continuous Wave LFM-CW Short-Range Radar for Detecting Subsurface Water Content with Deep Learning*.

Youssouf, A., Nasr, I. H., Traor, B., Amiri, A., Inoubli, M. H., Sangar, S., & Qaysi, S. (2021). *Geophysical Contributions to Gold Exploration in Western Mali According to Airborne Electromagnetic Data Interpretations*. 1–15.

Zainal Abidin, M. H., Madun, A., Ahmad Tajudin, S. A., Tajul Baharuddin, M. F., Yusof, M. F., Zakaria, M. N., & Rahmat, S. N. (2017). Evaluation of Unknown Tube Well Depth Using Electrical Resistivity Method. *MATEC Web of Conferences*, *103*. https://doi.org/10.1051/matecconf/201710307002

APPENDICE

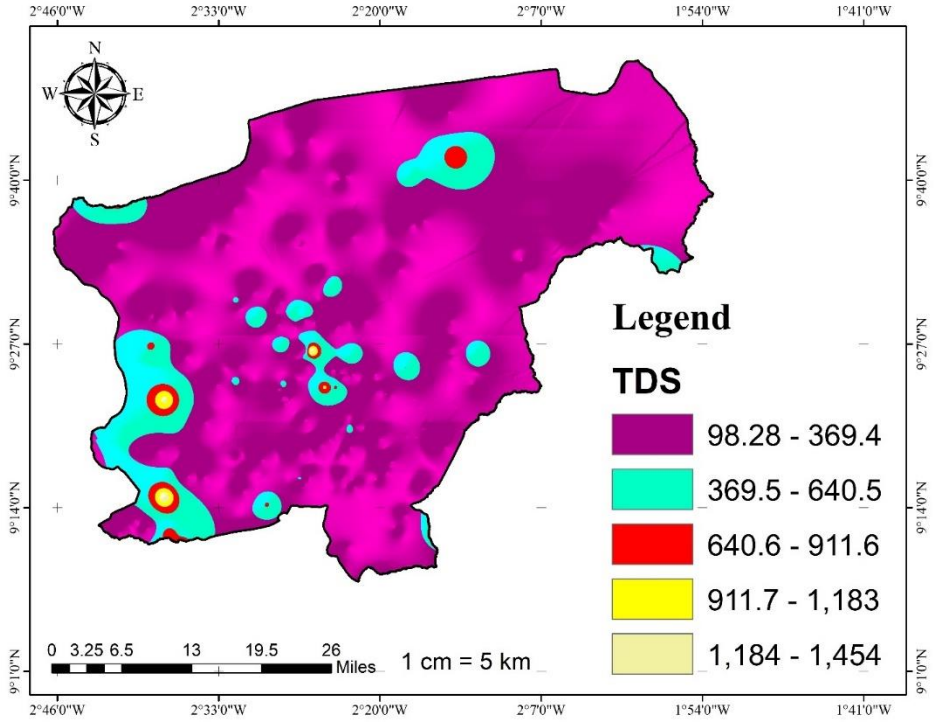

Figure 1 Spatial variation of Total Dissolved Solids in the study area

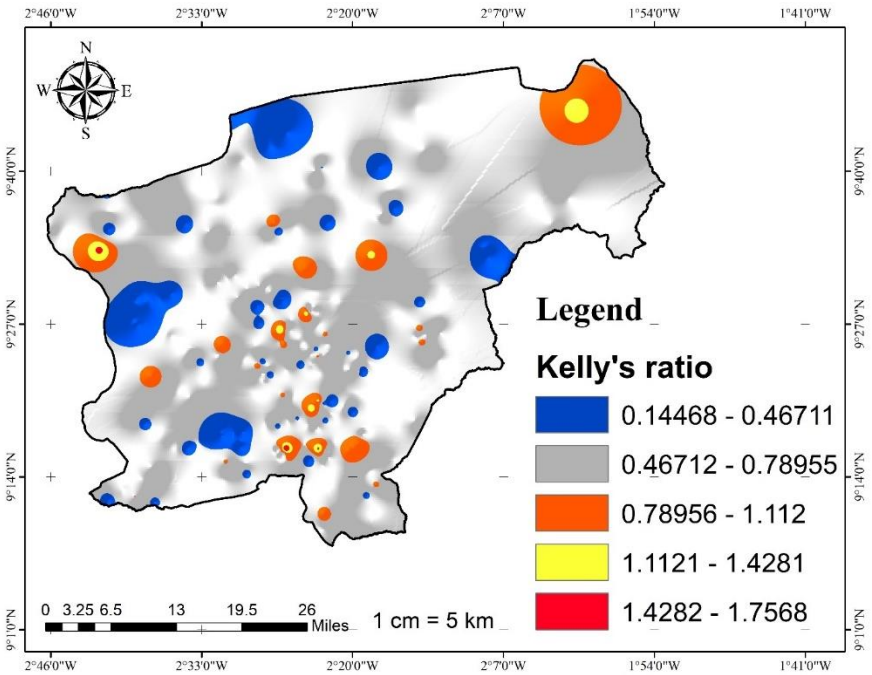

Figure 2 Spatial variation of Kelly's Ratio in the study area

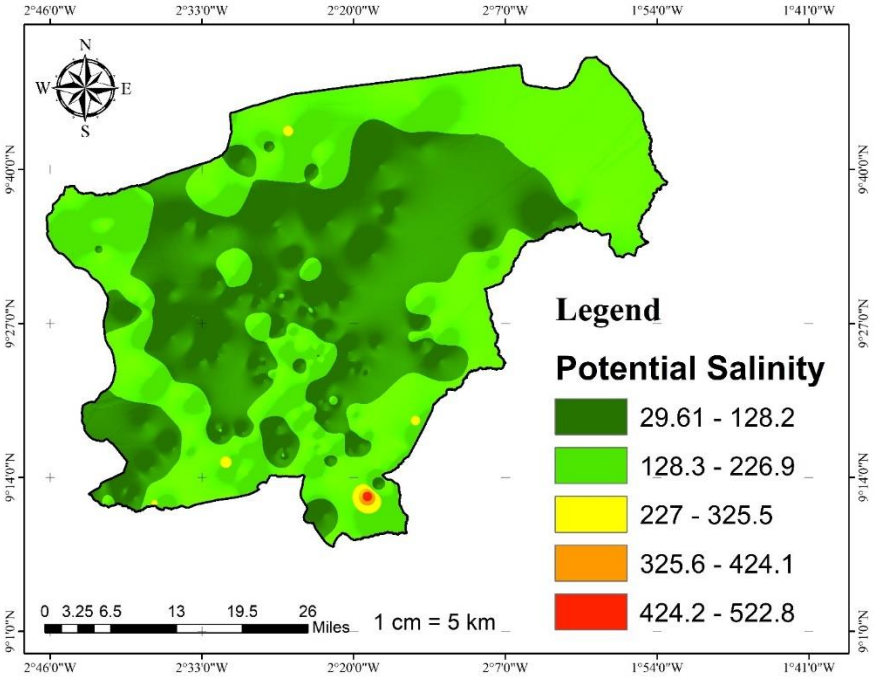

Figure 3 Spatial variation of Potential Salinity in the study area

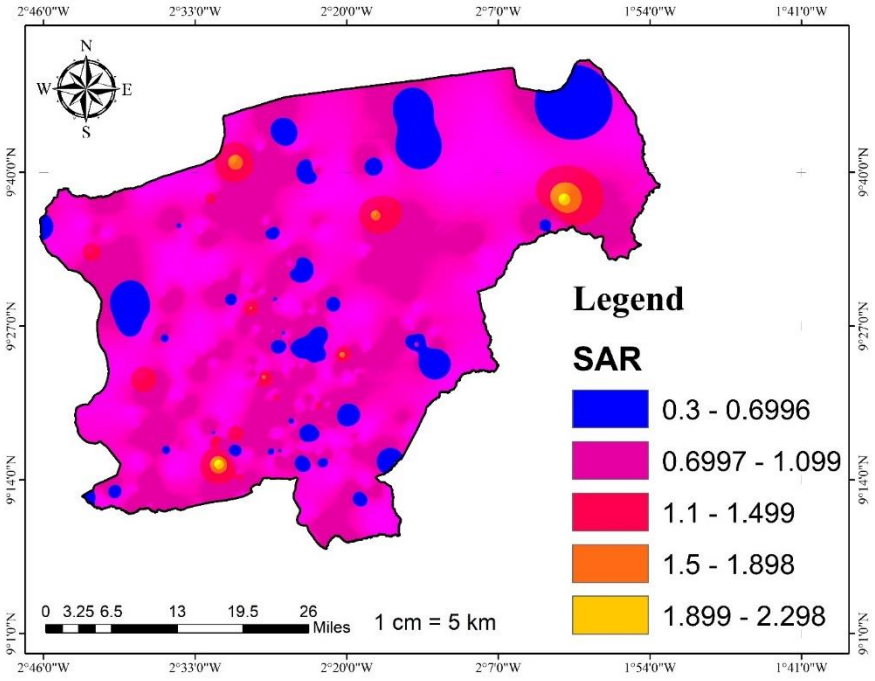

Figure 4 Spatial variation of Sodium Absorption Ratio in the study area

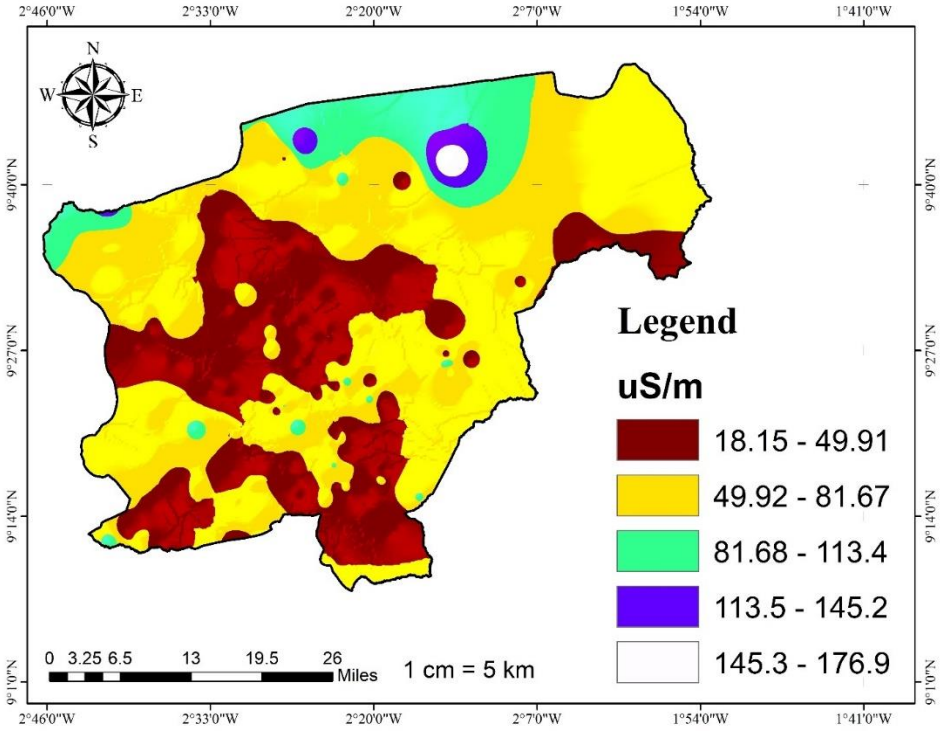

Figure 5 Spatial variation of Electrical Conductivity in the study area

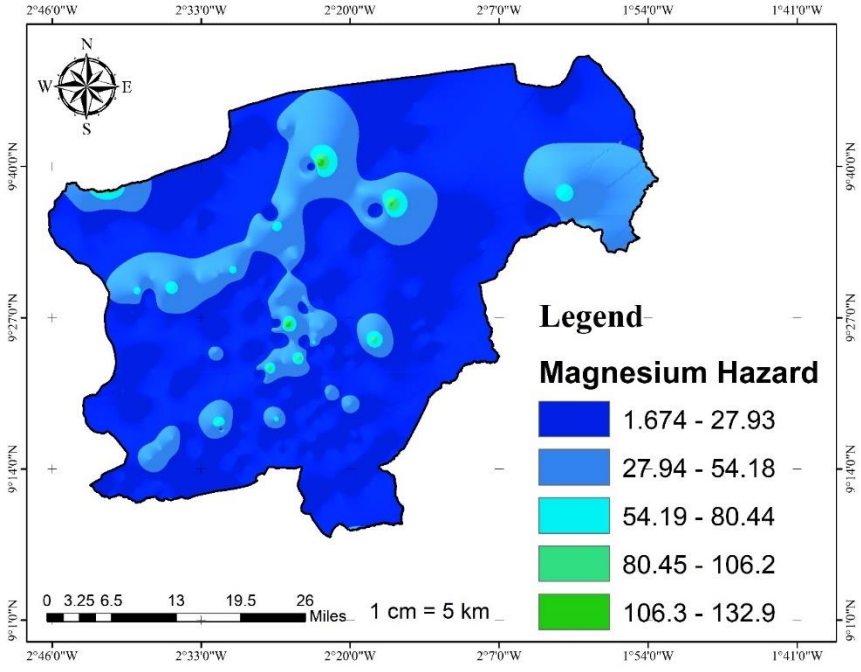

Figure 6 Spatial variation of Magnesium Hazard in the study area

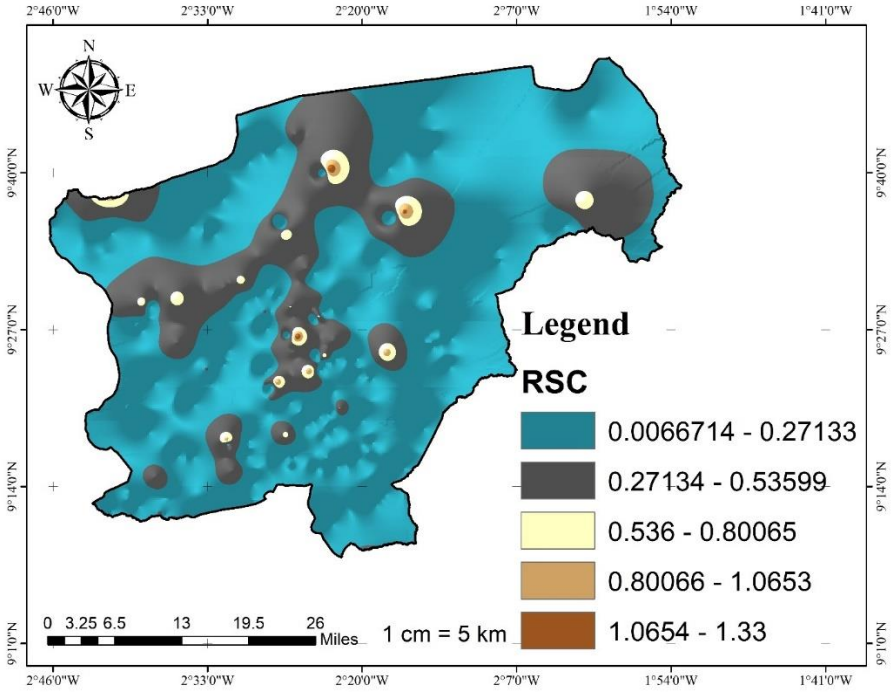

Figure 7 Spatial variation of Residual Sodium Carbonate in the study area